Optimizing Storm Surge Barrier Performance
Enhancing Closure Reliability to Reduce Coastal Flood Risk

Mooyaart, L.F.

DOI
10.4233/uuid:bf43d240-a460-40e7-bbbe-1a2111e37cb3

Publication date
2025

Document Version
Final published version

Citation (APA)
Mooyaart, L. F. (2025). *Optimizing Storm Surge Barrier Performance: Enhancing Closure Reliability to Reduce Coastal Flood Risk*. [Dissertation (TU Delft), Delft University of Technology]. https://doi.org/10.4233/uuid:bf43d240-a460-40e7-bbbe-1a2111e37cb3

L.F. Mooyaart

OPTIMIZING STORM SURGE BARRIER PERFORMANCE

Enhancing Closure Reliability to Reduce Coastal Flood Risk

Optimizing Storm Surge Barrier Performance: Enhancing Closure Reliability to Reduce Coastal Flood Risk

Dissertation

for the purpose of obtaining the degree of doctor
at Delft University of Technology,
by the authority of the Rector Magnificus
prof.dr.ir. T.H.J.J. van der Hagen,
chair of the Board for Doctorates,
to be defended publicly on
Monday 6 October 2025 at 15:00 o'clock

by

Leslie Freek MOOYAART
Master of Science in Civil Engineering, Delft University of Technology,
the Netherlands born in Groningen, the Netherlands

This dissertation has been approved by:

Prof.dr.ir. S.N. Jonkman	Promotor
Dr.ir. A.M.R. Bakker	Copromotor

Composition of the doctoral committee:

Rector Magnificus,	Chairperson
Prof.dr.ir. S.N. Jonkman	Delft University of Technology, promotor
Dr.ir. A.M.R. Bakker	Delft University of Technology, copromotor
Dr.ir. J.A. van den Bogaard	Rijkswaterstaat, external advisor

Independent members:

Prof.dr.ir. P.H.A.J.M. van Gelder	Delft University of Technology
Prof.dr. I.D. Haigh	University of Central Florida, USA
Prof.dr.ir. M.J.C.M. Hertogh	Delft University of Technology
ir. H. van Waveren	Rijkswaterstaat
Dr.ir. B. Hofland	Delft University of Technology, reserve member

This research was funded by Rijkswaterstaat

Book design, layout and print: Gildeprint, Enschede
Cover design by Vincent de Gooijer
ISBN: 978-94-6496-433-2

An electronic version of this dissertation is available at: http://repository.tudelft.nl

One cannot talk about risk in isolation. One needs to adopt a decision theory point of view and ask: "What are my options, what are the costs, benefits, and risks of each?' That option with the optimum mix of cost, benefit, and risk is selected. The risk associated with that option is acceptable. All others are unacceptable.

Kaplan & Garrick, 1981

Summary

Sea level rise and coastal urbanization motivate the improvement of coastal flood protection such as storm surge barriers. These large movable hydraulic structures (the largest one features 62 gates, each 42 meters wide) close during a storm surge to prevent coastal flooding in bays and estuaries. Barrier improvements lower their susceptibility to operational, structural, or height-related failures.

Storm surge barriers are often perceived as rigid structures that are difficult to adjust. In reality, these barriers undergo continuous repairs and renovations. Furthermore, there are many more options available to improve performance at storm surge barriers. These options vary in size (whether to replace the entire barrier or just a component) and type (human, software, hardware, system properties, maintenance & operation, model). Given the large number of options, identifying effective improvements can be challenging.

This thesis focuses on identifying improvements to storm surge barriers, particularly those that improve closure reliability. It addresses the following research question:

> ***How can closure reliability of existing storm surge barriers be systematically assessed and improved to enhance coastal flood protection?***

The key tool to assess and improve closure reliability is the reliability and availability analysis (RA analysis), which quantifies the probability of failure to close. This thesis uses the results of such an RA analysis to answer this research question.

The research is structured into four parts from coarse to fine. In each section, the Maeslant barrier in the Netherlands serves as a case study to illustrate the methods developed.

The first part addresses the question of how to determine the importance of (the lack of) closure reliability relative to other main failure mechanisms (structural failure and hydraulic overload) at storm surge barriers. Here, the exceedance frequency of the critical water level of interior flood defenses is assumed to be a good proxy for the flood frequency. The method then elaborates on how these failure mechanisms contribute to the exceedance frequency of a critical water level. The method uses descriptions, experiences, and results from current Dutch probabilistic water system models (Hydra-NL & Prestatiepeilen). This part clarifies how these models work and

explains how they can be applied and adjusted to assess storm surge barrier failure mechanisms, as opposed to those of interior flood defenses. The method helps to get better insight into the weak spots of storm surge barriers in protecting the hinterland. Storm surge barrier managers can use the method to examine which failure mechanisms contribute most to the flood frequency and, hence, are promising to improve. The method is applied at the Maeslant barrier and demonstrates that the probability of a failure to close accounts for more than 70% of the flood frequency in Rotterdam.

The second part analyses how an optimal requirement for closure reliability can be determined. Here, the economic optimization model for dike raising by van Dantzig (1956) is extended to include improvements in closure reliability. Based on this model, optimal requirements for a probability of a failure to close are determined and for the flood protection system including both storm surge barriers and interior flood defenses such as dikes. The costs associated with improving closure reliability are found to be crucial for determining the optimal requirements. The Maeslant barrier case study demonstrates that with a slight increase in risk (a factor of 2 to 3, corresponding to about 0.25 meter rise in sea level), the requirements for failure to close could become ten times more stringent.

The third part investigates how to identify and select closure reliability improvements without overlooking important ones. Here, a three-stage screening method is proposed to choose the top 5 performance improvements from a checklist of 85 principal performance improvements. The first stage is a desk study aimed at selecting only those principal performance improvements that could potentially have a major effect on the probability of a failure to close. The second stage is an expert session aiming to exclude principal performance improvements which are irrelevant. Another aim of this second session is to make promising performance improvements specific to the analyzed object. The third state is again an expert session, now aiming at ranking the remaining performance improvements after the previous stage. The method is applied to a historical RA analysis of the Maeslant barrier and identifies both crucial implemented performance improvements (such as formalizing human recovery) and new ones (examining common-cause failures, which refer to failures of identical components due to a shared cause).

The final part examines whether and how an existing RA analysis should be adjusted when improvements in closure reliability are identified. The developed method determines the value of model refinements and weighs them against their disadvantages (costs, impact on planning, and quality). The case study explores how to refine common-cause modeling, specifically at the ballast system, which is part of the Maeslant barrier and contains many identical components. Analyzing test data from ballast system components is identified as a first step to find better reliability estimates.

Combined, these parts constitute to a method to find and select closure reliability improvements and determine their effect on flood risk reduction. As such, it can be applied by storm surge barrier managers worldwide to combat rising flood risk when the lack of closure reliability is the dominant failure mechanism. Moreover, the third and fourth parts could also be useful for asset managers of other safety-critical objects aiming to improve their performance.

The study revealed a need for new and improved risk analyses specific for addressing risk associated with storm surge barriers. Current practices at Dutch storm surge barriers are based on the risk analysis of the Maeslant barrier, developed between 2001 and 2008. This analysis is large (> 1200 pages of fault trees and more than 7000 lines in a database file), and there are many inconsistencies with the fault tree model and the report. As a result, this model is difficult – if not impossible – to adapt. Moreover, current risk analyses rely on data and practices from other industries, which may not necessarily apply to storm surge barriers. Since 2008 new storm surge barriers have been constructed (e.g., New Orleans, St. Petersburg), and considerable operational experience has been gained. It is recommended to develop risk analyses and storm surge barrier failure and performance data based on that experience.

Samenvatting

De kust dient beter beschermd te worden door de toename van het overstromingsrisico door zeespiegelstijging en verstedelijking nabij de kust. Dit geldt ook voor stormvloedkeringen. Deze grote beweegbare waterbouwkundige kunstwerken (de Oosterscheldekering bestaat uit 62 schuiven van 42 meter breedte) sluiten tijdens een stormvloed om overstromingen vanuit zee via baaien en estuaria te voorkomen. Verbeteringen aan stormvloedkeringen zorgen ervoor dat de kans op operationeel, constructief of hoogte-gerelateerd falen afneemt.

Stormvloedkeringen worden vaak gezien als rigide constructies die moeilijk aan te passen zijn. In werkelijkheid vinden er continu reparaties en renovaties aan deze keringen plaats. Bovendien zijn er veel meer opties om stormvloedkeringen te verbeteren. Deze opties verschillen onder andere in grootte (vervangen kering, vervangen component) en type (menselijk handelen, software, hardware falen, systeemeigenschappen, onderhoud & bediening en model). Gezien het grote aantal opties is het moeilijk om effectieve verbeteringen te vinden.

Dit proefschrift gaat over het vinden van effectieve verbeteringen voor stormvloedkeringen, specifiek diegene die de betrouwbaarheid van de sluiting verbeteren. Het behandelt de volgende onderzoeksvraag:

> ***Hoe kan de betrouwbaarheid van de sluiting van bestaande stormvloedkeringen systematisch worden beoordeeld en verbeterd om de bescherming tegen overstromingen vanuit zee te verbeteren?***

De betrouwbaarheids- en beschikbaarheidsanalyse (RA analyse) is de belangrijkste tool om de betrouwbaarheid van de sluiting te beoordelen, aangezien deze de kans op het falen van een sluiting kwantificeert. Dit proefschrift gebruikt de uitkomst van deze RA analyse om te komen tot beantwoording van de onderzoeksvraag.

Het onderzoek is georganiseerd in vier delen van grof naar fijn. In alle delen wordt de Maeslantkering gebruikt als praktijkvoorbeeld om de ontwikkelde methodes te verduidelijken.

Het eerste deel gaat in op hoe het gebrek aan betrouwbaarheid van de sluiting bijdraagt aan het totale overstromingsrisico ten opzichte van andere belangrijke faalmechanismen (constructief falen en hydraulische overbelasting). Uitgangspunt daarbij is dat de overschrijdingsfrequentie van het waterpeil waarbij verwacht

wordt dat achterliggende keringen bezwijken een goede proxy is voor de overstromingsfrequentie. De methode bekijkt dan hoe faalmechanismen van de stormvloedkering bijdragen aan deze overschrijdingsfrequentie. De methode maakt gebruik van beschrijvingen, ervaringen en resultaten van huidige Nederlandse probabilistische watersysteemmodellen (Hydra-NL & Prestatiepeilen). Dit deel verduidelijkt hoe deze modellen werken en legt uit hoe ze kunnen worden toegepast en aangepast om faalmechanismen van stormvloedkeringen te beoordelen, in plaats van slechts voor achterliggende dijken. Daarmee kan beter inzicht verkregen worden in de zwakke plekken van stormvloedkeringen in de bescherming van het achterland. Stormvloedkeringbeheerders kunnen deze methode gebruiken om te beoordelen welke faalmechanismen het meest bijdragen aan de overstromingsfrequentie en daarmee het meest kansrijk om te verbeteren zijn. De methode is toegepast bij de Maeslantkering en toont aan dat de kans op het falen van de sluiting meer dan 70% van de overstromingsfrequentie uitmaakt.

In het tweede deel wordt nagegaan hoe een economisch optimale eis voor de betrouwbaarheid van de sluiting kan worden bepaald. Hier wordt het optimalisatiemodel voor dijkverhoging van Van Dantzig (1956) uitgebreid met verbeteringen van de betrouwbaarheid van de sluiting. Dit model bepaalt economisch optimale eisen voor de kans op een gefaalde sluiting en overstromingsfrequenties. De mate waarin de betrouwbaarheid van de sluiting aangepast kan worden, blijkt cruciaal voor het vaststellen van deze eisen. Het praktijkvoorbeeld van de Maeslantkering laat zien dat met een geringe toename van het risico (factor 2 tot 3, overeenkomstig met circa 0,25 meter zeespiegelstijging), de optimale eis voor de kans op een gefaalde sluiting meer dan een factor 10 strenger kan worden.

Het derde deel gaat in op hoe verbeteringen in de betrouwbaarheid van sluitingen kunnen worden gevonden en geselecteerd zonder belangrijke over het hoofd te zien. Hier wordt een selectieprocedure, die bestaat uit drie fasen, voorgesteld om een top 5 van prestatieverbeteringen te selecteren uit een lijst van 85 generieke prestatieverbeteringen. De eerste fase is een bureaustudie, gericht op het selecteren van prestatieverbeteringen die mogelijk een groot effect kunnen hebben op de kans op falen van de sluiting. De tweede fase is een expertsessie die generieke prestatieverbeteringen uitsluit als ze niet kansrijk worden beoordeeld. In deze fase worden tevens kansrijke generieke prestatieverbeteringen specifiek gemaakt voor de betreffende stormvloedkering. De derde fase is wederom een expertsessie, deze keer gericht op het rangschikken van de overgebleven prestatieverbeteringen. De methode is toegepast op een historische RA analyse van de Maeslantkering en vindt belangrijke geïmplementeerde prestatieverbeteringen (formaliseren van menselijk herstel) en nieuwe (onderzoek naar common-cause falen, dat wil zeggen falen van identieke componenten als gevolg van een gemeenschappelijke oorzaak).

In het laatste deel wordt onderzoek gedaan hoe bestaande RA analyses aangepast moeten worden wanneer er verbeteringen in de betrouwbaarheid van de sluiting worden gevonden. De ontwikkelde methode bepaalt de waarde van modelverfijningen en weegt deze af tegen hun nadelen (kosten, effect op planning en kwaliteit). Het praktijkvoorbeeld onderzoekt hoe common-cause modellering verfijnd kan worden, specifiek voor het ballastsysteem dat deel uitmaakt van de Maeslantkering en veel identieke componenten bevat. Het analyseren van testgegevens van ballastsysteem-componenten is geïdentificeerd als een kansrijke eerste stap om de RA analyse aan te passen.

Gecombineerd vormen deze onderdelen een methode om verbeteringen in de betrouwbaarheid van sluitingen te vinden en te selecteren, en hun effect op de vermindering van overstromingsrisico's te bepalen. Als zodanig kan het door asset managers van stormvloedkeringen worden toegepast om het stijgende overstromingsrisico te bestrijden, wanneer het falen van de sluiting het dominante faalmechanisme is. Bovendien kunnen het derde en vierde deel ook bruikbaar zijn voor beheerders van andere veiligheidskritieke objecten om hun prestaties te verbeteren.

Uit het onderzoek is een behoefte aan nieuwe en verbeterde RA analyses gebleken, specifiek voor het aanpakken van risico's die betrekking hebben op stormvloedkeringen. De huidige praktijk bij Nederlandse stormvloedkeringen is sterk gebaseerd op de RA analyses van de Maeslantkering, ontwikkeld in de periode van 2001 tot 2008. Het model van deze analyse is groot (>1200 pagina's aan foutenbomen + >7000 regels in een database-bestand) en de rapportage is inconsistent met dit model. Daardoor is dit model moeilijk – misschien wel onmogelijk – om aan te passen. Bovendien leunen huidige RA analyses op data en praktijken uit andere toepassingen (kernenergie, offshore-industrie), die kunnen leiden tot een onterechte focus op onderdelen die kritiek zijn binnen de betreffende toepassing. Sinds 2008 zijn er veel nieuwe stormvloedkeringen gebouwd (bijvoorbeeld bij New Orleans en St. Petersburg) en is er veel ervaring opgedaan met het beheer en onderhoud van Nederlandse stormvloedkeringen. De aanbeveling is om RA analyses en bijbehorende prestatie- en faalkansdatabases te ontwikkelen op basis van deze ervaringen.

Table of Contents

1

Introduction

1.1 Coastal floods and storm surge barriers[1]

Coastal zones are vulnerable to various natural hazards (Small and Nicholls, 2003). A particularly devastating hazard is a coastal flood due to storm surges. Notable examples include the 1900 flood in Galveston, the 1953 flood in the southwestern Netherlands, and the 2005 flood in New Orleans due to Hurricane Katrina. In each of these instances, there were over a thousand casualties, and cities, towns, and other properties suffered severe damage (see Figure 1.1).

Figure 1.1: Pictures of flood damages from the 1900 flood (left), 1953 flood (middle) and flood damages after Hurricane Katrina (right)

Storm surge-induced flood risk is rising due to two main factors. First, floods are occurring more frequently due to the effects of climate change, including sea level rise, increased storminess, and higher river flows (Calafat et al., 2022). Second, coastal areas become more vulnerable due to growing populations and the rising value of assets (Hallegatte et al., 2013).

1 The introduction contains parts of the introductions of the following three scientific papers: Mooyaart and Jonkman (2017), Mooyaart et al. (2023, 2025)

Already in ancient times, flood protection was built to protect against storm surge-induced floods. An important example of such flood protection is dikes. These earthen structures are placed at the transition between land and water to prevent storm surges from entering the land. In the UK, a dike is referred to as an embankment, and in the USA, it is known as a levee.

Due to the increasing risk of coastal floods, dike settlement, and land subsidence, dikes are often raised and reinforced. However, raising existing dikes — and consequently widening them — poses challenges in urban areas where space is limited. The social impact can be significant since there are businesses, homes, and ports in close proximity to these dikes. An economically viable alternative is a coastal barrier (see Figure 1.2), particularly for regions with long, exposed coastlines, such as larger bays, estuaries, and coastal waterways.

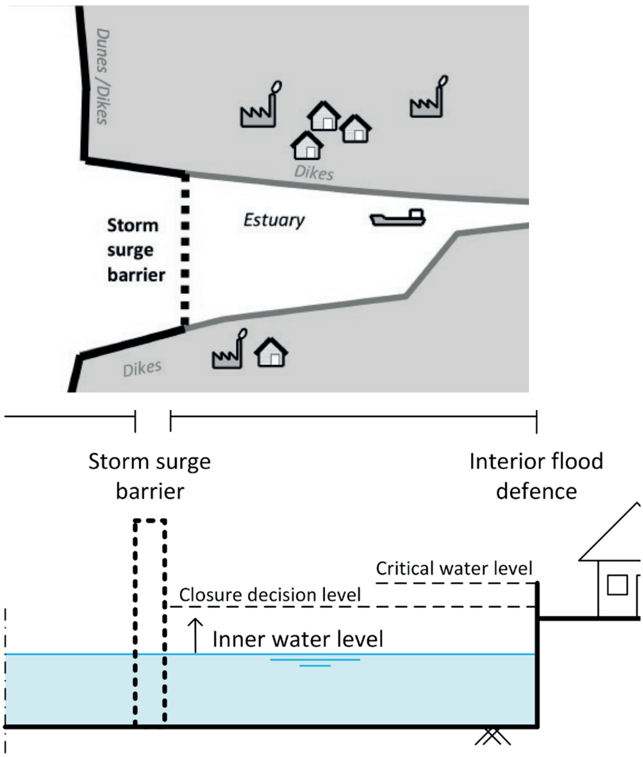

Figure 1.2: Schematic plan (top) and cross-section (bottom) of an estuary with a storm surge barrier as a coastal protection strategy. A storm surge barrier is open in normal conditions and, therefore, indicated with a dotted line. At the critical water level, interior flood defenses are expected to fail and result in a catastrophic flood. The closure decision level is a forecasted water level maximum at which a closure decision is taken. This level is below the critical water level to account for water level forecast errors, river inflow in the inner basin and local wind set-up.

Two main types of coastal barriers can be distinguished: closure dams and storm surge barriers. Closure dams permanently block an estuary or bay from the sea, preventing seawater from entering the newly formed lake and minimizing the risk of floods behind the dam. Typically, impounding an estuary with a closure dam creates a freshwater lake, which provides suitable conditions for agricultural expansion through land reclamation, although it negatively affects fisheries. Examples include the new polders built between 1930 and 1970 behind the Afsluitdijk (Closure Dam) in the Netherlands and the land reclamation project at Saegmungeum in South Korea. Closure dams often feature navigation locks and sluices for shipping and river runoff, respectively.

A storm surge barrier is a fully or partly moveable barrier that is temporarily closed to limit extreme water levels in the inner basin, thereby preventing a coastal flood. During normal conditions, the barrier is kept open to allow for tidal exchange and shipping. Table 1.1 presents an overview of storm surge barriers worldwide.

Table 1.1: overview of six storm surge barriers with the largest cumulative span – sum of the width of all openings – worldwide.

Storm surge barrier	Constr. year	Number of openings	Width of largest opening [m]	Gate type largest opening
Thames, London, UK	1982	10	61	Rotary segment
Eastern Scheldt, the Netherlands	1986	62	42	Vertical lift
Maeslant, the Netherlands	1997	1	360	Floating sector
Ems, Germany	2002	7	60	Rotary segment
St. Petersburg, Russia	2011	66	200	Floating sector
MOSE, Venice, Italy	2025	4	400	Flap

A storm surge barrier is closed using a predefined closure strategy. This strategy consists of closure criteria and control instructions. At all barriers except one [2], the most important closure criterion is the forecasted water level maximum, which in this thesis is referred to as the *closure decision level*. The closure decision level is below the critical water level of interior flood defenses to account for forecast errors, internal wind set-up, and river discharge accumulating behind the barrier (see Figure 1.2). Interior flood defenses consist of dikes, flood walls, and elevated land. The critical level is a certain water level at which the interior flood defenses are expected to fail and consequently result in a catastrophic flood.

2 The Ramspol barrier uses measured and not forecasted water levels to take a decision with respect to a closure.

The objective of the storm surge barrier is to prevent exceedance of the critical water level of the interior flood defenses. Three principal failure mechanisms can harm this objective (see Figure 1.3):

a) Operational failure: Mechanical, electrical, forecast, or control error resulting in a (partial) failure to open or close the barrier.
b) Structural failure: Collapse of the barrier structure due to instability, insufficient structural strength or seepage erosion.
c) Hydraulic overload: Despite successful barrier closure, water levels surpass the critical water level due to either excessive flow over and/or through the barrier, river flow accumulating behind the barrier, internal wind set-up, or a combination of these effects.

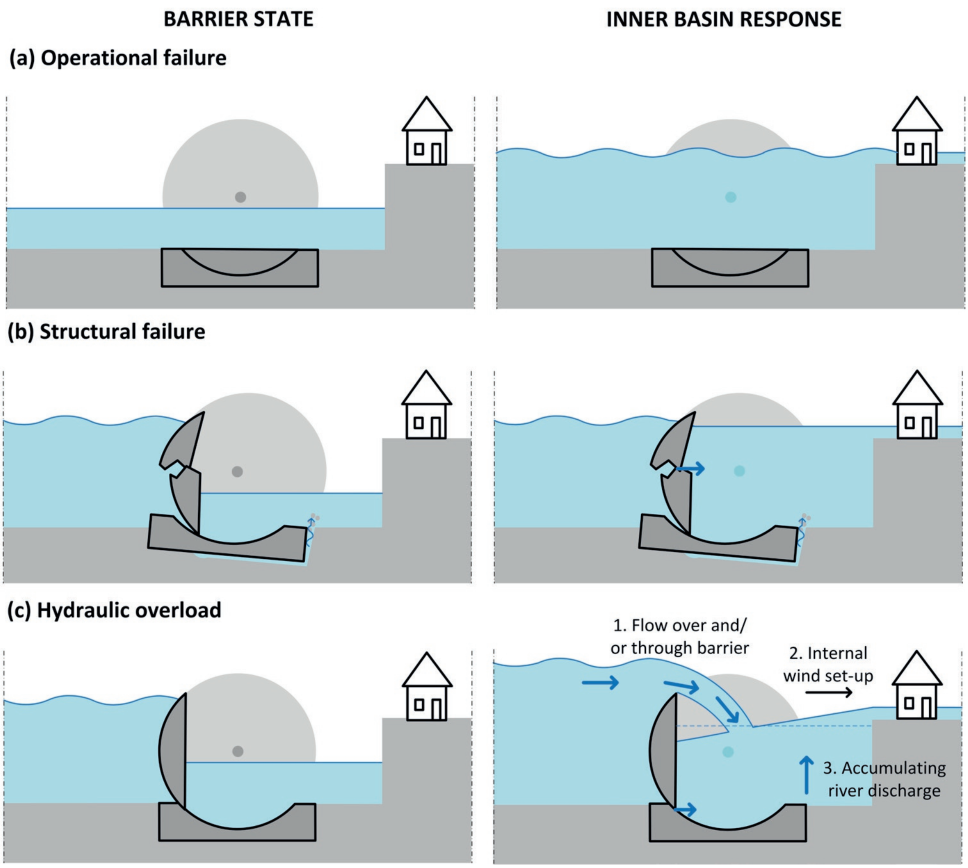

Figure 1.3: Principal system failure mechanisms. The left figure presents the barrier (failure) mode, while the right figure shows the corresponding inner basin response, which leads to exceedance of the critical water level.

This thesis is about reducing the susceptibility of operational failures, and more specifically the failure to close the barrier. In other words, this thesis is about improving closure reliability, that is, the annual frequency that the barrier successfully closes given severe storm conditions. If the barrier does not close in these severe storm conditions, the critical level is exceeded, resulting in interior flood defense failure and a coastal flood.

Closure reliability is crucial for storm surge barrier performance. Therefore, four Dutch storm surge barriers have legal requirements for the maximum probability of a failure to close. Chapter 2 demonstrates that a failure to close is the dominant failure mechanism of the Maeslant barrier. As the next section shows, this failure mechanism is important for other barriers as well. Thus, enhancing closure reliability at storm surge barrier flood protection systems is a promising approach for addressing rising flood risk.

1.2 Historic closure reliability assessment and improvement

The Hollandsche IJssel barrier (see Figure 1.4) is the oldest storm surge barrier, which was constructed quickly after the disastrous storm of 1953. Its initial assessment of closure reliability was relatively simple. Two movable gates, one behind the other,

Figure 1.4: Hollandsche IJssel barrier in 1983, source: beeldbank Rijkswaterstaat, photographer Bart van Eyk

could replace each other in case of a gate failure. Furthermore, by using vertical lift gates, there is no need for external electrical power, as the gate can close by gravity. They argue that such a barrier is as reliable as a closure dam with a shipping lock and sluices (Delta Committee, 1953). The barrier was completed in 1958, but the second gate was not installed until 1976 (Rijkswaterstaat, 1977).

An important development that influenced later closure reliability assessments of Dutch storm surge barriers is the introduction of acceptable annual frequencies of design water levels. These annual frequencies were assumed to be a good proxy for flood frequencies. For Central Holland, they proposed design water levels with an average return period of 10,000 years. For other regions, an average return period of 4,000 years was applied to account for the lower economic value of these regions (Delta Committee, 1960). Dams and dikes were then designed to resist this water level.

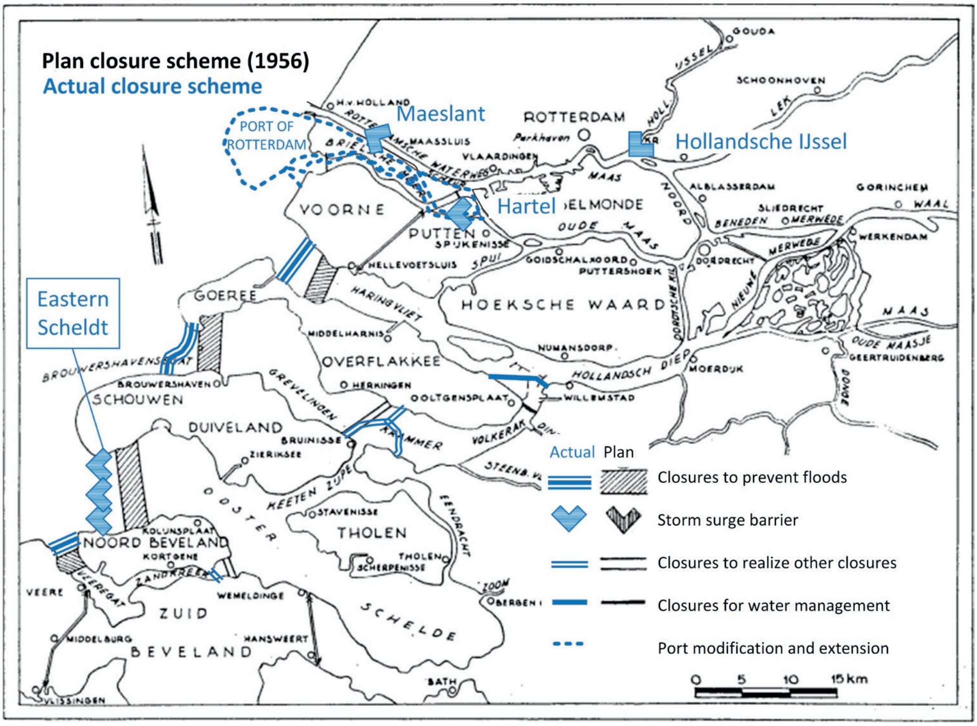

Figure 1.5: Schematic Deltaplan (Delta Committee, 1960) adapted in blue to indicate actual closure scheme. The Hollandsche IJssel barrier was the only storm surge barrier initially considered in the plan. It is constructed at the location indicated by the Delta Committee. The Deltaplan foresaw a closure dam at the Eastern Scheldt and dike raise along the New Waterway & Hartel canal, while storm surge barriers were realized here

In their original plan, the Delta Committee proposed dike reinforcements along important navigation routes (Rotterdam & Antwerp) and closure dams for other sea arms. Later, this plan was adapted to include more storm surge barriers (see Figure 1.5). At the Eastern Scheldt, not a closure dam but a storm surge barrier was constructed.

The design water level approach was not considered appropriate for the Eastern Scheldt barrier. First, because this approach did not account for a reverse load, that is, a scenario with high water levels in the Eastern Scheldt and low water levels on the North Sea. Second, because with the design water level approach, it is unclear how low the probability of a failure to close needs to be.

Therefore, the project goal was to achieve a maximum allowable flood frequency corresponding to the frequency of the design water level (Rijkswaterstaat, 1986). With this approach, the cumulative operational, structural and hydraulic overload failure frequency was designed to remain below the maximum flood frequency. Consequently, closure reliability was assessed probabilistically (TNO, 1980; KEMA, 1984) rather than pragmatically. Subsequently, this probabilistic approach was also implemented at the Maeslant and Hartel barriers.

Probabilistic closure reliability assessments are set up in a similar manner as probabilistic safety assessments of nuclear power plants, which are used to estimate the probability and/or frequency of significant radioactive releases (NUREG, 1975). Reliability experts conduct these assessments and describe a plant as a system with a certain functionality with respect to safety. These experts use fault and event trees to graphically represent how a combination of (lower level) failure events result in undesired outcomes (Paté-Cornell, 1984). Examples of these failure events are malfunctioning hardware and human errors. Reliability experts estimate probabilities of failure events, after which they use the fault or event tree to quantify the probability and/or frequency of significant radioactive releases. Probabilistic closure reliability assessments are similar but consider a coastal flood as an undesired outcome. From here onwards, this thesis refers to these probabilistic closure reliability assessments as reliability and availability analysis (RA analysis).

The Maeslant barrier, which was constructed between 1989 and 1997, has had the most issues with closure reliability. The Maeslant barrier is located at the entrance of the New Waterway and protects the cities of Rotterdam and Dordrecht against extreme storm surges. The barrier consists of two floating sector gates. When an extreme storm surge is expected, these gates float out from a dock and then sink down onto the bottom of the New Waterway (see Figure 1.6). When it is positioned,

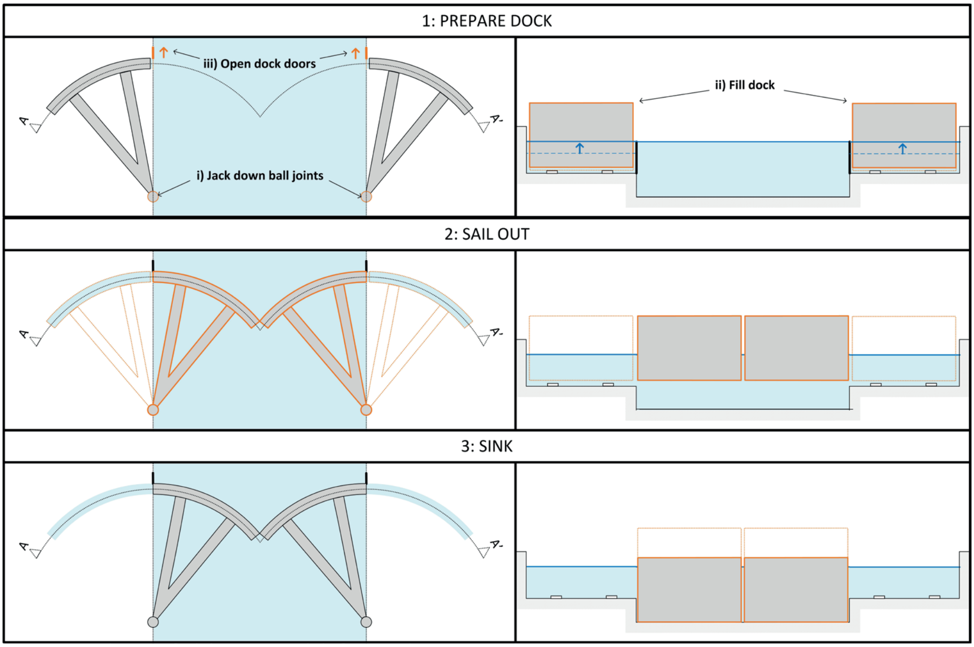

Figure 1.6: Schematic top view (left) and cross-section (right) of floating sector arms during three main closure procedure steps. Orange solid lines highlight gate parts that have moved during the main closure steps, and orange dotted lines indicate where the gate part was positioned in the previous step.

its structure needs to withstand the hydraulic forces given by the storm surge. In some storm scenarios, the barrier has to float again to release river discharge before it closes again. After this closure procedure, the barrier is floated and positioned back into the dock.

The design criterion for closure reliability was formulated as a maximum failure probability of 1/1000 on demand. The contractor used the design criterion to determine dimensions, types, and use of closure equipment. An important design decision which followed from the requirement was a completely automatic closure procedure to avoid failures due to human error (Bouwkombinatie Maeslant Kering, 1989).

Shortly after the delivery, experts within Rijkswaterstaat claimed that the maximum probability for a failed closure (<1/1000 on demand) was not achieved due to technical and organizational issues. In 2000, Rijkswaterstaat decided to redo the initial

RA analysis. NRG (2003) estimated the probability of a failed closure for the Maeslant barrier to be about 1/10 per closure request, which is a factor hundred lower than the initial design requirement.

Already early after the delivery, experts within Rijkswaterstaat claimed that the maximum probability of failed closure (<1/1000 on demand) was not met due to technical and organizational problems. In the year 2000, it was decided to redo the initial closure reliability assessment (van Akkeren, 2004). NRG (2003) found an estimated probability of a failed closure for the Maeslant barrier of about 1/10 per closure request and, thus, a 100 times lower than the design requirement.

There were two important reasons for the difference between the design assessment and that of NRG. In the design assessment, a total failure probability for all software tasks was estimated, while in the NRG analysis, a software failure probability per software task was determined. Already the minimum failure probability of a single task exceeded the design estimate for all software failures. Additionally, the design assessment assumed a high standard safety organization, which Rijkswaterstaat had not implemented. This led to different perspectives on many of the assumptions regarding the probability of failures.

Although it was possible to lower the probability of a failed closure, Rijkswaterstaat estimated that reaching the original design criterion (1/1000 on demand) was not possible based on the insights from the NRG analysis. Therefore, they investigated the possibility of lowering the criterion for the probability of failure on demand by analyzing the effect on critical water levels of interior flood defenses (HKV, 2006). The study showed that loosening the requirement for the probability of a failed closure to 1/100 on-demand only resulted in 6 to 12 kilometers of dike raise. Therefore, Rijkswaterstaat adopted this less stringent requirement.

To meet this new requirement, Rijkswaterstaat implemented two main improvements. First, it formalized the option of repairing or recovering hardware or software failures during operation. Second, it implemented risk-based asset management, referred to as ’ProBo’ by Rijkswaterstaat. Kharoubi et al. (2024) most eloquently describe how Rijkswaterstaat applied risk-based asset management at the Maeslant barrier and other Dutch storm surge barriers.

Still, barrier managers continue to have difficulties to meet the renewed requirement. Bi-annual assessments have often reported a probability of failure lower than 1/100 on demand (TNO, 2014; Rijkswaterstaat, 2022). Therefore, Rijkswaterstaat implemented a closure reliability improvement: an alternative control of the ballast system in case of failure. Still, reliability experts of Rijkswaterstaat claim the assessment misses important failure modes and has a too low quality to validate (Rijkswaterstaat, 2022).

While the issues with closure reliability are most persistent at the Maeslant barrier, other storm surge barriers have had issues with RA analyses as well.

The regional water authority Schieland & Krimpenerwaard (Dutch: Hoogheemraadschap Schieland & Krimpenerwaard) assessed the interior flood defenses of the Hollandsche IJssel barrier as insufficiently safe. At an early stage of the dike reinforcement project, the environmental impact assessment committee (EIA-committee, in Dutch: m.e.r.-commissie) advised against focusing solely on dike improvement and recommended considering enhancements to closure reliability as well (Hoogheemraadschap van Schieland en de Krimpenerwaard, 2020). In their subsequent advice, the EIA-committee remained unconvinced that dike improvement was necessary (M.e.r.-commissie, 2023b). In their final advice (M.e.r.-commissie, 2023a), they acknowledged the necessity of dike improvement but stressed that further study was needed for optimizing closure reliability.

Closure reliability is assessed at storm surge barriers in the UK and USA as well. At the storm surge barriers in New Orleans, these assessments were used to find closure reliability improvements that fit within the maintenance and operation budget and permitting requirements (Bowles et al., 2017). One of the gates of the IHNC barrier - the barge gate - requires more costly and drastic adaptation for reliable gate operation. Federal representatives (US Army Corps of Engineers) and local authority (Flood Authority East) struggle how to deal with this issue appropriately.

At the Thames, the Environment Agency and its partners have developed a plan to provide sufficient flood safety until 2100 (Environment Agency, 2023). As part of the plan, they are considering improvements to water level forecasting at the barrier. Moreover, they are investigating options to add and replace storm surge barriers in and along the Thames. However, from personal communication with local staff, it followed that upgrades of closure equipment could also be promising.

1.3 Literature review

Most research on storm surge barriers originates from their design stage. Much of this research is stored in large design archives and is highly specialized. For instance, research into the properties of a new material applied to storm surge barriers. van Oorschot and Wijmans (1979) published a study regarding information systems, which exemplifies such specialized research. More general information is found in barrier design summaries published in professional journals and conference proceedings (de Bruijn, 1955; Jonker, 1955; Cordes et al., 1972; Horner, 1979; Fleming et al., 1980; Gerrard et al., 1983; Tappin et al., 1984; Janssen et al., 1994; Daniel, 1996; Starke and Wolff, 2000). For the Thames and Eastern Scheldt barrier, more comprehensive design notes are available (Institution of Civil Engineers, 1978; Rijkswaterstaat, 1986). Recent scientific publications (Christian et al., 2015; Davlasheridze et al., 2019; Chen et al., 2020; Kirshen et al., 2020; Rasmussen et al., 2023; Jonkman and Merrell, 2024) can be associated with plans to construct a storm surge barrier near Houston, Texas, and other projects in the USA. All the design considerations from these documents provide valuable background information for adapting barriers. Furthermore, these documents reveal that while these structures serve similar functions, they possess many distinct physical properties, such as their gate types. This storm surge barrier literature has two key issues: 1) the research pertains to individual barriers and cannot be directly applied to others, and 2) the research focuses on the design stage rather than enhancing existing barriers.

Most research on storm surge barriers originates from their design stage. The majority of this research is stored in huge design archives and is highly specific. For instance, a research into the properties of a new material applied at the storm surge barrier. Some of this specific research was published in a scientific journal (van Oorschot and Wijmans, 1979). More general information is found in barrier design summaries, published in professional magazines and conference proceedings (de Bruijn, 1955; Jonker, 1955; Cordes et al., 1972; Horner, 1979; Fleming et al., 1980; Gerrard et al., 1983; Tappin et al., 1984; Janssen et al., 1994; Daniel, 1996; Starke and Wolff, 2000). For the Thames and Eastern Scheldt barrier, more extensive design notes are available (Institution of Civil Engineers, 1978; Rijkswaterstaat, 1986). More recent scientific publications (Christian et al., 2015; Davlasheridze et al., 2019; Chen et al., 2020; Kirshen et al., 2020) can be associated with plans to construct a storm surge barrier near Houston (TX, USA). All the design considerations from these documents provide useful background information for adapting barriers. However, this storm surge barrier literature has two main issues: 1) the research is specific to an individual barrier and cannot directly be applied at others and 2) the research concerns the design stage rather than enhancing existing barriers.

Mooyaart and Jonkman (2017) studied storm surge barriers more generally. They explain their role in the flood protection system and address important design considerations for them. Orton et al. (2023) present a research agenda on estuary impacts by storm surge barriers. While these studies are more general, they also do not address how to enhance existing barriers.

Other research investigates when storm surge barriers need to be replaced. Haasnoot et al. (2013) propose to analyze different pathways, with each pathway corresponding to significant system changes, such as removing a storm surge barrier and transforming inner basins from saline to freshwater systems. De Bruijn et al. (2022) and Rijcken et al. (2023) looked more specifically at the Rhine-Meuse Delta and investigated the option to lower the probability of failure by more than a factor ten by replacing or adding a barrier, respectively. Vader et al. (2022) assessed the end of the lifetime of the Hollandsche IJssel barrier. These studies only consider the period after the end of their lifetime; they do not explore how to adapt barriers during their operational lifespan.

Adapting maintenance and operations has been extensively researched in the scientific field of safety-critical objects. Safety-critical objects must address low-probability, high-consequence risks, such as nuclear power plants. The book by Moubray (1997) is renowned for identifying effective maintenance actions for these objects. Guidelines by Rijkswaterstaat (2011, 2018) for the maintenance and operation of storm surge barriers derive from this scientific domain (Kharoubi et al., 2024). Consequently, these guidelines often remain abstract and lack specificity regarding storm surge barriers. For example, when implementing asset management practices at Rijkswaterstaat facilities, a functional analysis is suggested, but without a concrete example pertaining to a storm surge barrier. Therefore, it is uncertain how to establish and quantify the performance of a storm surge barrier. This knowledge gap complicates the application of maintenance and operational insights from other safety-critical objects specifically to storm surge barriers.

Moreover, there is a lack of knowledge on how to establish closure reliability requirements. Currently, four Dutch storm surge barriers have such a requirement: the Maeslant barrier, Hollandsche IJssel barrier, Hartel barrier, and Ramspol barrier. For the Maeslant barrier, this requirement is based on an extensive study that is over

20 years old (HKV, 2006). The closure reliability requirements for other barriers are based on expert judgment (Ministerie van Infrastruur en Milieu, 2016). As a simple and better-supported method is absent, it is unclear whether closure requirements should be updated to response to rising flood risk and if so, how.

Academically, the question of "how safe is safe enough" has been studied for decades. Specifically, regarding coastal defense structures, van Dantzig (1956); Vrijling (2001); Eijgenraam et al. (2014); Kind (2014); Jonkman et al. (2011) and Dupuits et al. (2017) have proposed methods to establish coastal flood safety standards. Their approach seeks to find the economic optimum between investments in flood defenses and the associated coastal flood risk. This economic optimum is then used to define a flood safety standard. However, these studies have only considered dikes and coastal dams as flood defense investments and have not included closure reliability improvements when setting flood safety standards. Thus, the knowledge gap lies in determining the economically optimal closure reliability requirements.

Other researchers have investigated topics related to closure reliability. Walraven et al. (2022) describe the design, maintenance, and operation of barriers. They suggest that learning from the maintenance and operation practices of existing barriers can help to adapt them. They also point out that due to the infrequent use of storm surge barriers, acquiring knowledge is challenging. Kamps et al. (2024a, b) discuss how to preserve and enhance knowledge among staff working on storm surge barriers. Trace-Kleeberg et al. (2023) examine how rising sea levels reduce maintenance windows at the Maeslant barrier, which – without countermeasures – would lead to a higher probability of a failure to close. Ponsioen et al. (2023) investigate the use of digital twins to improve the maintenance and operation of storm surge barriers. (Bakker et al., 2025) explore the impact of multi-peak storms and clustered storm surges on the likelihood of a closure failure. All of this research effectively demonstrates that many closure reliability improvements are possible.

However, there are many more options to improve the operational reliability of storm surge barriers. These options differ in various aspects, including size (replacement of the barrier or its components), type (human, software, hardware), and location (at the barrier or within interior flood defenses). Given the large number of options, identifying effective improvements in closure reliability poses a challenge, and a method for addressing this issue is currently unavailable.

1.4 Research questions

The main research question addressed in this dissertation is:

Main research question

> ***How can closure reliability of existing storm surge barriers be systematically assessed and improved to enhance coastal flood protection?***

The literature review revealed that a framework is missing for identifying, evaluating, and prioritizing coastal flood risks in areas protected by storm surge barriers. Consequently, it is difficult to apply knowledge from other safety-critical objects to storm surge barriers. Moreover, it is challenging to determine the significance of closure reliability. Thus, this dissertation addresses the following sub-question:

Sub-question chapter 2

> ***How to determine the importance of closure reliability relative to other main failure mechanisms (structural failure and hydraulic overload) for storm surge barriers?***

Next, no method was found to determine how to establish economically optimal closure reliability requirements. Therefore, Chapter 3 treats the following sub-question:

Sub-question chapter 3

> ***How to determine an economically optimal requirement for closure reliability?***

As explained in the literature review, there are a lot of options to improve closure reliability. A method is lacking to consider these options systematically. Therefore, chapter 4 responds to this sub-question:

Sub-question chapter 4

> ***How to find and select closure reliability improvements without overlooking important ones?***

When improvements in closure reliability are identified, their impact has to be quantified by refining the current RA analysis. Modifying such an analysis is not always straightforward; therefore, the concluding chapter addresses the following sub-question:

Sub-question chapter 5

> ***How can the RA analysis be refined to address identified improvements in closure reliability?***

1.5 Research approach

The research is organized from coarse to fine (see Figure 1.7). First, it starts at the flood protection system level, investigating the role of barrier failure mechanisms on coastal flood risk. Then, closure reliability is looked into and balanced with dike raise and monetized coastal flood risk. The last part investigates how to lower the probability of a failure to close.

To answer the sub-questions, each chapter proposes a method that is evaluated using the Maeslant barrier as a case study. For each method, a good-quality RA analysis is assumed to be available. These methods are based on existing methods and then tailored and adapted to answer the sub-question.

Chapter 2 presents a method to prioritize barrier failure mechanisms based on their impact on extreme water level maxima at interior flood defenses. This method uses descriptions, experiences, and results from HydraNL (HKV, 2011) and Prestatiepeilen models (Rijkswaterstaat, 2008). The chapter clarifies how these models work and explains how they can be applied to assess storm surge barriers instead of interior flood defenses.

Chapter 3 presents an economic optimization model – also known as a cost-benefit analysis - that balances improvements in closure reliability with monetized flood risk and dike raise. The dike raise economic optimization model by van Dantzig (1956) is extended to include closure reliability enhancements. Based on this balance, the economically optimal closure reliability requirements are determined.

Chapter 4 proposes a three-stage screening method to select the top 5 performance improvements from a checklist of 85 principal performance improvements. This method uses useful elements from well-developed risk assessment methods (e.g., FMECA, HAZOP). Moreover, an existing RA analysis establishes the effect of closure reliability improvements on the probability of a failure to close.

Chapter 5 introduces a method to screen how the model can be effectively refined while considering implementing a performance improvement. This method describes and uses current practices regarding RA analyses.

Chapter 6 concludes the dissertation. Moreover, this chapter reflects on current flood risk management in the Netherlands based on the newly developed knowledge in this thesis.

1.6 Programmatic network

This research was part of a programmatic network of research on Storm Surge Barriers, aiming at developing knowledge on asset management of storm surge barriers. Ponsioen et al. (2023) developed and tested a prototype of a digital twin for the Maeslant barrier to evaluate the feasibility of using digital twins in storm surge barriers. Kharoubi et al. (2024) analyzed the risk-based asset management of Dutch storm surge barriers. Kamps et al. (2024a, b) investigated the knowledge necessary for maintaining a storm surge barrier. Van Gijzen and Bakker (2023) examined the significance of pump reliability and availability for the pump station at IJmuiden. Together with this thesis this work increases the body of knowledge on storm surge barriers.

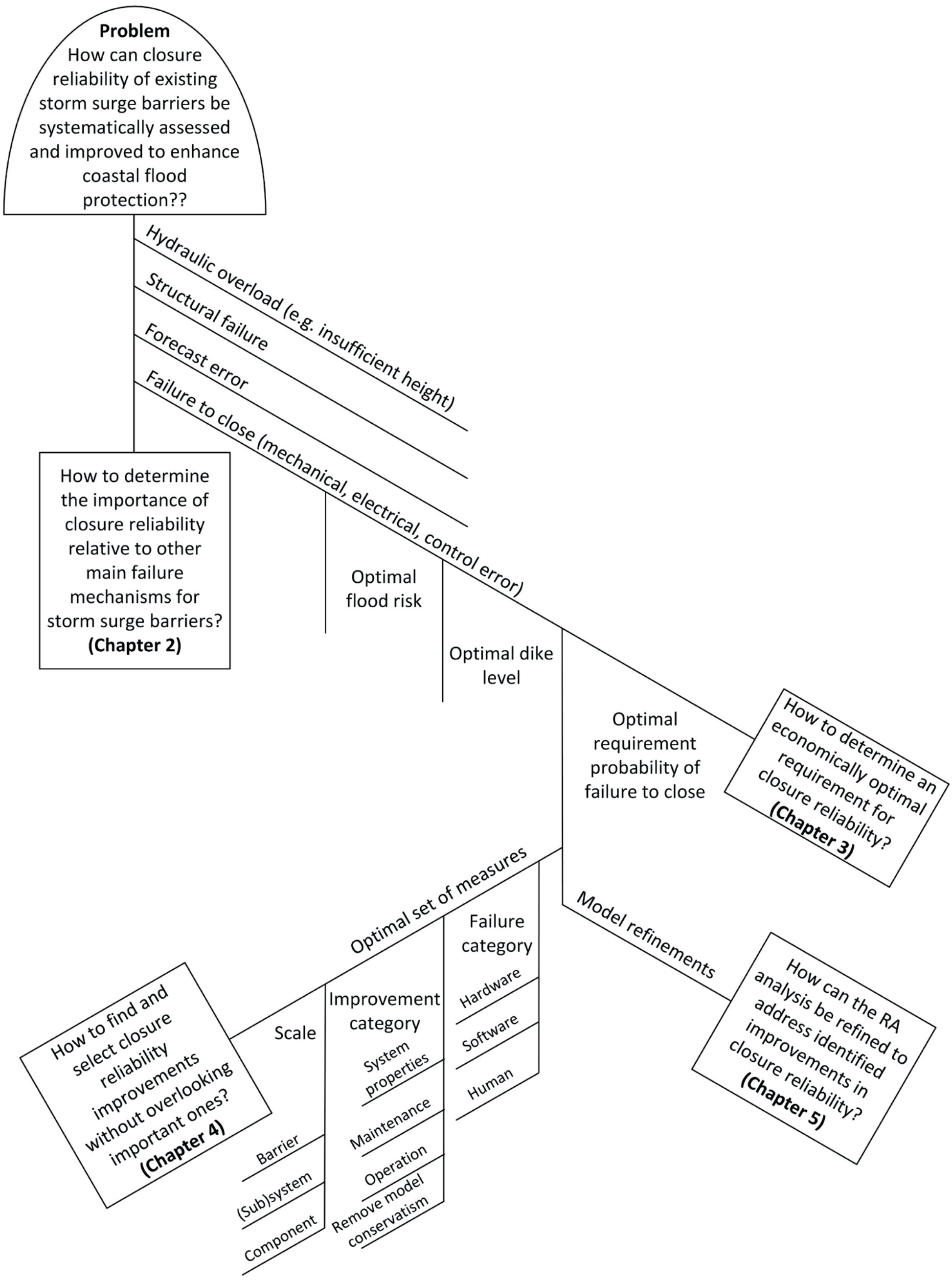

Figure 1.7: Fish-bone diagram presenting the trade-offs which each chapter investigates to answer the research sub-questions

1.7 References

Bakker, A. M., Rovers, D. L., and Mooyaart, L. F. (2025). Storm Surge Clusters, Multi-Peak Storms and Their Effect on the Performance of the Maeslant Storm Surge Barrier (The Netherlands). *Journal of Marine Science and Engineering*, 13(2).

Bouwkombinatie Maeslant Kering (1989). Sector gate barrier, design documents (Dutch: Sectordeur-kering, document ontwerp deel 1 en 2). Technical report, Rijkswaterstaat Directie Sluizen en Stuwen.

Bowles, D. S., Moore, D., Turner, R., and Chauhan, S. S. (2017). Risk assessment of the New Orleans Hurricane Storm Damage Risk Reduction System complex closure structures. *2017 ASDSO - Dam Safety, Conference Proceedings*, (November):403–424.

Calafat, F. M., Wahl, T., Tadesse, M. G., and Sparrow, S. N. (2022). Trends in Europe storm surge extremes match the rate of sea-level rise. *Nature*, 603(7903):841–845.

Chen, Z., Orton, P., and Wahl, T. (2020). Storm surge barrier protection in an era of accelerating sea-level rise: Quantifying closure frequency, duration and trapped river flooding.

Christian, J., Fang, Z., Torres, J., Deitz, R., and Bedient, P. (2015). Modeling the Hydraulic Effectiveness of a Proposed Storm Surge Barrier System for the Houston Ship Channel during Hurricane Events. *Natural Hazards Review*, 16(1):04014015.

Cordes, F., Fedder, H., and Albrecht, U. (1972). Der Wehrtrager des Eidersperrwerkes [Water retaining beams at the Eider barrier]. *Beton- und stahlbetonbau*, 67(10):217–228 (in German).

Daniel, R. (1996). Hartelkering - Schuiven met mogelijkheden [Hartel barrier - gates with possibilities]. *Bouwen met staal*, (130):38–45.

Davlasheridze, M., Atoba, K. O., Brody, S., Highfield, W., Merrell, W., Ebersole, B., Purdue, A., and Gilmer, R. W. (2019). Economic impacts of storm surge and the cost-benefit analysis of a coastal spine as the surge mitigation strategy in Houston-Galveston area in the USA. *Mitigation and Adaptation Strategies for Global Change*, 24(3):329–354.

De Bruijn, K. M., Diermanse, F. L., Weiler, O. M., De Jong, J. S., and Haasnoot, M. (2022). Protecting the Rhine-Meuse delta against sea level rise: What to do with the river's discharge? *Journal of Flood Risk Management*, 15(3):1–15.

de Bruijn, M. (1955). A flood protection in the estuary of the Hollandse IJssel near Krimpen. (Dutch: Een stormvloedkering aan de mond van de Hollandse IJssel bij Krimpen a/d IJssel). *De Ingenieur*, 67(21):B.67 – B.76.

Delta Committee (1953). Afsluiting van de Hollandse IJssel, Toelichting op het 2e interim-advies van de Deltacommissie. Technical report, Rijkswaterstaat.

Delta Committee (1960). Eindverslag en interimadviezen. *Rapport Deltacommissie*, Deel 1:15.

Dupuits, E. J., Schweckendiek, T., and Kok, M. (2017). Economic optimization of coastal flood defense systems. *Reliability Engineering and System Safety*, 159(October 2016):143–152.

Eijgenraam, C., Kind, J., Bak, C., Brekelmans, R., Den Hertog, D., Duits, M., Roos, K., Vermeer, P., and Kuijken, W. (2014). Economically efficient standards to protect the Netherlands against flooding. *Interfaces*.

Environment Agency (2023). What needs to be done across the estuary (outcomes): Thames Estuary 2100.

Fleming, J., McMillan, P., and Williams, B. (1980). The River Hull Tidal Surge Barrier. In *Institution of Civil Engineers, Part 1*, pages 417–454.

Gerrard, R., Long, J., and Shah, H. (1983). Barking Creek Tidal Barrier. *Proceedings of the Institution of Civil Engineers*, 74(3):525–541.

Haasnoot, M., Kwakkel, J. H., and Walker, W. E. (2013). Dynamic adaptive policy pathways: A method for crafting robust decisions for a deeply uncertain world. *Global Environmental Change*, 23(2):485–498.

Hallegatte, S., Green, C., Nicholls, R. J., and Corfee-Morlot, J. (2013). Future flood losses in major coastal cities. *Nature Climate Change*, 3(9):802– 806.

HKV (2006). Achterlandstudie Maeslantkering, Hydra-B. Technical report.

HKV (2011). Hydra-Zoet for the fresh water systems in the Netherlands Probabilistic model for the assessment of dike heights. Technical Report December.

Hoogheemraadschap van Schieland en de Krimpenerwaard (2020). Notitie Reikwijdte en Detailniveau. MER Fase 2. Technical report.

Horner, R. W. (1979). The Thames Barrier Project. *The Geographical Journal*, 145(2):242–253.

Institution of Civil Engineers (1978). Thames Barrier Design. In Harding, B., editor, *Proceedings of the conference held in London on 5 October, 1977*, pages 1–202, London. T. Telford.

Janssen, J., van Ieperen, A., Kouwenhoven, B., Nederend, J., Pruijssers, A., and de Ridder, H. A. (1994). The design and construction of the New Waterway storm surge barrier in the Netherlands. In *28th PIANC World Congress - Seville, Spain*, Seville.

Jonker, L. (1955). Stormvloedkering in de Hollandsche IJssel nabij Krimpen. *Weg en Waterbouw*, (1-2):22–26.

Jonkman, S. N., Jongejan, R., and Maaskant, B. (2011). The Use of Individual and Societal Risk Criteria Within the Dutch Flood Safety Policy Nationwide Estimates of Societal Risk and Policy Applications. *Risk Analysis*, 31(2):282–300.

Jonkman, S. N. and Merrell, W. J. (2024). Discussion of “Coastal Defense Megaprojects in an Era of Sea-Level Rise: Politically Feasible Strategies or Army Corps Fantasies?”. *Journal of Water Resources Planning and Management*, 150(4).

Kamps, M., van den Bogaard, J., Van den Boomen, M., and Hertogh, M. (2024a). Knowledge Continuity Aspects in Designs and Contracts of Dutch Storm Surge Barriers. *European Conference on Knowledge Management*, 25(1):342–350.

Kamps, M., van den Boomen, M., van den Bogaard, J., and Hertogh, M. (2024b). Intergenerational transfer of engineering expertise: knowledge continuity management in storm surge barrier engineering. *Built Environment Project and Asset Management*.

KEMA (1984). Analysis of the operating system of the gates of the storm surge barrier in the Easter Scheldt (Dutch: Analyse van het bewegingssysteem voor de schuiven van de stormvloedkering in de Oosterschelde). Technical report, Rijkwaterstaat Direktie Bruggen.

Kharoubi, Y., van den Boomen, M., van den Bogaard, J., and Hertogh, M. (2024). Asset management for storm surge barriers: how and why? *Structure and Infrastructure Engineering*, 0(0):1–15.

Kind, J. M. (2014). Economically efficient flood protection standards for the Netherlands. *Journal of Flood Risk Management*.

Kirshen, P., Borrelli, M., Byrnes, J., Chen, R., Lockwood, L., Watson, C., Starbuck, K., Wiggin, J., Novelly, A., Uiterwyk, K., Thurson, K., McMann, B., Foster, C., Sprague, H., Roberts, H. J., Bosma, K., Jin, D., and Herst, R. (2020). Integrated assessment of storm surge barrier systems under present and future climates and comparison to alternatives: a case study of Boston, USA. *Climatic Change*, 162(2):445–464.

M.e.r.-commissie (2023a). Krachtige IJsseldijken Krimpenerwaard, Toetsingsadvies over het milieueffectrapport en de aanvulling daarop. Technical report.

M.e.r.-commissie (2023b). Krachtige IJsseldijken Krimpenerwaard, voorlopig toetsingsadvies over het milieueffectrapport. Technical report.

Ministerie van Infrastruur en Milieu (2016). Factsheets flood safety standards primary flood defences (Dutch: Factsheets normering primaire waterkeringen). Technical report.

Mooyaart, L. F., Bakker, A. M., van den Bogaard, J. A., Jorissen, R. E., Rijcken, T., and Jonkman, S. N. (2025). Storm surge barrier performance—The effect of barrier failures on extreme water level frequencies. *Journal of Flood Risk Management*, 18(1):1–17.

Mooyaart, L. F., Bakker, A. M. R., van den Bogaard, J. A., Rijcken, T., and Jonkman, B. (2023). Economic optimization of coastal flood defence systems including storm surge barrier closure reliability. *Journal of Flood Risk Management*, 16(3).

Mooyaart, L. F. and Jonkman, S. N. (2017). Overview and Design Considerations of Storm Surge Barriers. *Journal of Waterway, Port, Coastal, and Ocean Engineering*, 143(4):06017001.

Moubray, J. (1997). *Reliability-centred Maintenance*. Biddles LtD, Guildford & King's Lynn, 2nd edition.

NRG (2003). Betrouwbaarheidsanalyse OKE. Technical report, Arnhem.

NUREG (1975). Reactor safety study – an assessment of accident risks in U.S. Commercial Nuclear Power Plants, WASH 1400, NUREG 75/014. Technical report.

Orton, P., Ralston, D., van Prooijen, B., Secor, D., Ganju, N., Chen, Z., Fernald, S., Brooks, B., and Marcell, K. (2023). Increased Utilization of Storm Surge Barriers: A Research Agenda on Estuary Impacts. *Earth's Future*, 11(3).

Paté-Cornell, M. E. (1984). Fault Trees vs. Event Trees in Reliability Analysis. *Risk Analysis*, 4(3):177–186.

Ponsioen, L., Jonkman, S., Bakker, A., and Nederend, J. (2023). Investigation and development of a Digital Twin for the Maeslant barrier: Exploring the application of digital twins in the maintenance and operation of storm surge barriers. Technical report, Delft University of Technology, Delft.

Rasmussen, D. J., Kopp, R. E., and Oppenheimer, M. (2023). Coastal Defense Megaprojects in an Era of Sea-Level Rise: Politically Feasible Strategies or Army Corps Fantasies? *Journal of Water Resources Planning and Management*, 149(2):1–14.

Rijcken, B. T., Mooyaart, L., Oerlemans, C., Ziel, F. V. D., Borghans, J., Botterhuis, T., Winden, A. V., Jorissen, R., and Kok, M. (2023). It takes two to tango with Sea level rise. *TU Delft DeltaLinks*, pages 1–16.

Rijkswaterstaat (1977). De tweede schuif voor de beweegbare stormvloedkering in de Hollandse IJssel. *Driemaandelijkse berichten Deltawerken*, (79):497–502.

Rijkswaterstaat (1986). Ontwerpnota Oosterscheldekering [Design documents Eastern Scheldt barrier]. Technical report.

Rijkswaterstaat (2008). Performance levels Eastern Scheldt, continuation (Dutch: Prestatiepeilen Oosterschelde, vervolg). Technical report.

Rijkswaterstaat (2011). Guideline Risk based asset management according to the ProBo approach (Dutch: Leidraad Risicogestuurd Beheer en Onderhoud conform de ProBo werkwijze). Technical report.

Rijkswaterstaat (2018). Manual performance-based risk analyses PRA (Dutch: Handreiking prestatiegestuurde risicoanalyses PRA). Technical report

Rijkswaterstaat (2022). Legislated assessment Europoort barrier (Dutch: Wettelijke beoordeling Europoortkering I Dijktraject 208). Technical report.

Small, C. and Nicholls, R. J. (2003). A global analysis of human settlement in coastal zones. *Journal of Coastal Research*, 19(3):584–599.

Starke, W.-D. and Wolff, R. (2000). Das Emssperrwerk und seine Verschlüsse [Ems barrier and its closures]. *Stahlbau*, 69(12):974–980 (in German).

Tappin, R. G. R., Dowling, P. J., and Clark, P. J. (1984). Design and model testing of the Thames Barrier gates. In *Ordinary Meeting of the Institution of Structural Engineers*, number 4, pages 115–124.

TNO (1980). Failure probability analysis of the Eastern Scheldt barrier (Dutch: Faalkans-analyse van de Oosterschelde Stormvloedkering). Technical report, Rijkswaterstaat Deltadienst, Delft.

TNO (2014). De stormvloedkeringen in Nederland en de toepassing van de ProBO. Technical report.

Trace-Kleeberg, S., Haigh, I. D., Walraven, M., and Gourvenec, S. (2023). How should storm surge barrier maintenance strategies be changed in light of sea- level rise? A case study. *Coastal Engineering*.

Vader, H., Bakker, A. M., Jonkman, S. N., van den Boomen, M., van Baaren, E., and Diermanse, F. L. (2022). A framework for assessing the remaining life of storm surge barriers. *Journal Structure and Infrastructure Engineering*, 20(12):2022–2034.

van Akkeren, K. (2004). Results As-Wished risk analysis and design water level model Europort barrier (Dutch: Resultaten As–Wished Risicoanalyse en MHW model Europoortkering) [PowerPoint presentation].

van Dantzig, D. (1956). Economic decision problems for flood protection. *Econometrica*, 24(3):276–287.

van Gijzen, L. and Bakker, A. M. (2023). Determining the future functional requirements of a pumping-weir station with the help of data-analysis. *Life-Cycle of Structures and Infrastructure Systems - Proceedings of the 8th International Symposium on Life-Cycle Civil Engineering, IALCCE 2023*, pages 2612–2619.

van Oorschot, J. and Wijmans, W. (1979). An Information System on Environmental Conditions for the Construction and Operation of a Storm-Surge Barrier. *IEEE Journal of Oceanic Engineering*, 4(2):40–45.

Vrijling, J. K. (2001). Probabilistic design of water defense systems in the Netherlands. *Reliability Engineering and System Safety*, 74(3):337–344.

Walraven, M., Vrolijk, K., and Kothuis, B. B. (2022). *Design, maintain and operate movable storm surge barriers for flood risk reduction*. Elsevier Inc.

2

The importance of closure reliability relative to other barrier failure mechanisms[2]

2 This chapter was published in the Journal of Flood Risk Management, Issue 18, volume 1 with the title: "Storm surge barrier performance – the effect of barrier failures on extreme water level frequencies"

As explained in the introduction, there are three main failure mechanisms: operational failure, structural failure, and hydraulic overload. Improvements in closure reliability reduce susceptibility to operational failures. The effectiveness of these improvements depends on the importance of other failure mechanisms. Although there are advanced methods for each failure mechanism individually, an overarching method that integrally evaluates these main failure mechanisms is lacking.

Therefore, this chapter presents a method to compare storm surge barrier failure mechanisms by comparing their effect on extreme water levels behind the barrier.

The literature review is presented in Section 2.1. Section 2.2 explains how storm surge barriers work and fail. Section 2.3 outlines the method for quantifying storm surge barrier performance in relation to the frequency of extreme water levels behind the barrier. Section 2.4 applies this method to a case study: Rotterdam and the Maeslant barrier. Sections 2.5 and 2.6 discuss and conclude the chapter, respectively.

Introduction

Storm surge barriers are an important type of coastal flood protection as they protect coastal cities such as London (UK), New Orleans (USA) and Rotterdam (The Netherlands). These large barriers mitigate flood disasters by closing during storm surges while allowing tidal movements and navigation during normal conditions (Mooyaart & Jonkman, 2017).

Storm surge barriers are part of a larger flood protection system, which consists of an inner basin and interior flood defenses. These interior flood defenses are constituted of elevated land, flood walls and dikes, the latter which are also referred to as embankments (UK) and levees (USA). Figure 2.1 presents a principal cross-section of this flood protection system. At the critical water level, interior flood defenses are expected to fail and result in a catastrophic flood.

The role of the storm surge barrier is to prevent extreme water levels in the inner basin which exceed the critical water level of the interior defenses. Thus, the more often a storm surge barrier averts exceedances of the critical water level, the better it performs. The exceedance frequency of extreme water levels is referred to as

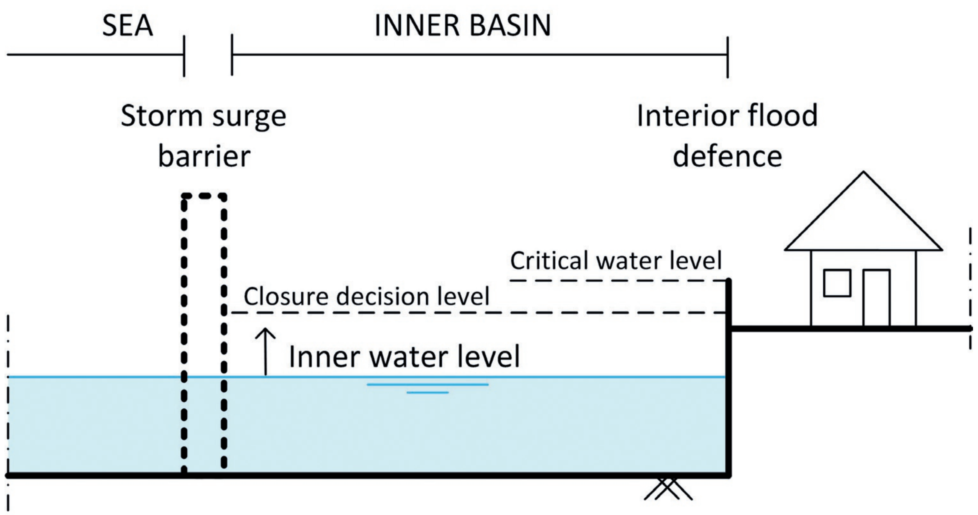

Figure 2.1: Schematic cross-section indicating the elements of a storm surge barrier flood protection system. A storm surge barrier is open in normal conditions and, therefore, indicated with a dotted line. At the interior flood defense, the critical water level is assumed to be equal to the crest level for visual clarity. The closure decision level is below the critical water level to account for water level forecast errors, the river gradient and local wind set-up.

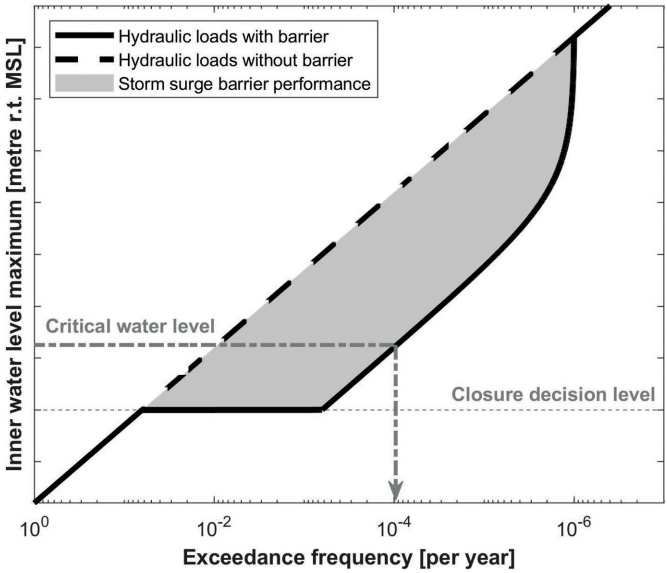

Figure 2: Schematic relations of exceedance frequencies of extreme water level maxima with and without a storm surge barrier based on the Maeslant barrier (Rotterdam, Netherlands), aiming at explaining the concept of "storm surge barrier performance". The method and case study describe how the hydraulic loads with a barrier are developed. Figure 2.12 presents how barrier failure mechanisms contribute to these hydraulic loads.

hydraulic loads. Storm surge barrier performance is defined as the difference between the hydraulic loads with and without the barrier (see Figure 2.2).

Three principal failure mechanisms determine the efficacy of the flood protection system with a storm surge barrier (see Figure 2.3):

1. **Operational failure**: Incorrect closing or opening of the barrier due to forecasting, mechanical, electrical and/or control errors.

2. **Structural failure**: Collapse of the barrier causing uncontrolled water flow.

3. **Hydraulic overload**: Despite successful barrier closure, water levels surpass critical water levels due to either excessive flow over and/or through the barrier, river flow accumulating behind the barrier, internal wind setup or a combination of these effects (see Figure 2.3).

Mooyaart et al. (2023) show that sea level rise motivates substantial investments into storm surge barrier performance in the future. Moreover, Trace-Kleeberg et al.

(2023) demonstrate the negative influence of sea level rise on the number and length of maintenance windows. This is expected to make operational failures more likely without additional measures. To determine the effectiveness of investments into storm surge barrier performance, there is a need for a method which systematically addresses all system failure mechanisms and their effect on storm surge barrier performance.

Recent scientific literature on storm surge barrier performance is usually restricted to only one or sometimes two of the three principal failure mechanisms. Christian et al. (2015) and Schlumberger et al. (2021) analyze the effect a barrier has on water levels behind the barrier. They analyze a recent event with some small alterations to that

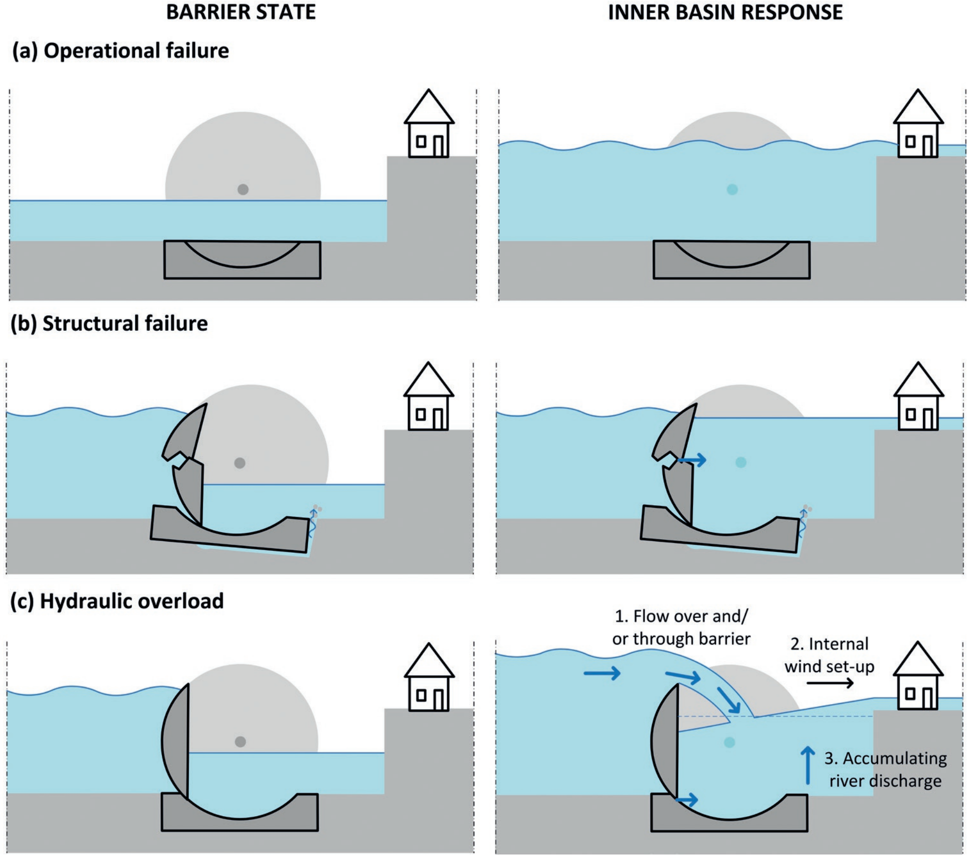

Figure 2.3: Principal system failure mechanisms. The left figure presents the barrier (failure) mode, while the right figure shows the corresponding inner basin response, which leads to exceedance of the critical water level.

event, without discussing the frequencies of these events. Gouldby & Sayers (2009) assess flood risk behind the Thames Barrier probabilistically, but neglect barrier failures. Vader et al. (2022) argue that structural and hydraulic overload are irrelevant for their case and, therefore, only consider operational barrier failure quantitatively. Zhong et al. (2012), Diermanse et al. (2015) and De Bruijn et al. (2022) include both operational failures and hydraulic overload due to river discharge. Their approach is also being used to determine loads for interior flood defenses in the Netherlands (Geerse, 2010). Dupuits et al. (2017) and van Berchum et al. (2019) optimize barrier flood protection systems taking into account structural failures and hydraulic overload due to barrier overflow. None of these authors consider both structural and operational failure mechanisms.

To our knowledge, the three principal failure mechanisms have only been jointly considered in design and assessment reports (Rijkswaterstaat, 1986; 2022) and a conference paper by Janssen & Jorissen (1992). The model they present is, however, difficult to reproduce, verify and apply to other barriers. As a result, it is unclear how barrier failure mechanisms influence storm surge barrier performance. Thus, there is no systematic method to evaluate the relative importance of the three principal failure mechanisms (operational failure, structural failure, hydraulic overload).

This chapter presents a probabilistic method that evaluates storm surge barrier performance by considering all three principal failure mechanisms and the uncertainties inherent in extreme events predictions. Our method is applied to the Maeslant barrier in Rotterdam (The Netherlands) providing insight into optimizing flood protection measures.

The chapter is structured as follows: Section 2 describes barrier operation and possible failures. Section 3 introduces the method to establish hydraulic loads and storm surge barrier performance. Section 4 applies the method to the Maeslant barrier (Rotterdam, Netherlands) followed by discussions and conclusions in Section 5 and 6.

Barrier operation and failure

Barrier operation

Each storm surge barrier has two distinct modes of operation: 1) the barrier is open under normal conditions and 2) the barrier closes in case a critical high water level is forecasted. In the first mode of operation, the barrier is maintained and tested (see Kharoubi et al. (2024) for more information on asset management of these type of structures), usually taking into account seasons with a lower risk of severe weather events (Trace-Kleeberg et al., 2023).

For the second mode, storm surge barrier managers use a predefined closure strategy to operate the barrier. This strategy consists of closure criteria and control instructions. At almost all barriers, the most important closure criterion is the forecasted water level maximum, which is referred to as the *closure decision level* (h_c).

When the forecasted water level exceeds the closure decision level, the moment to start the closure is planned. Adequate time allowance to close the barrier is considered for potential operational disruptions. Closing around slack tide allows for more storage of river discharge with minimal flow conditions. However, a shorter closure time reduces the impact on navigation and tidal exchange and can reduce structural loads. In any case, the closure must be sufficiently planned ahead to communicate its timing to local stakeholders, the most important often being the port authority.

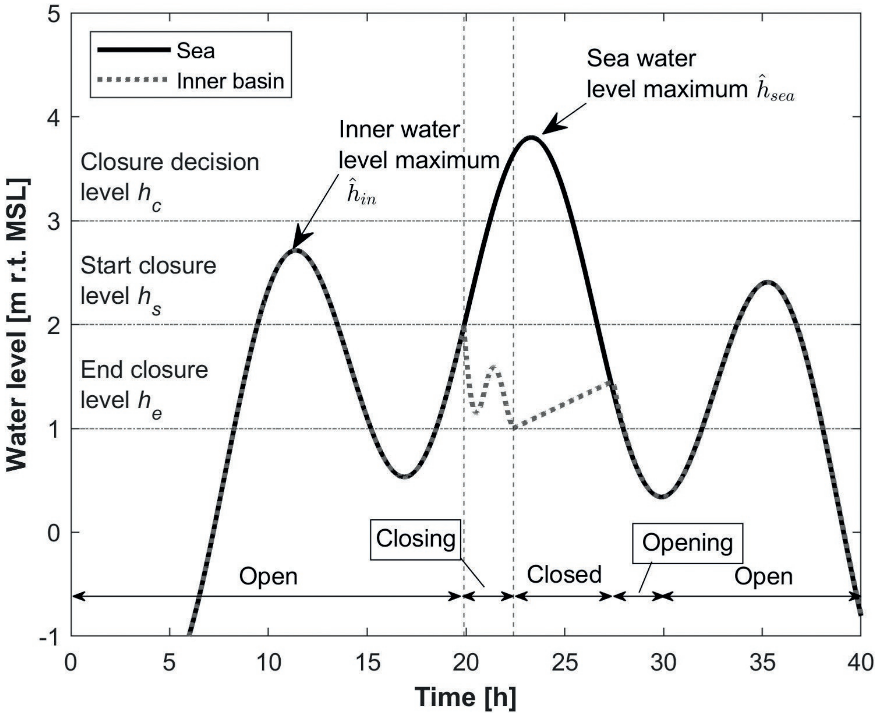

Figure 2.4: Example of inner and sea water levels during a closure procedure, based on the Maeslant barrier (Rotterdam, Netherlands). Water levels are expressed in meters relative to mean sea level (MSL).

Operators employ machinery, including operating mechanisms, drives, electronic switchboards, control computers, and power supplies, to move the gates into position — a process that on average takes two and a half hours at the Maeslant barrier. Consequently, the water level at the start (*start closure level*) differs from the water level at the end (*end closure level*) especially at estuaries with a significant tidal range (>1 meter). Once closed, the barrier structure, consisting of gates and foundation, withstands the hydraulic loads securing the inner basin. During the closure, the inner basin water levels are subject to falls and rises due to the abrupt tidal closure (translation waves), leakage of the barrier, river discharge and internal wind set-up.

The barrier reopens when an equilibrium of water levels on both sides of the barrier is reached. For longer lasting storms at regions with significant astronomic tides, for instance at the Thames barrier (London), the barrier can close and open several times around low tide to drain the inner basin. After the storm has passed, the barrier remains open until the next storm surge event arrives.

Figure 2.4 illustrates the closure procedure and its effect on the inner water level h_{in}. The inner water level maximum is the highest water level during a storm surge event in the inner basin, which is indicated with a circumflex: $\hat{h}_{in}$. In this example, the storm surge barrier operation resulted in a reduction of the inner water level maximum by approximately one meter.

Barrier and system failures

In the introduction, it was stated that a failure of a storm surge barrier flood protection system is an event in which the critical water level z is exceeded. This can be caused by three principal failure mechanisms: operational, structural and hydraulic overload failure.

Operational failures are a (partial) failure to close or to open. These failures result from decision and control errors, unavailability of staff and malfunctioning equipment. Decision errors are more likely if the storm conditions are close to the closure criteria. Other types of operational failures are not necessarily related to the conditions at the peak of the storm.

With structural failures, storm surge barriers fail to resist the hydraulic loads. Most important hydraulic loads are the hydraulic head and wind wave impacts. They can cause the barrier to collapse, break or undermine the foundation.

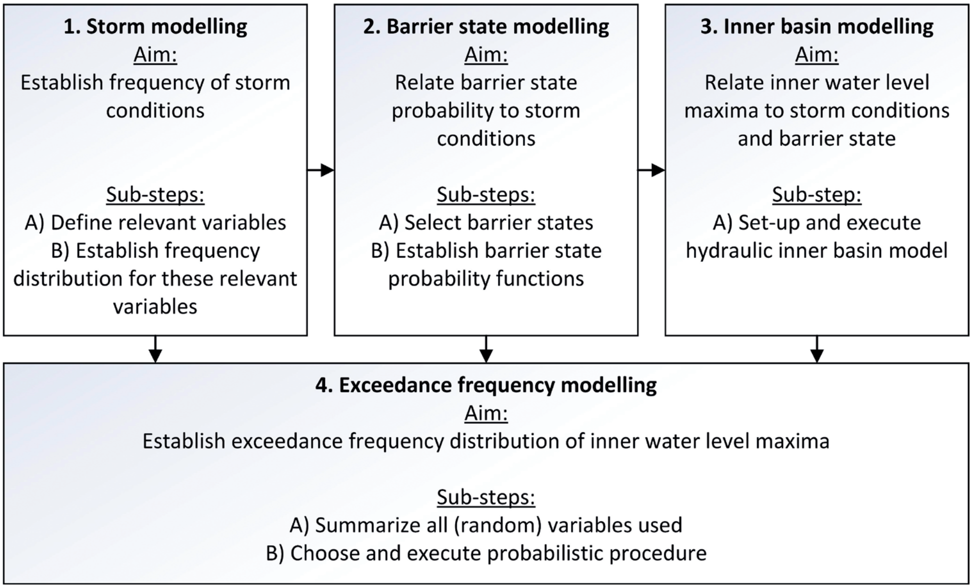

Figure 2.5 provides a flow diagram of these four steps.

The hydraulic overload principal system failure mechanism represents scenarios where despite successful barrier operation, extreme storm surge, astronomic tide and river conditions still cause the critical level *z* to be exceeded. Most barriers have considerable flow through them during a storm. The sector arms of the Maeslant barrier do not touch each other in closed position. At the Eastern Scheldt barrier, the foundation consists of highly permeable rock mattresses. Flow through the barrier alone will not result in critical water level exceedance. However, combined with (a combination of) barrier overflow, river discharge behind the barrier and internal wind set-up a catastrophic flood can occur.

Finally, there are important partial failures scenarios. Closures can be too late due to an operational error, resulting in a relatively full inner basin, making critical water level exceedance more likely. At multiple gate barriers, a single gate failure results in large flow velocities through this opening. These large flow velocities can erode bed protections or cause gates to vibrate, resulting in a structural failure.

Method to quantify storm surge barrier performance

The section outlines the four-step method to quantify storm surge barrier performance. The four steps are:

1. Storm modelling
2. Barrier state modelling
3. Inner basin modelling
4. Exceedance frequency modelling.

Storm modelling

The aim of this first step is to establish frequency distributions of relevant (random) variables of storms. These variables can be properties of the storm itself (e.g., sea level maximum, maximum wind speed), but also the astronomic tide (e.g., tidal amplitude, tidal phase) and the river (e.g., discharge). Depending on the aim of the analysis, assumptions with respect to sea level rise can be included here. All these properties together are referred to as storm conditions S.

The more variables are considered relevant in this stage, the more complex the modelling in the next stages becomes. Therefore, it is advocated to start with the most important variable(s) and build the model onwards based on the initial results.

Barrier state modelling

In this step, system failure mechanisms are organized according to barrier states. Barrier states are the state and/or position a barrier is in during a storm, which results in a certain degree of obstruction of flow. A barrier state k can be a failed, a partially failed or a successful state.

First, barrier states are to be defined. The analysis should at least consider two barrier states: fully open and successfully closed. Other principal barrier states which can be included are a failure to close and a structural failure. Based on the initial insights from this analysis, the number of the barrier states K can be extended. Those barrier states which are not expected to lead to critical water level exceedance are excluded.

The probability of a barrier state is related to storm conditions S. The relation is referred to as the *barrier state probability function* $P_k(S)$. These probability functions are mutually exclusive and combined encompass the entire probability space.

An event tree is applied to visualize the progression of events and, thereby, determine barrier states. The probability of the barrier state is the product of the conditional probabilities of the intermediate events in the event tree.

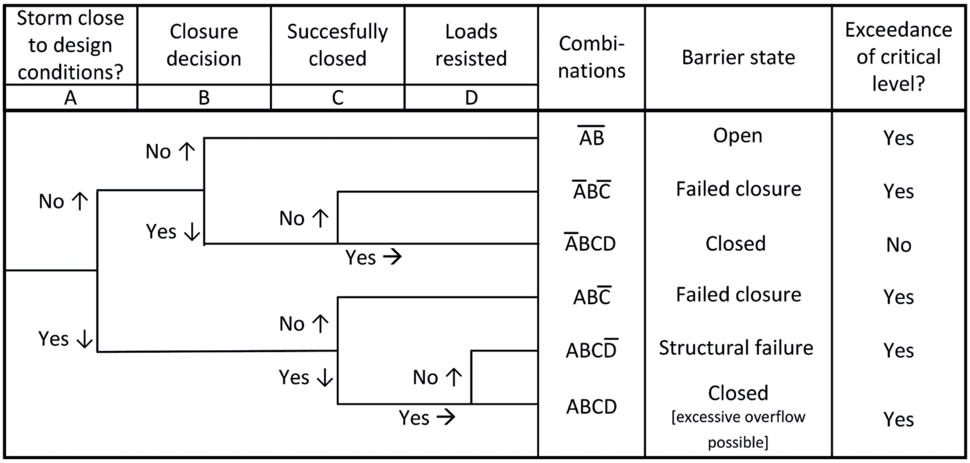

Figure 2.6: Event tree of a closure procedure. Two types of storm events are analyzed; one which results in a flood in case the barrier remains open $\overline{A}$ and a more severe one which will result in structural or hydraulic overload failure (A). For the first storm type, a structural failure cannot occur {$P(\overline{D}) = 0$} and for the second type, there is always a closure decision {$P(B) = 1$} and, therefore, these paths were removed.

The event tree of Figure 2.6 is used to demonstrate the development of barrier state probability functions. Two types of storm events are analyzed; one which results in a flood in case the barrier remains open $\overline{A}$ and a more severe one which will result in structural or hydraulic overload failure (A). Three successful events are defined: B) a closure decision, C) a successful closure, D) hydraulic loads resisted. The failure events are indicated with a macron ‾ : no closure decision, $\overline{C}$) a failed closure due to mechanical, electrical or control errors and, $\overline{D}$) structural failure.

The frequencies of storms (events A and $\overline{A}$) are the result of the first step in this method: storm modelling. Barrier state probability functions are combinations of probability functions of Events B to D and their opposites $\overline{B}$ to $\overline{D}$. The probability of successful closure decision $P(B)$ is related to the sea level maximum $\hat{h}_{sea}$ [meter relative to mean sea level (m r.t. MSL)], using a normal cumulative distribution function (Φ) with the closure decision level h_c [m r.t. MSL] as a mean and the water level forecast error σ_c [m] as the standard deviation. Likewise, the (conditional) structural failure probability $P(\overline{D})$ depends on the sea level maximum $\hat{h}_{sea}$ [m r.t. MSL] with normal distribution parameters: the mean structural fragility z_{str} [m r.t. MSL] and its standard deviation σ_{str} [m]. The constant P_{FC} is used to determine the probability of a failed closure $P(\overline{C})$ on demand. The barrier states are listed in the following order: 1) open, 2) failure to close, 3) structural failure and 4) closed and find the following barrier state probability functions:

$$P_1\left(\hat{h}_{sea}\right) = P(\overline{B}) = 1 - \Phi\left(\frac{\hat{h}_{sea} - h_c}{\sigma_c}\right)$$

$$P_2\left(\hat{h}_{sea}\right) = P(B\overline{C}) = \Phi\left(\frac{\hat{h}_{sea} - h_c}{\sigma_c}\right) \cdot P_{FC}$$

$$P_3\left(\hat{h}_{sea}\right) = P(BC\overline{D}) = \Phi\left(\frac{\hat{h}_{sea} - h_c}{\sigma_c}\right) \cdot \left(1 - P_{FC}\right) \cdot \Phi\left(\frac{\hat{h}_{sea} - z_{str}}{\sigma_{str}}\right)$$

$$P_4\left(\hat{h}_{sea}\right) = P(BCD) = \ldots$$

$$\ldots = \Phi\left(\frac{\hat{h}_{sea} - h_c}{\sigma_c}\right) \cdot \left(1 - P_{FC}\right) \cdot \left\{1 - \Phi\left(\frac{\hat{h}_{sea} - z_{str}}{\sigma_{str}}\right)\right\}$$

Figure 2.7 presents these barrier state probability functions, which will later on be used in the case study. The blue line presents the probability of the barrier being open. With sea level maxima approaching the closure decision level h_c = MSL+3.1m, the probability of an open barrier declines. Due to the small water level forecast error σ_c = 0.2m, it is unlikely that the barrier remains open with sea level maxima higher than MSL + 3.5m.

The barrier state probability function of a failed closure due to mechanical, electrical or control errors (red line) is the result of two events: a closure decision being taken and a failed closure. Until approximately MSL + 3.5m, the probability rises as the barrier with these water level maxima the barrier can remain open due to the lack of a closure decision. For water level maxima higher than MSL + 3.5 meter, the probability of a failed closure remains constant (P_{FC} = 1/100 on demand).

The barrier state probability function of structural failure is the combination of three events: a closure decision, a successful closure and a structural failure. Structural failure becomes more likely for sea level maxima above MSL+4.0m. Due to structural fragility (values z_{str} = MSL + 6.6m and σ_{str} = 0.5m), the probability of structural failure rises to a maximum 99/100, as in 1/100 cases the closure failed due to mechanical, electrical and/or control errors.

Successful closure is a barrier state which occurs if there is a closure decision, no failure to close and no structural failure. As a result, for each sea level maximum, the sum of the probabilities is one.

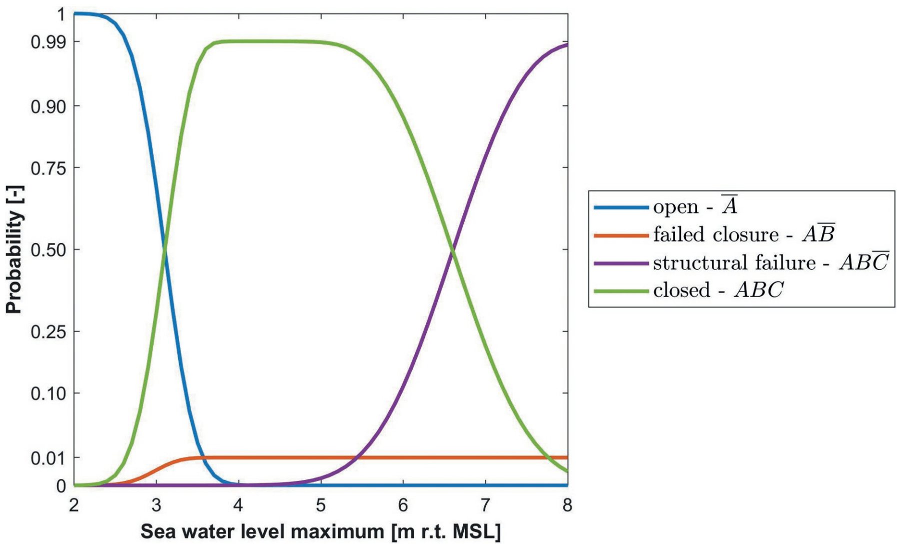

Figure 2.7: Example of barrier state probability functions used for the Maeslant barrier case study. Sea level maxima are presented in meters relative to mean sea level [m r.t. MSL]. The vertical axis was scaled using a beta distribution (2,2) to emphasize probabilities near zero and one. The symbols in the legend correspond with the events as indicated in the event tree of Figure 2.6.

Inner basin modelling

The inner basin modelling aims to relate storm and river conditions and barrier states to inner water levels in front of interior flood defenses and near the barrier. Preferably, the inner basin modelling accounts for all relevant hydraulic phenomena. The inner basin model used at the Maeslant barrier covers the lower part of the Rhine and Meuse Delta, accounting for translation waves, flow through and over the barrier, river flow, internal wind set-up, water storage, the hydraulic properties of the more southerly Haringvliet sluices and friction in channels. For the Galveston Bay, a similar model is applied to assess the feasibility of a storm surge barrier (Christian et al., 2015). However, for this chapter, a simpler analytical model is used which only includes a few of the relevant hydraulic phenomena to emphasize our approach with respect to barrier state and probabilistic modelling.

Furthermore, it is assumed that inner water levels do not affect the probability of barrier states. Both structural loads and closure criteria can, however, be influenced by inner water levels. When there is a demand to include these effects, a feedback loop between step 3 (inner basin modelling) and step 2 (barrier state modelling) should be added.

Exceedance frequency modelling

In this final modelling step, the exceedance frequency of the critical water level z is determined. In this section, first the method is explained on an abstract level, after which some practical issues are pointed out concerning this abstract method. Then, the method is introduced and applied for the Maeslant barrier case.

The frequency of a single event that exceeds the critical water level z is composed of (see Figure 2.8):

1. the frequency of a storm event $F(S)$ [per year] with properties S (= result of step 1: storm surge modelling).
2. the probability of a barrier state k given storm properties S, which are the barrier state probability functions $P_k(S)$ (= result of step 2: barrier state modelling), and
3. the probability of exceedance of the critical water level z given the storm event S, the barrier state k and inner basin properties B: $P\left(\hat{h}_{in} > z \middle| S, k, B\right)$

Imagine that there are m possible events which exceed the critical water level. Then, the sum of the frequencies of these events amount to the frequency of critical water level exceedance $F\left(\hat{h}_{in} > z\right)$ [per year]:

$$F\left(\hat{h}_{in} > z\right) = \sum_{i=1}^{m} F(S) \cdot P_k(S) \cdot P\left(\hat{h}_{in} > z \middle| S, k, B\right) \qquad (1)$$

For continuous parameters, frequency and probability functions could be resolved by integration of probability density functions. However, the conditional probability density of the inner water level $p\left(\hat{h}_{in} \middle| S, k, B\right)$ is an indirect result of the inner basin modelling and remains difficult to interpret. Therefore, the three terms $\{f, P_k$ and $p\left(\hat{h}_{in} \middle| S, k, B\right)\}$ are combined to introduce the partial distribution g_k, which presents the density of inner water levels for an individual barrier state. Using this approach, the contribution of the individual barrier states to the exceedance frequency of the critical water level can still be recognized, which is the main aim of this chapter.

The partial distributions g_k can be established with several probabilistic procedures. If there is only one random variable affecting the partial inner water level distribution, an analytical procedure can be applied. With more random variables, numerical procedures are needed. In the case study (section 4), both an analytical and a numerical procedure (a Monte Carlo Simulation) are demonstrated.

The exceedance frequencies result from integration of the partial distributions for water level maxima higher than the critical water level. The number of random

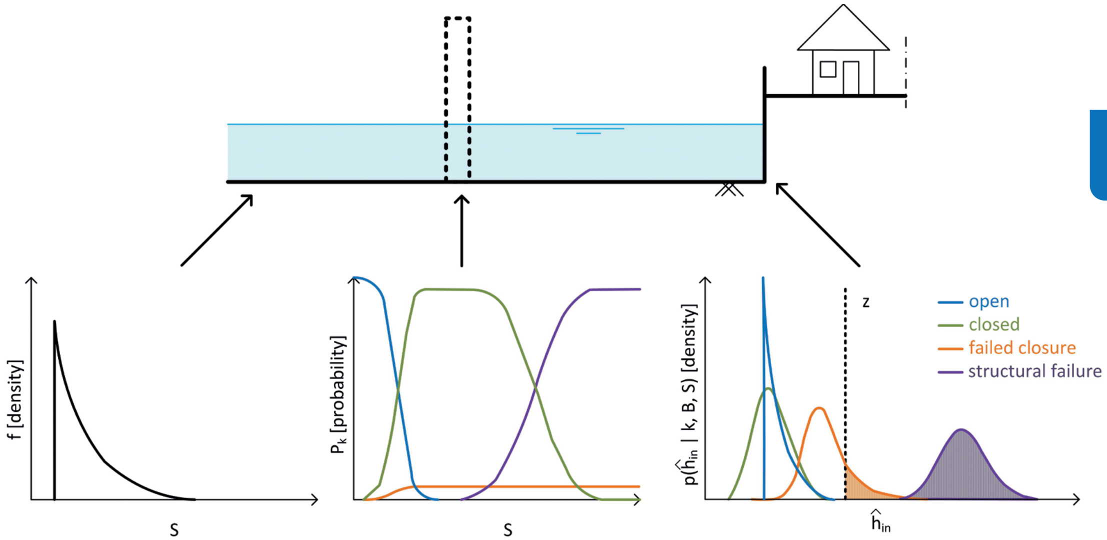

Figure 2.8: Overview of three main stochastic variables required to establish the exceedance frequency of the critical water level, corresponding to formula 2: the frequency density S, the barrier probability state functions P_k and the density of inner water level maxima at a certain location behind the barrier given the storm conditions and barrier state $p(\hat{h}_{in}|k, S)$. The plots in the lower panels present example functions of these main stochastic variables with a single variable describing storm severity S and four barrier states (open, closed, failed closure and structural failure). The lower right panel indicates the critical level *z* with a dashed line, hatching the probability density exceeding this level.

variables *n* determines the tuple of the integral. For example, if there are three random variables, the exceedance frequency is found with a triple integral. The exceedance frequency of a critical water level for a specific barrier state $G_k(\hat{h}_{in} > z)$ [per year] is

$$G_k(\hat{h}_{in} > z) = \int \dots \int_{\hat{h}_{in} > z} g_k\{\hat{h}_{in}(X_1, X_2, \dots, X_n)\} dX_1 \dots dX_n \qquad (2)$$

In this equation *X* is a set of *n* random variables which affect the frequency of the inner water level maxima. The random variables encompass the storm conditions *S* and variables for the barrier state probability functions and could include random variables of inner basin properties.

In the final step, the exceedance frequencies of the barrier states are summed over all states to find the exceedance frequency of the critical water level $F(\hat{h}_{in} > z)$ [per year]:

$$F(\hat{h}_{in} > z) = \sum_{i=1}^{K} G_k(\hat{h}_{in} > z) \qquad (3)$$

This formula is also applied to examine more extreme water level maxima than the critical level *z* alone to find the hydraulic loads with a storm surge barrier.

Rotterdam case study

Introduction

This case study applies the method to quantify storm surge barrier performance to the Maeslant barrier in Rotterdam. Three examples of the method are presented: 1) an analytical probabilistic procedure with a single random variable, 2) a Monte Carlo Simulation including seven random variables and 3) the same probabilistic procedure, but with a lower failure probability to close as a result of a performance improvement.

The Maeslant barrier was constructed to protect the cities of Rotterdam and Dordrecht against coastal floods (see Figure 2.9). The barrier is positioned at the New Waterway, which is the main canal connecting Rotterdam to the sea. The barrier consists of two floating sector arms. In normal conditions, these hydraulic gates are positioned in a dry dock. If the closure decision level h_c of Mean Sea Level (MSL) + 3.0 meter is predicted to be exceeded, the closure procedure starts and the gates are positioned into the New Waterway.

In this case study, the flood frequency at Rotterdam is investigated, which interior flood defenses have a critical water level *z* of MSL + 3.6 meter.

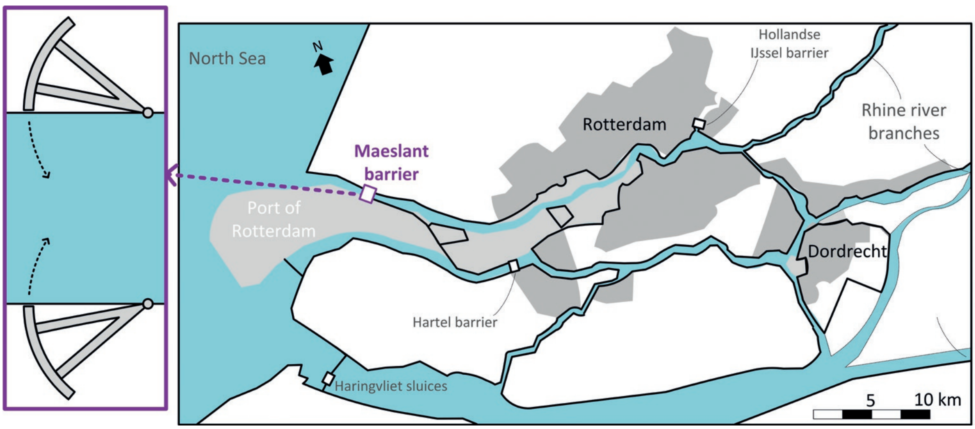

Figure 2.9: Schematic map with top view of the Maeslant barrier (left) and region protected by this barrier (right). Urban areas are hatched dark grey, port areas light grey. Solid black lines are used to indicate flood defenses.

Analytical procedure

Storm modelling

For the analytical procedure, only the sea level maximum is analyzed. Moreover, sea level rise is not accounted for, as the study aims at finding current exceedance frequencies.

Like Mooyaart et al. (2023), an exponential distribution is used for annual water level maxima with an annual maximum H_A of MSL + 2.1 meter and a decimal height H_B of 0.75 meter. Thus, the probability density function of this distribution is

$$f_{sea}\left(\hat{h}_{sea}\right) = \frac{ln10}{H_B} \cdot 10^{-\frac{\hat{h}_{sea} - H_A}{H_B}} \quad (4)$$

Barrier state modelling

Four barrier states are defined: open, failed closure, structural failure and successful closure. A failure to re-open again is excluded as its likelihood of leading to critical level exceedance is low. The event tree in Figure 2.6 was used to arrange barrier states.

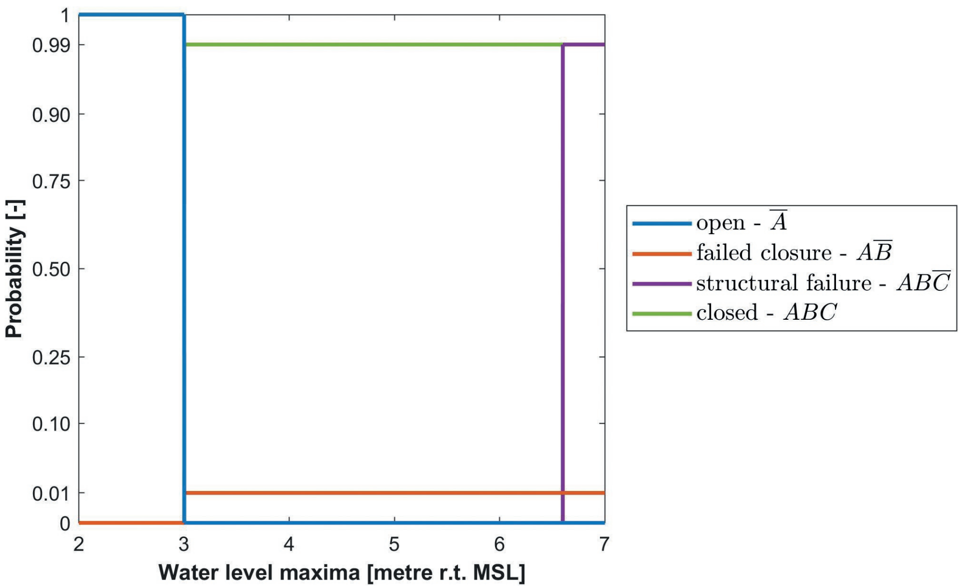

Figure 2.10: Barrier state probability functions for the analytic procedure. The barrier remains open below the closure decision level (blue line) and always fails structurally above the structural failure level z_{str}. Between these closure decision and structural failure level, the barrier closes successfully with a rate of 99/100 on demand and thus fails in 1/100 demands. The vertical axis was scaled using a beta distribution (2,2) to emphasize probabilities near zero and one. The symbols in the legend correspond with the events as indicated in the event tree of Figure 2.6.

The following barrier state probability functions are applied (see Figure 2.10):

1. Open: If predicted the sea level maximum is lower than the closure decision level h_c, the barrier remains open. For all other sea level maxima, a closure decision is taken.
2. Failed closure: if the sea level maximum exceeds the closure decision level, the probability of a failed closure is P_{FC}= 1/100 on demand (Wat, 2021) regardless of the sea level maximum.
3. Structural failure: The structural design was based on hydraulic loads with a return period of 1,000,000 years (Janssen et al., 1994). A sea level maximum of MSL +6.6 meter corresponds to this return period. It is assumed that if this level z_{str} is exceeded, the barrier fails structurally, and that no structural failure occurs below this level.
4. Successful closure: In all other cases, closure is successful, hence $P_4(h_c \leq \hat{h}_{sea} < z_{str})$ = 99/100 on demand.

Inner basin model

In case of successful closure, the barrier obstructs the flow. For the analytical procedure, it is assumed that all inner water level maxima result in the closure decision level. Thus, the role of river discharge and barrier overflow is neglected.

For the open and failed closure mode, the storm surge can freely enter the New Waterway. It is assumed that the flow is unobstructed in case of structural failure as well. With unobstructed flow (open, failed closure and structural failure barrier states) sea level maxima are equal to inner water level maxima. As Rotterdam is located near the Maeslant barrier, this is a realistic assumption. It is demonstrated that for the failed closure barrier state, this approach leads to similar results as previous studies, which use a more accurate inner basin model.

Exceedance frequency modelling

With the assumption of the previous paragraph, the partial density function g_k is merely the product of the barrier probability functions and the sea level density functions for the open and failed barrier states (1: open, 2: failed closure and 3: structural failure):

$$g_k\left(\hat{h}_{in}\right) = f_{sea}\left(\hat{h}_{sea}\right) \cdot P_k\left(\hat{h}_{sea}\right) \tag{5}$$

in which P_i is the barrier state probability function and f_{sea} is the probability density of sea water level maxima [per year per meter].

For the closed barrier state (barrier state 4), the closure frequency F_4 is added at the closure decision level:

$$g_4\left(\hat{h}_{in} = h_c\right) = F_4 = \int f_{sea}\left(\hat{h}_{sea}\right) \cdot P_4\left(\hat{h}_{sea}\right) d\hat{h}_{sea} \tag{6}$$

Equation 2 is used to determine the exceedance frequency of the critical water level per barrier state. Equation 3 finds the hydraulic loads with a storm surge barrier.

Results

Figure 2.11 shows the partial densities of the four barrier states. The open barrier state density is equal to the density without a barrier until the closure decision level. The closed barrier state has a frequency equal to the closure frequency at the closure decision level, which results in an infinitely high density at this water level.

The densities of the barrier failure mechanisms are much smaller and, therefore, plotted on two separate panels. The density of the failed closure is a factor hundred lower than without a barrier. Above MSL + 6.6m, the combination of structural failure and a failure to close result in a density equal to the density without a barrier.

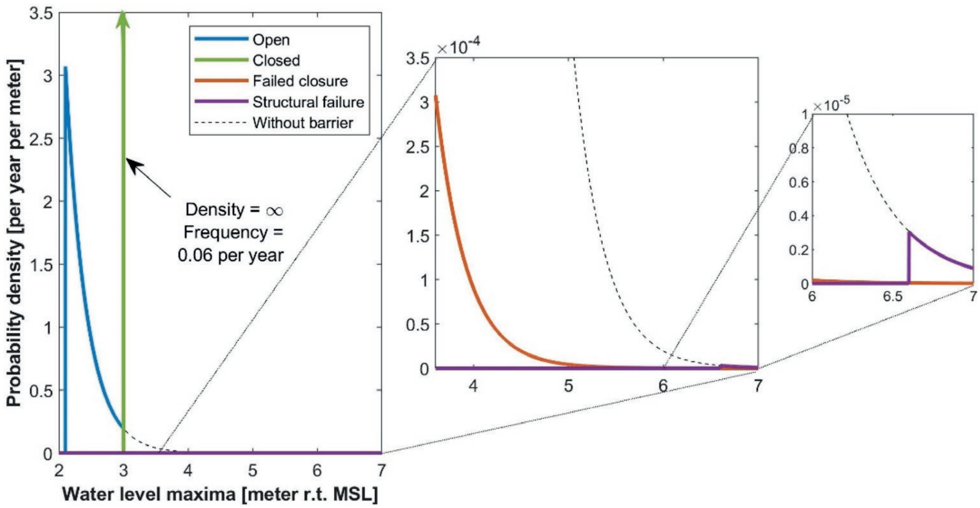

Figure 2.11: Probability density of water level maxima at Rotterdam with and without a barrier. Colored lines are used to indicate the contribution of specific barrier states to the density, while a thin dashed black line shows the density without a barrier. The left figure shows the density over the entire range of water level maxima. The middle figure presents the density for water levels higher than the critical water level (MSL + 3.6m), while the right figure zooms in even smaller probability densities for water levels exceeding MSL + 6m.

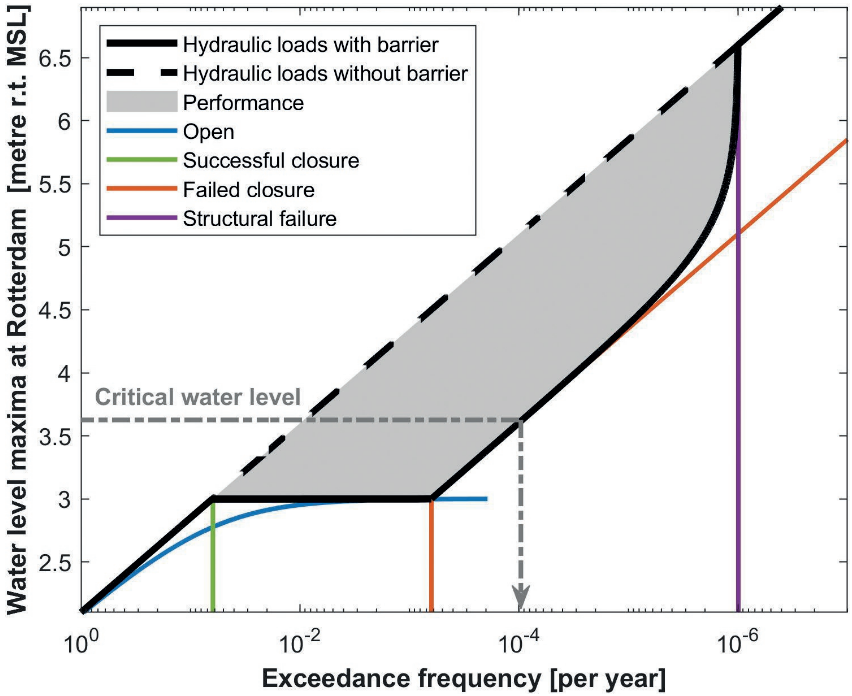

Figure 2.12: Hydraulic loads at Rotterdam with and without a barrier using the analytical procedure expressed in meters relative to mean sea level (MSL). Exceedance frequencies of the yearly water level maximum (10^0) are dominated by the storm surge barrier remaining open (blue line). With higher water level maxima, it becomes less likely that the barrier remains open (blue line), and, therefore, the blue line reaches an asymptote equal to the closure decision level. This blue line (open barrier) does not follow the black dashed line (without a barrier), as with a barrier there are also other barrier states which result in exceedances of these extreme water level maxima. The barrier closes successfully with a frequency of 99/100 per year, all resulting in an extreme water level maximum equal to the closure decision level (green line). For extreme water level maxima above the closure decision level, a failure to close (red line) occurs every once in a hundred times and, hence, exceedance frequencies of inner water level maxima are one hundred times as low as without a barrier. Structural failures (purple) occur with extreme water level maxima above the structural failure level of MSL + 6.6 meter. The hydraulic loads with a barrier (black) are the sum of the inner water level maxima exceedance frequency of the four barrier states (open, closed, failed closure and structural failure).

Figure 2.12 presents the results with exceedance frequencies on the horizontal axis in reverse direction. In this example, the critical water level can only be exceeded if the barrier is in one of two barrier states (failed closure or structural failure). The exceedance frequency with the failed closure is 10^{-4} per year, which is similar as was found in a previous study (HKV, 2006). Exceedance of the critical level due to structural failure is a hundred times less likely: 10^{-6} per year.

Storm surge barrier performance can be found by comparing the hydraulic loads with and without the barrier. The figure shows that between the closure decision and structural failure level, the hydraulic load is affected by the storm surge barrier. The exceedance frequency of MSL + 5.1m provides insight into how the model functions. At this water level the exceedance frequency of a failed closure and a structural failure are equal (10^{-6} per year). The sum of the exceedance frequencies of all barrier states $2 \cdot 10^{-6}$ is the exceedance frequency with a storm surge barrier (see equation 3). Below MSL +5.1m, failure to close is most important for storm surge barrier performance, while for higher levels structural failure is.

The open and closed barrier states contribute to lower extreme water levels. The closed barrier state has a constant exceedance frequency until the closure decision level, equal to the closure frequency. The open barrier state exceedance frequency approaches an asymptote equal to closure decision level. When combined these two barrier states result in a hydraulic load equal to the hydraulic load without a barrier.

Monte Carlo Simulation

For the second probabilistic procedure, the following is adapted:

- More variables describing the storm conditions are included; the sea level maximum is split in storm surge and astronomic tide. Moreover, river discharge is considered which can accumulate behind the barrier.
- The same four barrier states are applied; however, barrier probability functions are used which include uncertainty with respect to forecasting and structural failure (see Figure 2.7).
- A slightly more sophisticated, but still simplified inner basin model is applied to account for the effect of accumulating river discharge, which is elaborated upon in the next section.

The properties of the additional variables describing storm conditions and the barrier probability functions are presented in Table 1.

Inner basin modelling

For all barrier states, the inner water level h_{in} [meter relative to mean sea level (MSL)] is modelled during a storm. Table 1 presents the meaning, dimension and value of these variables. The inner water level is constituted of three components: the storm surge h_{storm}, the astronomic tide h_{tide} and the river component h_{river}. Using similar assumptions regarding storm pattern and river influence as Zhong et al. (2012), the following equation for the open barrier states is used:

$$h_{in}(t) = h_{barrier}(t) = h_{storm}(t) + h_{tide}(t) + h_{river}(t) \quad (7)$$

$$h_{storm}(t) = \zeta_{storm} \cdot cos^2\left\{\frac{\pi}{T_{storm}} \cdot \left(t - \frac{1}{2} \cdot T_{storm}\right)\right\}$$

$$h_{tide}(t) = \zeta_{tide} \cdot sin\left\{\frac{2 \cdot \pi}{T_{tide}} \cdot (t - \varphi)\right\}$$

$$h_{river}(t) = \frac{1}{2 \cdot g} \cdot \left(\frac{8/9 \cdot Q_{Rhine}}{\mu \cdot A_{mouth}}\right)^2$$

For all barrier states, any water level differences between Rotterdam and the Maeslant barrier are neglected $\{h_{in}(t) = h_{barrier}(t)\}$.

The start of the closure takes place at the start closure level h_s (MSL+2m) closest before the first exceedance of the closure decision level, corresponding to the closure procedure of the Maeslant barrier.

Multiple effects cause the water level to drop after the start of the closure (negative translation wave, tidal phase difference between Maeslant barrier, Haringvliet and the rest of the lower rivers and internal wind set-up). To account for these effects, an end closure level h_e of MSL + 1m is used.

River flow and overflow over the barrier cause the inner basin to rise gradually during closure. River flow spreads over a wide area: Besides the New Waterway also the larger Haringvliet Lake. A single basin approximation is used to estimate the water level rise, considering the entire area (300 km^2, based on publicly available data on lake sizes and estimates using Google Maps). The effect that for higher water levels (h_{in} > MSL + 2.5m), the storage area rapidly increases is ignored. Like Zhong et al. (2012), only the Rhine flow is considered, neglecting the smaller Meuse flow and account for 1/9th of the flow being diverted upstream through the IJssel to the Northern part of the Netherlands.

In this model, flow through the barrier is neglected and only barrier overflow $Q_{overflow}$ is considered [m^3/s]. The within the hydraulic engineering field common applied formula (Ministerie van Verkeer en Waterstaat, 1990) is used:

$$Q_{overflow}(t) = c \cdot W \cdot \left\{h_{barrier}(t) - z\right\}^{1.5} \quad (8)$$

To find the water level rise due to overflow, again the single basin approximation is applied. However, it is assumed that the water spreads over a smaller area ($A_{overflow}$ = 50km^2). The inner water level with barrier closure is then:

$$h_{in,closed} = h_{ECL} + \frac{8/9 \cdot Q_{Rhine}}{A_{Rhine}} \cdot (t - t_{EC}) + \sum_{t_{EC}}^{t} \frac{Q_{overflow}}{A_{overflow}} \cdot \Delta t \quad (9)$$

In which t_{EC} is the time at the end of the closure and Δt is the time step, which was taken at 1200 seconds (20 minutes).

For extreme high river discharges (>6,000 m^3/s), the barrier closes around low tide. However, this specific closure procedure was excluded from the inner basin model as it had little effect on inner water level maxima. Very extreme river discharges were maximized until 18,000 m^3/s to account for upstream river flooding.

Exceedance frequency modelling

Table 1 presents the properties of all variables applied in this case. A Monte Carlo simulation is performed where 10^8 random samples are taken from the seven distributions presented in Table 1. For each sample of all distributions, the inner basin model is run to find the inner water level maximum. The inner water level maxima are grouped in the four barrier states: open, closed, failed closure and structural failure.

Table 1: Properties of variables of Monte Carlo Simulation.

Variable	Symbol	Unit	Distr.	μ	σ	Source
Storm surge	ζ_{storm}	m	Exp.	1.2	0.75	1
Storm duration	T_{storm}	s	Logn.	12.2	0.11	2
River discharge	Q_{river}	m^3/s	Logn.	7.7	0.5	3
Tidal phase	φ	s	Unif.	0	44712	
Closure decision level	h_c	m*	Normal	3.1	0.2	4
Prob. failed closure	P_{FC}		Bern.	1/100		
Structural fragility	z_{str}	m*	Normal	6.6	0.5	
Tidal amplitude	ζ_{tide}	m	Det.	0.9		5
Tidal period	T_{tide}	s	Det.	44712		
Start closure level	h_s	m*	Det.	2		6
End closure level	h_e	m*	Det.	1		7
River flow section	μA_{mouth}	m2	Det.	3620		3
Rhine basin	A_{Rhine}	km^2	Det.	300		8
Crest level barrier	z_{crest}	m*	Det.	5		6
Overflow constant	c	m/s1/2	Det.	1.9		9
Width barrier	W	m	Det.	360		6
Overflow basin	$A_{overflow}$	km^2	Det.	50		8
Grav. acc.	g	m/s^2	Det.	10		

m* is meter relative to Mean Sea Level. Exp., Logn., Det., Unif. are abbreviations for exponential, lognormal, deterministic and uniform, respectively. The lognormal cumulative distribution has the following structure: $\frac{1}{2}\left[1+\operatorname{erf}\left(\frac{\ln x-\mu}{\sigma\sqrt{2}}\right)\right]$. For the exponential distribution, the value μ corresponds to the annually exceeded water level and σ is the decimal height. For the uniform distribution μ and σ are the lower and upper bound, respectively. Sources: [1] Annual maximum minus average tidal range, [2] Deltares (2017), [3] Zhong et al. (2012), [4] HKV (2011) [5] semi-diurnal component (M2) of tide, [6] Janssen et al. (1994), [7] assumption is based on a small number of hydraulic model run outputs, [8] based on satellite images and publicly available data of lake sizes, [9] Ministerie van Verkeer en Waterstaat (1990)

Results

Figure 2.13 shows the number of samples within bins of 0.1 meter. Most samples result in an open situation. Closures occur often as well, but barrier failures are rarely drawn. Exceedances of the critical water level of MSL + 3.6 meter are, however, mostly the result of barrier failures to close.

Figure 2.14 presents the hydraulic loads with and without a barrier. The exceedance frequency of the critical water level is $1.4{\cdot}10^{-4}$ per year with a barrier and $1.0{\cdot}10^{-2}$ per year without a barrier. The storm surge barrier performance is mainly influenced by the possibility of a failed closure ($1 \cdot 10^{-4}$ per year), but is significantly affected by the open ($1 \cdot 10^{-5}$ per year) and closed ($2 \cdot 10^{-5}$ per year) barrier states as well. Although structural fragility was included, structural failure remains an unlikely cause for exceedance of the critical water level ($2 \cdot 10^{-6}$ per year).

Overflowing events almost never result in exceedance of the critical water level. Severe overtopping events were analyzed, but found that the difference between end closure and critical water level provides sufficient storage for overflow even in rare cases.

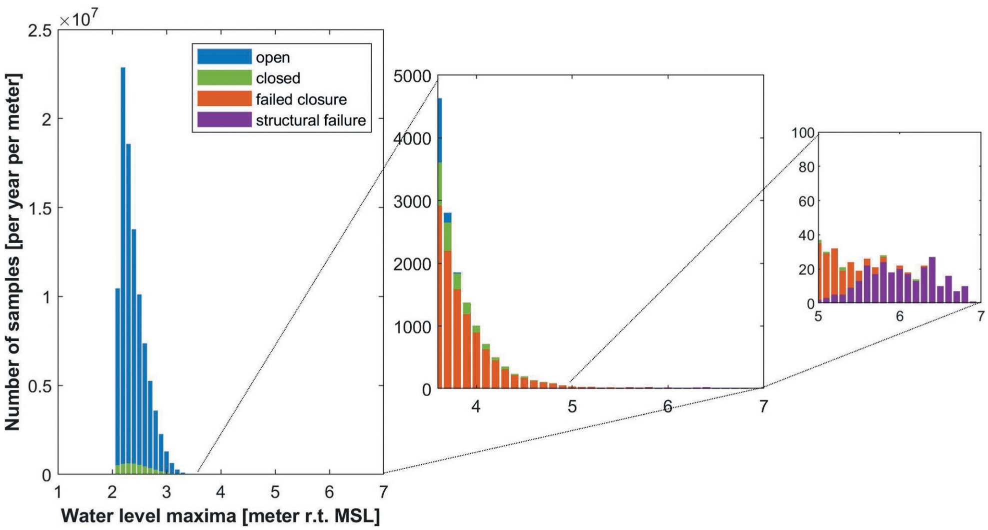

Figure 2.13: Histograms with the number of samples from the Monte Carlo Simulation (10^8 samples) that resulted in an inner water level maximum (bins 0.1 meter). The left figure presents all samples and the middle figure presents those which exceed the critical water level. The right figure zooms in on water levels exceeding MSL+5m.

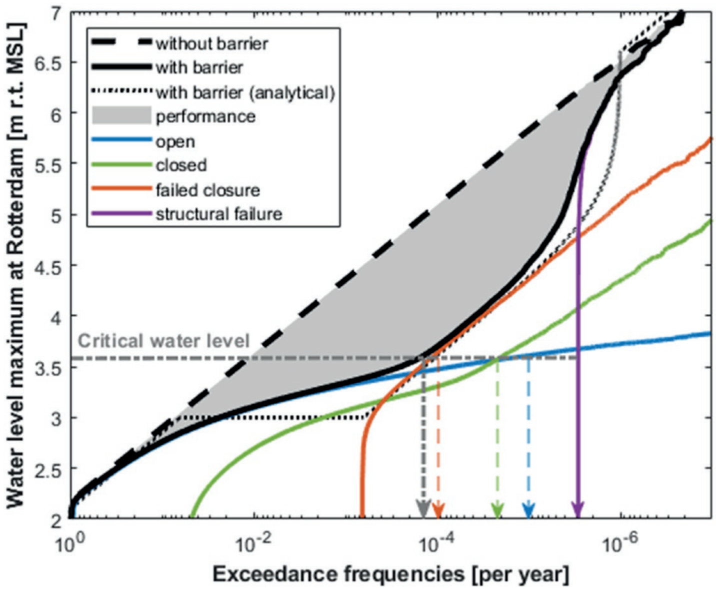

Figure 2.14: Hydraulic loads with and without a barrier with a Monte Carlo Simulation with 10^8 samples. The colored lines indicate the exceedance frequencies of the inner water levels for each barrier state. The open (blue) and closed (green) barrier state occur most often, typically resulting in extreme water level maxima below the critical level. Forecast errors at the open barrier state and high river discharges accumulating behind the barrier at the closed barrier state can cause the critical water level to be exceeded, with frequencies of about 10^{-5} per year (see dashed arrows). Failed closures and structural failures occur less frequent than open and closed barrier states, but have relatively high water level maxima. Near and above the critical level, failed closures occur at a constant rate of once in a hundred relative to the hydraulic loads without a barrier. Structural failures occur at the higher extreme water level maxima and due to the assumed structural fragility, this curve approaches the hydraulic loads without a barrier in a curved manner. The hydraulic load with a barrier is the sum of the four exceedance frequencies of the barrier states. The critical water level of the flood defenses behind the barrier is indicated with a grey dash dot line.

Comparing both methods (Analytical and Monte Carlo), the Monte Carlo approach revealed additional scenarios where open and closed barrier states lead to critical level exceedances. For the open and closed mode, the exceedance frequency is about $2 \cdot 10^{-5}$ per year. The failed closure partial distribution is similar to the analytical solution, which was expected because the same input was used. The structural failure frequency is slightly higher at the critical water level than the analytical method ($2{\cdot}10^{-6}$ per year) as the possibility of structural failure with lower levels was included.

Performance improvement

As a final example, only the probability of a failed closure is changed from 1/100 to 1/1000 on demand. This lower probability is the result of a performance improvement of the Maeslant barrier such as an additional barrier which was proposed by Rijcken et al. (2023).

Figure 2.15 (left) presents the exceedance frequencies of extreme water levels with the performance improvement. Compared to the previous example, the partial distribution of the failed closure has moved to the right, having exceedance frequencies exactly a factor ten lower. Due to this shift, the hydraulic overload failure mechanism has the highest contribution to the exceedance frequency of the critical level (48%).

Figure 2.15 (right) and Table 2 reference show that the exceedance frequency of the critical level was lowered from $1.4 \cdot 10^{-4}$ to $4.2 \cdot 10^{-5}$ per year. Thus, a performance improvement of the failed closure of a factor 10 resulted in a flood frequency three times as low.

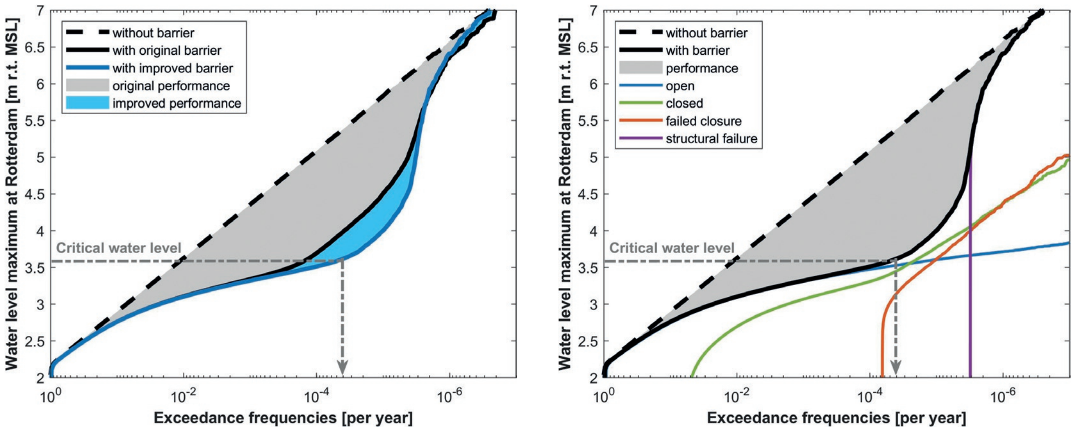

Figure 2.15: Exceedance frequencies with a performance improvement, which has lowered the probability of failed closure from 1/100 to 1/1000 on demand. Differences in performance for frequencies below 10^{-6} per year are caused by the inaccuracy of the Monte Carlo Simulation for lower frequencies.

Table 2: Overview of exceedance frequencies of the critical water level [per year] for the Analytical procedure, the Monte Carlo Simulation and the Performance improvement which has lowered the probability of a failed closure from 1/100 to 1/1000 on demand.

Failure mechanism	Analytical procedure	Monte Carlo simulation	Performance improvement
Operational f., forecast error	0	$1 \cdot 10^{-5}$	$1 \cdot 10^{-5}$
Hydraulic overload *	0	$2 \cdot 10^{-5}$	$2 \cdot 10^{-5}$
Operational f., failed closure	$1 \cdot 10^{-4}$	$1 \cdot 10^{-4}$	$1 \cdot 10^{-5}$
Structural failure	$1 \cdot 10^{-6}$	$2 \cdot 10^{-6}$	$2 \cdot 10^{-6}$
Total	$\mathbf{1.0 \cdot 10^{-4}}$	$\mathbf{1.4 \cdot 10^{-4}}$	$\mathbf{4.2 \cdot 10^{-5}}$

* Exceedance of the critical level is mainly (> 99%) caused by high river discharges accumulating behind the barrier, the contribution due to excessive barrier overflow is negligible.

Discussion

This study introduces a method for assessing the relative importance of various principal failure mechanisms in storm surge barrier systems. The method is transparent as it explicitly quantifies the performance of the storm surge barriers and shows how failure mechanisms contribute.

The method has several applications: It can detect weak spots of the coastal protection, as barriers often have a crucial position and, thus, their most important failure mechanism is likely to be such a weak spot. The method can also be used to aid decision-making with respect to effectiveness of maintenance and upgrades. For instance, if a more advanced forecasting system is considered, the method can indicate whether forecasting errors are the most important failure mechanism. If so, together with the economic optimization model by Mooyaart et al. (2023), the method can indicate the return on investment of a more advanced forecasting system.

Furthermore, the method is highly flexible. It can incorporate more detailed models to become more accurate, such as more advanced inner basin and structural models. The method can consider many barrier states, which might be useful for storm surge barriers with multiple gates (Eastern Scheldt barrier (the Netherlands) has 62) or inner basins that are affected by multiple structures (West Closure Complex (New Orleans, LA, USA) contains 11 pumps and a sector gate). More complex system failure mechanisms can be incorporated such as a barrier failure due to a collapse of the bed protection. In this scenario, the barrier gate(s) fail partially resulting in high flow velocities in the remaining opening.

Another example of a factor that could drive outcomes for other barriers is the role of spring astronomic tides. For instance, at the Thames barrier, sea level maxima dominated by astronomic spring tides can be well-predicted in advance and are not necessarily accompanied with bad weather. Storm surge dominated sea level maxima have unfavorable conditions and, thus, higher failure probabilities. It could be relevant to include this effect in the barrier state modelling.

Probabilistic methods such as presented in this chapter explicitly model uncertainty. Storm surge barriers have to deal with relatively large uncertainties as storm surges are rare, there are only a few dozens of storm surge barriers worldwide[3], each of them has unique characteristics and no barrier failures have been reported yet. As a result of this data sparsity, results are generally difficult to validate. Adding more complex models as suggested in the previous paragraph, can increase this validation challenge.

In this method, the effect storm surge barriers have on inner water levels is analyzed. For some barrier systems, the role of wind waves and flood duration is important as well. In Venice, for instance, the closure decision level is lower with more severe wind, as the inner waves are higher and are likely to cause more damage. If those parameters are relevant, the hydraulic load and subsequent performance definition and the corresponding probabilistic method should include these parameters.

In the case study, two probabilistic techniques were applied. The analytical technique was efficient and for failed barrier states equally accurate. The Monte Carlo Simulation was especially valuable with the closed barrier state, with more variables affecting inner water level maxima. An optimal balance between model efficiency and accurateness could be to use different probabilistic techniques per barrier state.

Conclusions

This study introduces a general method for evaluating how structural, operational and hydraulic overload failures in storm surge barriers affect the critical level exceedance frequency in the inner basin. The applicability of the method was demonstrated on the basis of a case study of the Maeslant barrier which protects Rotterdam (Netherlands). Applied to the Maeslant barrier in Rotterdam, the method identified

3 Mooyaart & Jonkman (2017) identified eighteen. I-storm (2021) presents an overview with 33 barriers using a wider definition than used in this chapter, but only five countries (Belgium, England, Italy, The Netherlands, USA) . Trace-Kleeberg et al. (2023) suggests that there are over 50 storm surge barriers.

the most significant failure mechanism: operational failure due to mechanical, electrical or control errors. Structural failure, hydraulic overload and forecast errors become more important if the probability of a failed closure is lowered by a factor of ten. Thus, it was proven that the method is able to assess multiple types of system failure mechanisms.

Given that coastal flood risk is rising, the method helps to get better insight into the weak spots of storm surge barriers in protecting the hinterland. Storm surge barrier managers can use the method to identify potential risk reduction measures and assess their effectiveness. Moreover, this method can be used to evaluate storm surge barrier improvements in coastal defense strategies against sea level rise.

Supplementary materials

The Matlab code developed for this chapter is available on
https://github.com/LeslieMooyaart/Storm-surge-barrier-performance/.

References

Christian, J., Fang, Z., Torres, J., Deitz, R., & Bedient, P. (2015). Modeling the Hydraulic Effectiveness of a Proposed Storm Surge Barrier System for the

Houston Ship Channel during Hurricane Events. *Natural Hazards Review*, *16*, 04014015. doi:10.1061/(asce)nh.1527-6996.0000150.

De Bruijn, K. M., Diermanse, F. L., Weiler, O. M., De Jong, J. S., & Haasnoot, M. (2022). Protecting the Rhine-Meuse delta against sea level rise: What to do with the river's discharge? *Journal of Flood Risk Management*, (pp. 1–15). doi:10.1111/jfr3.12782.

Deltares (2017). Stochasts for Flood Protection Assessment (*Dutch: Basisstochasten WBI-2017)*. Technical Report.

Diermanse, F. L., De Bruijn, K. M., Beckers, J. V., & Kramer, N. L. (2015). Importance sampling for efficient modelling of hydraulic loads in the Rhine–Meuse delta. *Stochastic Environmental Research and Risk Assessment*, *29*, 637–652. doi:10.1007/s00477-014-0921-4.

Dupuits, E. J., Schweckendiek, T., & Kok, M. (2017). Economic optimization of coastal flood defense systems. *Reliability Engineering and System Safety*, *159*, 143–152. URL: http://dx.doi.org/10.1016/j.ress.2016.10.027. doi:10.

1016/j.ress.2016.10.027.

Dutch Law on Water (Dutch: Waterwet), (2021), URL: https://wetten.overheid.nl/BWBR0025458/2021-01-01.

Geerse, C. (2010). Summary of probabilistic models for fresh water *(Dutch:*

Overzichtsdocument probabilistische modellen zoete wateren Hydra-VIJ , Hydra-B en Hydra-Zoet). Technical Report HKV and Rijkswaterstaat.

Gouldby, B., & Sayers, P. (2009). A methodology for regional-scale flood risk assessment. *Water Management*, doi:10.1680/wama.2009.00084.

HKV (2006). *Achterlandstudie Maeslantkering, Hydra-B*. Technical Report.

HKV (2011). *Hydra-Zoet for the freshwater systems in the Netherlands Probabilistic model for the assessment of dike heights*. Technical Report December. URL: http://publicaties.minienm.nl/download-bijlage/23355/ hydra-zoet-for-the-fresh-water-system-in-the-netherlands.pdf.

I-storm (2021), *Storm surge barriers within the I-STORM network*, Retrieved August 27, 2024, from https://www.i-storm.org/initiatives/downloads

Janssen, J., van Ieperen, A., Kouwenhoven, B., Nederend, J., Pruijssers, A., & de Ridder, H. A. (1994). The design and construction of the New Waterway storm surge barrier in the Netherlands. In *28th PIANC World Congress -*

Seville, Spain. Seville.

Janssen, J. P., & Jorissen, R. E. (1992). Integrating forecast effects and operational behaviour in designing the Rotterdam storm surge barrier. In *Floods and Flood Management. Fluid Mechanics and its Applications* January. Dordrecht: Springer. doi: https://doi.org/10.1007/978-94-011-1630-5_22.

Yara Kharoubi, Martine van den Boomen, Johan van den Bogaard & Marcel Hertogh (19 Aug 2024): Asset management for storm surge barriers: how and why?, Structure and Infrastructure Engineering, DOI: 10.1080/15732479.2024.2391034

Ministerie van Verkeer en Waterstaat (1990). *Design Formulae for Hydraulic*

Structures (Dutch: rekenregels voor Waterbouwkundig Ontwerpen). Technical Report. URL: https://repository.tudelft.nl/islandora/object/uuid: 2fe77080-bf43-4c06-80b4-4d7ce84f7b70/datastream/OBJ/download.

Mooyaart, L. F., Bakker, A. M. R., van den Bogaard, J. A., Rijcken, T., & Jonkman, B. (2023). Economic optimization of coastal flood defense systems including storm surge barrier closure reliability. *Journal of Flood Risk Management*. URL: https://onlinelibrary.wiley.com/doi/10.1111/jfr3. 12904. doi:10.1111/jfr3.12904.

Mooyaart, L. F., & Jonkman, S. N. (2017). Overview and Design Considerations of Storm Surge Barriers. *Journal of Waterway, Port, Coastal, and Ocean Engineering*, *143*, 06017001. doi:10.1061/(asce)ww.1943-5460.0000383.

Rijcken, T., Mooyaart, L.F., Oerlemans, C., Van der Ziel, F., Borghans, J., Botterhuis, T., Winden, A. V., Jorissen, R.E. & Kok, M. (2023). It takes two to tango with sea level rise. *TU Delft DeltaLinks*, (pp. 1–16). URL: https://flowsplatform.nl/{#}/ it-takes-two-to-tango-with-sea-level-rise-1682542508929.

Rijkswaterstaat (1986). *Design documents Eastern Scheldt barrier [Dutch: Ontwerpnota Oosterscheldekering]*. Technical Report. URL: https://repository.tudelft.nl/islandora/object/uuid%3Adda73a61-a199-4e6b-ad8c-6dd8a68bf147

Rijkswaterstaat (2022). *Legal assessment trajectory 218, Eastern Scheldt barrier [Dutch: Wettelijke beoordeling traject 218, Oosterscheldekering]*. Technical report.

Schlumberger, J., Ferrarin, C., Jonkman, S. N., Loaiza, A. D., Antonini, A., & Fatori, S. (2021). Developing a framework for the assessment of current and future flood risk in Venice, Italy. *Natural Hazards and Earth System Sciences Discussions*, (pp. 1–30). URL: https://nhess.copernicus.org/ preprints/nhess-2021-272/. doi:10.5194/nhess-22-2381-2022.

Trace-Kleeberg, S., Haigh, I. D., Walraven, M., & Gourvenec, S. (2023). How should storm surge barrier maintenance strategies be changed in light of sea level rise? A case study. *Coastal Engineering*, 184, p.104336.

Vader, H., Bakker, A. M., Jonkman, S. N., van den Boomen, M., van Baaren, E., & Diermanse, F. L. (2022). A framework for assessing the remaining life of storm surge barriers. *Journal Structure and Infrastructure Engineering*.

van Berchum, E. C., Mobley, W., Jonkman, S. N., Timmermans, J. S., Kwakkel, J. H., & Brody, S. D. (2019). Evaluation of flood risk reduction strategies through combinations of interventions. *Journal of Flood Risk Management*, *12*, 1–17. doi:10.1111/jfr3.12506.

Zhong, H., van Overloop, P. J., van Gelder, P., & Rijcken, T. (2012). Influence of a storm surge Barrier's operation on the flood frequency in the rhine delta area. *Water (Switzerland)*, *4*, 474–493. doi:10.3390/w4020474.

3

Economic optimization of closure reliability requirements[5]

5 This chapter is largely based on Mooyaart, L. F., Bakker, A. M. R., van den Bogaard, J. A., Rijcken, T., & Jonkman, B. (2023). Economic optimization of coastal flood defence systems including storm surge barrier closure reliability. *Journal of Flood Risk Management,* 16(3), doi:10.1111/jfr3.12904.

The introduction, discussion and concluding remarks were adapted to improve readability and consistency in this thesis. Moreover, the discussion responds to a study performed by Rijkswaterstaat to investigate the effectiveness of a double barrier at the Maeslant barrier.

The previous chapter compared the importance of operational failures relative to other failure mechanisms (structural, hydraulic overload). When the lack of closure reliability is the dominant failure mechanism, measures may be necessary. However, it is uncertain to what extent such measures are required.

To tackle this issue, this chapter presents a model that balances the cost of measures at the barrier, cost of raising interior flood defenses and (monetized) flood risk. This model builds upon the well-known optimization model for dike raising by Van Dantzig (1956) to include options for reducing the probability of failed closures.

Section 3.1 presents the current state-of-the-art literature on economic decision-making in flood risk management. Section 3.2 describes the economic optimization model. Sections 3.3 and 3.4 illustrate the model using a case study (Maeslant barrier, Rotterdam) and its results, respectively. Sections 3.5 and 3.6 discuss and conclude the chapter.

3.1 Introduction

In the previous chapter, it was established that there are three principal system failure mechanisms: operational failure, structural failure and hydraulic overload. Yet, at four out of the five regions protected by Dutch storm surge barriers, the risk of operational failures, specifically the risk of a failed closure, is the largest (Maeslant barrier (previous chapter); Hollandsche IJssel barrier (Vader et al., 2022)) or the second largest (Eastern Scheldt barrier (Rijkswaterstaat, 2008), Ramspol (Rijkswaterstaat, 2002)). Therefore, it is expected that the risk of non-closure, i.e., the lack of closure reliability, is important for storm surge barriers outside the Netherlands as well.

Closure reliability is defined as the frequency that the barrier successfully closes in severe storm conditions which otherwise would result in interior flood defense failure and consequent coastal flooding. A coastal flood occurs if both the storm surge barrier fails to close and secondary protection behind the barrier collapses. Many technical components, such as operating mechanisms, drives, switchboards, and computers, but also on the reliability of operating and maintenance staff, affect the ability to close (Lewin et al., 2003). Although individual components are often highly reliable, the number of components and maintenance and operation actions can accumulate to probabilities of non-closure around 1:100 on demand (Maeslant & Eastern Scheldt barrier).

Although relevant, current economic decision-making models do not include closure reliability. Most recent developments in coastal flood risk decision-making focus on the effect of uncertainty or robustness of measures (Haasnoot et al., 2013; Kim et al., 2019; Ruig et al., 2019; Van der Pol et al., 2021). Groves and Sharon (2013) explore a wide range of flood risk reduction measures, and Aerts et al. (2014) even include storm surge barriers, but they do not consider improving closure reliability. Kind (2014) and Eijgenraam et al. (2017) built upon the well-known Van Dantzig model, balancing dike raise cost and coastal flood risk. These models are, however, only suitable for optimizing a single flood defense. As non-closure of a storm surge barrier can only lead to coastal floods if secondary flood protection fails as well, an economic decision-making model is required which can handle double barrier systems. The CPB Netherlands Bureau for Economic Policy Analysis (2013) and Dupuits et al. (2017) address these types of systems. However, they only consider structural and overtopping failure modes, which are often not dominant for coastal flood defense systems with storm surge barriers. Consequently, no economic optimization models are available which include closure reliability as a parameter.

This chapter presents an economic optimization model for a coastal flood defense system with a storm surge barrier, which takes closure reliability into account. It was chosen to include closure reliability into the simple, but widely used economic optimization model of Van Dantzig (1956) for two reasons: First, the model of van Dantzig is analytical and, therefore, relatively simple. As Vezér et al. (2018) indicate, simple economic decision-making models are better affordable, more transparent, and more amenable to reproducibility and scrutiny. Moreover, simpler models can assess a wider range of options and scenarios, as Van Berchum et al. (2019, 2020) and Ceres et al. (2019, 2022) promote. They also help in policy-making preceding more detailed analyzes supporting the final investments. Second, the model optimizes dike raise, which is still a popular flood risk reduction measure in the Netherlands. Other measures such as improving evacuation or raising hinterland are considered, but are not applied. Figure 3.1 indicates the principle of the model of Van Dantzig (1956) and how closure reliability is added to this model.

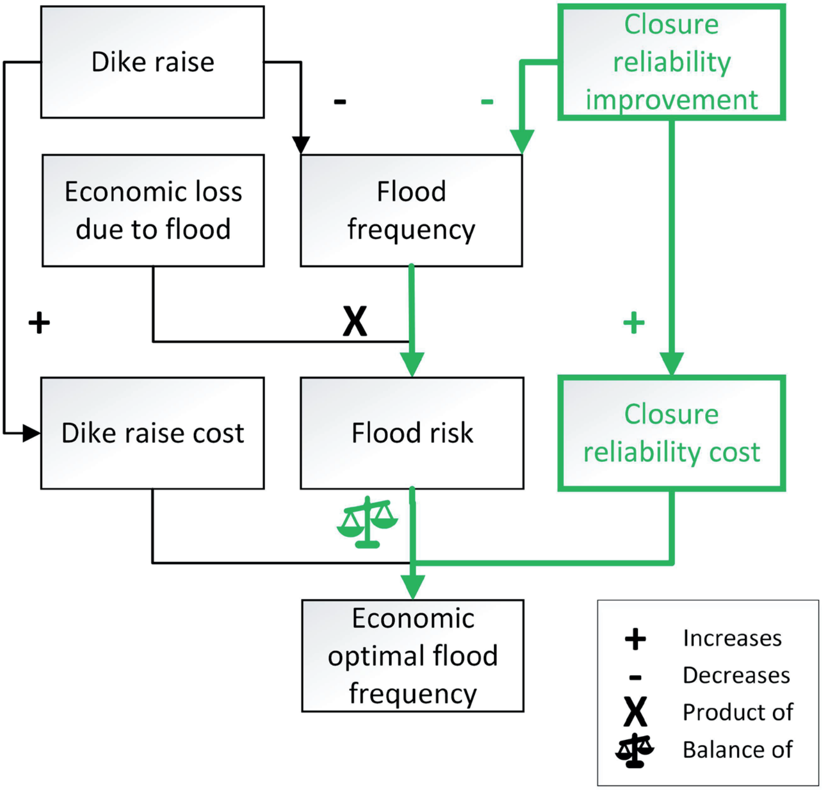

Figure 3.1: Process to find economic optimal flood frequencies. In black, the principle of the model of van Dantzig (1956) is shown. In green, the addition proposed by this chapter is indicated.

The model is applied to the region protected by the Maeslant barrier (Rotterdam, the Netherlands), which is presented in section 3. Section 4 shows the results of the optimization, where the effect of sea level rise is also explored. Section 5 discusses the model, followed by concluding remarks in section 6.

3.2 Optimization model

3.2.1 Optimization problem

In this optimization problem, investments in closure reliability (C_{SSB}) are looked into as well as raising polder dikes behind the barrier (C_D). Investments in both measures reduce flood frequency in the polder and, thus, lower coastal flood risk. Here, coastal flood risk is expressed as the present value of expected damage over the considered lifetime *R* [M€]. The economic optimal solution has the lowest total cost *TC* [M€], i.e., the lowest sum of investment cost and expected damage:

$$min(TC) = min\left(C_{SSB} + C_D + R\right) \quad (1).$$

3.2.2 Flood frequency

Figure 3.2 presents a schematic top view of the basic coastal defense system considered in this chapter. Figure 3.3 shows the corresponding schematic cross-section. As these figures indicate, both the storm surge barrier and the dike need to fail before a coastal flood takes place. These two failure events are considered to be independent of each other. Hence, the flood frequency F_f [per year] is

$$F_f = F_D \cdot P_{NC} \quad (2).$$

In which F_D is the failure frequency of a dike [per year] and P_{NC} is the probability of non-closure [on demand]. In this chapter, consistently frequency, with the corresponding symbol *F*, is used to describe the likeliness of an event to occur for a specified unit of time, in our case a year. For the likeliness of other events such as that of non-closure, the term probability with the corresponding symbol *P* is applied.

Independence for the risk of non-closure is often assumed (see for instance HKV, 2006 and Vader et al., 2022), as failure of the dike mainly depends on the extreme water level and closure reliability does not. Unavailability of electro-mechanical equipment often occurs in rest, due to dormant failures or equipment being under repair. Other unavailability of electro-mechanical equipment is related to the hydraulic conditions at the closure, which are not necessarily related to those at the peak of the storm.

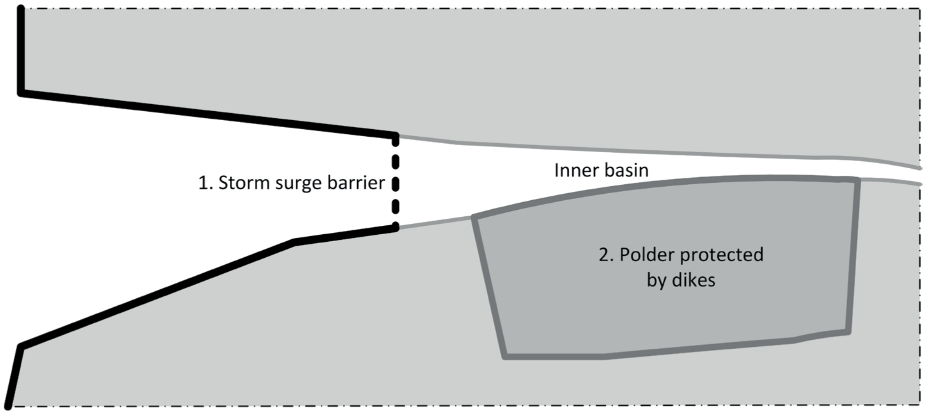

Figure 3.2: Schematic overview of a storm surge barrier flood protection system with one polder considered for the economic optimization model.

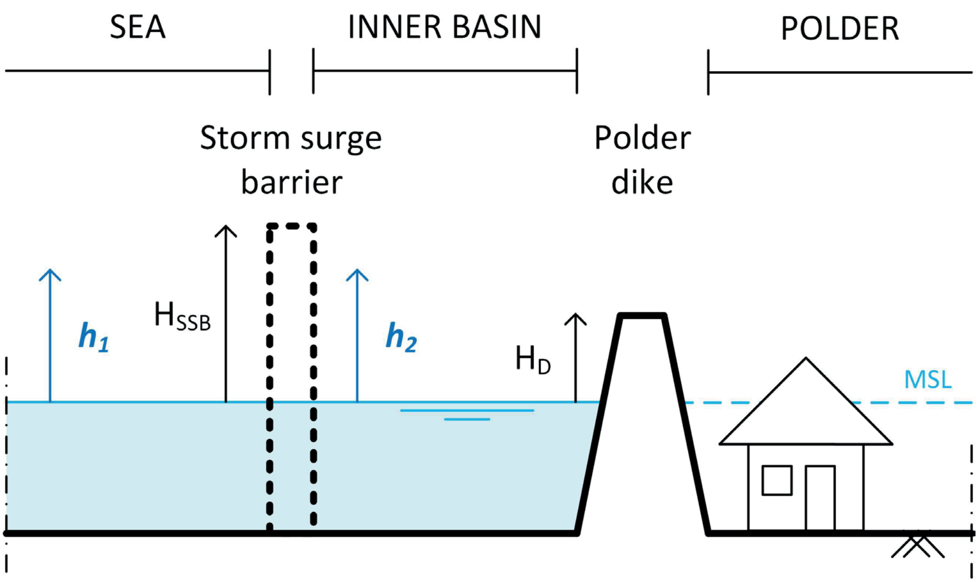

Figure 3.3: Schematic cross-section of a storm surge barrier flood protection system with one polder considered for the economic optimization model.

Software reliability is related to the complexity of the software, the production process, quality of software engineers and quality of testing (Van Manen et al., 2015). Reliability of human operation depends on staff and training quality (Lewin et al., 2003). None of these main reasons for non-closure is, however, related to the water level. Only non-closure due to a too low water level forecast depends on the extreme water level (Janssen and Jorissen, 1992). Often the closure criteria are chosen in a way, that this risk is insignificant. Therefore, the effect of the water level forecast error is neglected in this chapter.

The failure probability of dikes highly depends on the water level. For many failure modes such as inner slope erosion due to overflow & overtopping, geotechnical stability and groundwater erosion, the water level is the most important load. Other loads such as wind waves are often related to the water level as well, as basins behind the barrier are often shallow. A modern approach is to consider the uncertainties in strength, load and models using fragility curves. The failure frequency of dikes is then a result of the frequency of extreme water levels and the probability of the dike failing given that extreme water level (Lendering et al., 2018).

As the main interest of this study is the basic choice between storm surge barrier and dike investments, a simplified approach is adopted. It is assumed that dikes resist the water level until a certain critical height H_D [meter r.t. mean sea-level (MSL)] (see Figure 3.3). Beyond this critical height, the dike will breach. Although this approach might seem highly simplified compared to the approach of Lendering et al. (2018), the optimization is not expected to be affected too much as in each approach the water level remains the most important factor. Both in older (van Dantzig, 1956) as more recent economic optimization models (Jonkman et al., 2009; Eijgenraam et al., 2014; Kind, 2014) the simplified approach was adopted to find optimal flood frequencies.

For the extreme water level distribution, an exponential distribution is used as initially proposed by Wemelsfelder (1939) and applied by Van Dantzig (1956). Although for extreme water level prediction, other extreme value distribution types such as the Generalized Extreme Value distribution are more common (Arns et al., 2013), the exponential distribution type has remained popular for economic optimization (Jonkman et al., 2009; Eijgenraam et al., 2017; Lendering et al., 2015; Dupuits et al., 2017). Furthermore, it is assumed that the water level in front of the dike h_2 is equal to the sea water level h_1, if the barrier is not closed. Hence, the exceedance probability of critical water levels H_D [meter r.t. MSL] is

$$F_D = F(h_1 > H_D) = 10^{-\frac{H_D - H_A}{H_B}} \quad (3).$$

In which h_1 is the sea water level [meter r.t. MSL], H_A [meter r.t. MSL] is the water level which is exceeded annually on average. The distribution parameter H_B is the decimal height [meter]. With an increase of one decimal height, the extreme water level is ten times less likely to occur. Combining equations 2 and 3 results in the following equation for flood frequency:

$$F_f = 10^{-\frac{H_D - H_A}{H_B}} \cdot P_{NC} \qquad (4).$$

3.2.3 Flood risk

Flood risk can be simplified to the product of flood frequency and its adverse economic consequences, when two assumptions are made (Lendering et al., 2020). First, the critical height approach has to be adopted, as was described in the previous section. Second, any dike breach is assumed to lead to maximum flood damage. At deep polders, a dike breach fills the polder with flood depths of several meters. With flood depths of one to two meter, flood damages tend to be close to maximum damage. Wing et al. (2020) show this flood damage behavior for the deep polders of New Orleans. Therefore, at a deep polder, the loss D [M€] can be related to the sea water level h_1 [meter r.t. MSL] in the following manner:

$$D = \begin{cases} 0 & if\, h_1 < H_D \\ \widehat{D} & if\, h_1 \geq H_D \end{cases} \qquad (5).$$

Here, $\widehat{D}$ is the maximum flood damage [M€].

To compare cost of flood risk reduction measures with residual flood risk, the present value of residual flood risk (R) needs to be determined. This value depends on interest, sea level rise, and the economic development in the protected area. Van Dantzig (1956) showed how the reduced discount rate δ′ could be applied to account for all these effects. This approach, however, only accounts for sea level rising at a constant rate. As almost all current sea level projections show an accelerated pace, the reduced discount rate is calculated for each year:

$$\delta' = \delta - \gamma - \beta \qquad (6).$$

In which δ is the interest rate [per year], γ is the rate of economic growth and consequent damage increase [per year], and β is the rate at which flood risk increases due to (relative) sea level rise [per year]. This latter rate β is equal to

$$\beta = \frac{r_{SLR}}{H_B} \cdot \ln 10 \qquad (7).$$

with r_{SLR} being the amount of sea level rise [meter/year].

A period of 100 years is applied, as flood risk reduction measures often have a long lifetime. With this approach, the present value of the residual flood risk R [M€] is

$$R = F_f \cdot \widehat{D} \cdot \sum_0^{100} (1 + \delta')^{-t} \quad (8),$$

with t being the number of years after the construction year of the flood protection measure [year].

3.2.4 Cost functions

For the cost functions, the present value of the flood risk reduction measures is required. Therefore, the cost functions include construction, maintenance and operation cost. Although future sustainability is an important part of investment considerations, the present value of the replacement after 100 years is small and, therefore, neglected in this chapter.

Like Van Dantzig (1956) and Jonkman et al. (2009), a cost relation for dike raise is taken which consists of fixed cost and linearly rising cost with dike raise:

$$C_D = C_{D,0} + k_D \cdot (H_D - H_{D,0}) \quad (9).$$

Here, C_D is the dike raise cost [M€], $C_{D,0}$ [M€] is the fixed investment cost, k_D is the additional cost per meter dike raise [M€ per m], $H_{D,0}$ is the initial critical dike level [meter r.t. MSL] and H_D is the raised critical dike level [meter r.t. MSL]. Van Dantzig (1956) stressed that the linear approximation is only valid for small dike raises. Eijgenraam et al. (2014), therefore, proposed to apply an exponential cost relation. Kind (2014), however, demonstrates that the results of Eijgenraam et al. (2014) can be linearized. Moreover, empirical studies of the cost of dike raises could only find a linear relation (Jonkman et al., 2013; Lenk et al., 2017; Aerts, 2018), most likely due to the relatively large variation in cost. A linear cost function for dike raise, therefore, seems reasonable. Similarly, maintenance cost of dike raise is not well known. Therefore, it is assumed that the dike raise cost include maintenance and, therefore, refers to the present value.

For the case, both the construction and the maintenance and operation cost of the Maeslant barrier are used. The cost of improving closure reliability is not well known. For this chapter, it is assumed that there are a discrete number of closure reliability improvements.

3.2.5 Optimization of total cost

This section explains how to find the solution with the least total cost, i.e., the optimal solution. To optimize more effectively, three steps are introduced to narrow the selection of solutions. Only for the selected solutions, the total costs are determined. The objective of this approach is to only investigate amount of dike raises which can be optimal.

In the first step, dike raise is optimized without considering any closure reliability improvement, applying the model of Van Dantzig:

$$\Delta\breve{H}_D = H_A - H_{D,0} - H_B \cdot log\left(\frac{k_D \cdot H_B}{ln(10) \cdot \widehat{D} \cdot \Sigma(1+r)^t}\right) \quad (10).$$

From this equation, it can be recognized that the optimal amount of dike raise is the sum of the yearly exceeded water level H_A, the initial dike height $H_{D,0}$ and a certain amount of decimal heights to optimally balance dike raise cost and risk. The term

$$\breve{F}_{f,D} = \frac{k_D \cdot H_B}{ln(10) \cdot \widehat{D} \cdot \Sigma(1+r)^t} \quad (11).$$

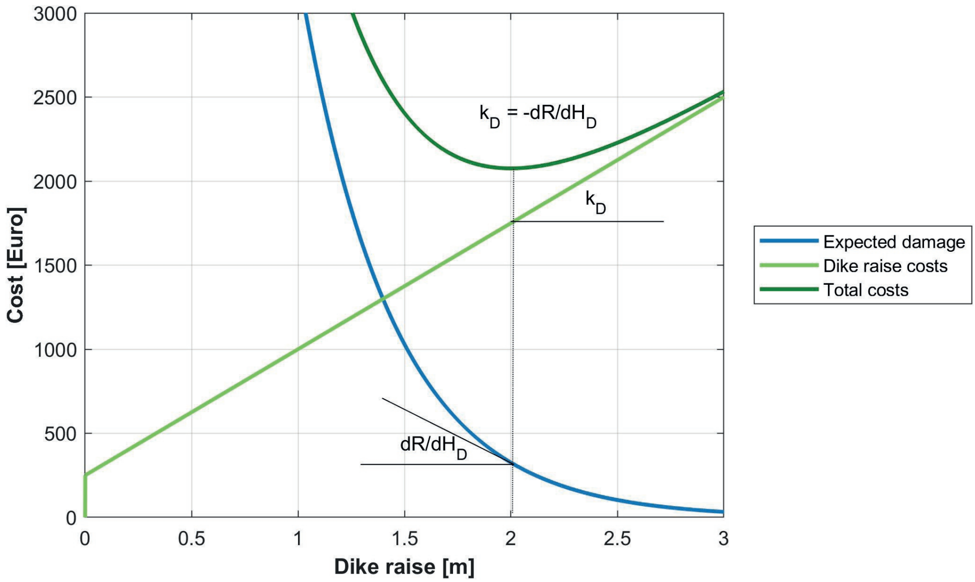

Figure 3.4: Classic optimization of dike raise with parameters: fixed costs dike raise $C_{D,0}$ = 250 M€, variable cost dike raise k_D = 750 M€, initial dike height $H_{D,0}$ equal to yearly exceeded water level H_A, decimal height H_B = 1.0 meter, maximal flood damage $\widehat{D}$ = 650 M€, reduced discount rate *d'* = 2%. The optimal solution is a dike raise of 2 meter, corresponding to a flood frequency of 1/100 years. At this optimum, the increase in dike raise cost (k_D) is opposite to the decline in risk (dR/dH_D).

corresponds to the optimal flood frequency with dike raise $\check{F}_{f,D}$ [per year]. Figure 3.4 shows the principle of Van Dantzigs optimization method. At the optimal amount of dike raise (and flood frequency), the dike raise cost increases with the same rate that coastal flood risk declines (see Figure 3.4).

In the second step, the amount of dike raise is optimized for every closure reliability improvement, using a similar approach. With the use of equations 2 and 11, the optimal failure frequency of the dike is established, including the probability of non-closure:

$$\check{F}_D = \frac{k_D \cdot H_B}{P_{NC} \cdot ln(10) \cdot \hat{D} \cdot \Sigma(1+r)^t} \quad (12).$$

The optimal amount of dike raise is then

$$\Delta\check{H}_D = H_A - H_{D,0} - H_B \cdot log\left(\check{F}_D\right) \quad (13).$$

To re-evaluate the equations, a storm surge barrier is considered with a probability of non-closure of 1/100. Equation 12 shows that the optimal dike frequency is a factor 100 higher. This higher optimal dike frequency results in an optimal amount of dike raise which is two decimal heights lower.

Figure 3.5 shows another example to explain how to optimize combinations of closure reliability improvements and dike raise. Figure 3.5 is based on Figure 3.4, but has a closure reliability improvement, which costs 1000 M€ and has a probability of non-closure of 4/100 per request. This improvement is illustrated with a grey arrow. The risk without any dike raise is 1300 M€, resulting in a total cost of 2300 M€, indicated with a black square. The light green line shows the additional cost for dike raise, which are the same as in Figure 3.4. As the risk curve and the dike raise costs are equal to the previous figure, also the optimum flood frequency is (10^{-2} per year). Hence, the optimal solution is to additionally raise the dike by 0.6 meter. This combination of improvements leads to a total cost of 2000M€, which is lower than 1) closure reliability alone and 2) dike raise alone.

Closure reliability improvements can lower flood frequency beyond the optimal flood frequency of dikes. In those cases, additional dike raise is never optimal anymore. Likewise, if closure reliability improvements lower flood frequency close to the optimal flood frequency of dikes, additional dike raise is infeasible. These additional dike raises are small, resulting in the cost being higher than the risk reduced. To overcome this issue, a selection criterion is introduced: the minimal amount of dike

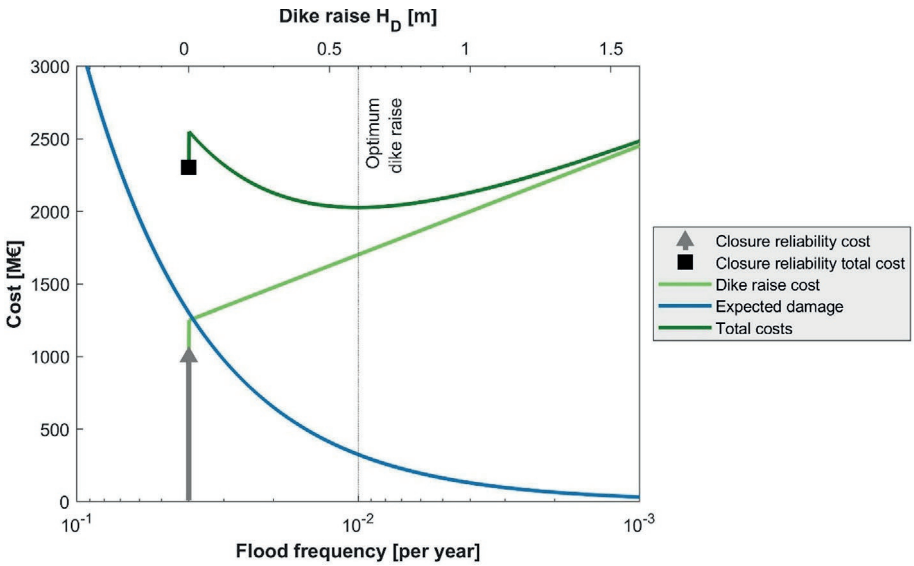

Figure 3.5: Optimization with storm surge barrier improvement. Dike raise parameters are the same as the previous figure. Storm barrier improvement with a cost of 1000 M€ has a probability of non-closure of 4/100 requests. The optimal solution is to combine this improvement with a dike raise of 0.6 meter, resulting in a flood frequency of 1/100 years.

raise. At the minimal amount of dike raise, cost is exactly equal to the risk reduction dike raise achieves. This minimal amount of dike raise ΔH_{min} [meter] is (see Appendix A for the derivation)

$$\Delta H_{min} = H_B \cdot \left(\frac{\Delta H_{min} \cdot \ln 10}{H_B} + \frac{C_{D,0} \cdot \ln 10}{k_D \cdot H_B} + 1 \right) \quad (14).$$

In the final step, the optimal solution of the selected solutions is found using equation 1.

3.3 Maeslant barrier case

3.3.1 Area and potential flood damages

The Rhine and the Meuse flow in the North Sea at the south-western part of the Netherlands (see Figure 3.6). After the catastrophic 1953 flood, many of the river branches were closed off by dams. Because of the importance of the local port (Rotterdam), this waterway remained open. To balance flood risk and navigation

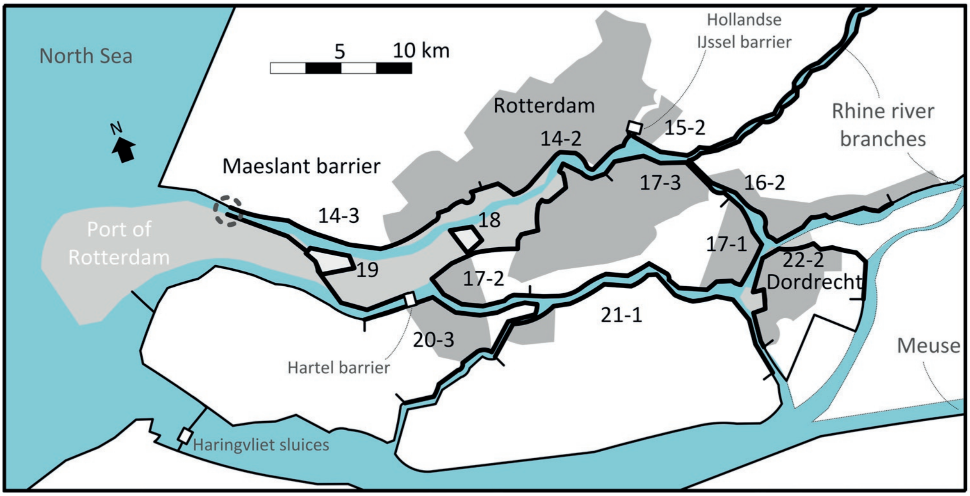

Figure 3.6: Map of dike ring parts (indicated with thick solid lines) significantly affected by the risk of a coastal flood due to the non-closure of the Maeslant barrier. Dike ring part numbers correspond to those presented by the Ministry of Infrastructure and Environment (2016). Thinner solid lines indicate dike rings which are not significantly affected by the Maeslant barrier. Thin dotted lines indicate river contours. Blue surfaces represent water bodies. Dark grey surfaces highlight inhabited areas behind dikes, while light grey indicates developed areas which are not protected by river dikes. Important hydraulic flood defense structures are presented with a square box.

interests, a storm surge barrier was constructed: The Maeslant barrier (construction year 1997). The model is illustrated on the basis of a case with this barrier.

The Maeslant barrier has most effect on floods directly behind the barrier. About 65 kilometer upstream, flood risk depends only on river discharges. In nearby river branches, other hydraulic structures the Haringvliet sluices and the Hollandsche IJssel barrier also affect flood risk. Therefore, with a more reliable Maeslant barrier, flood risks following from river discharge or malfunctioning hydraulic structures become relatively more important. Hence, improving reliability of the Maeslant barrier reduces the size of the area influencing coastal flood risk and vice versa. For this case though, this dependency is ignored and, therefore, the size of the area influenced by Maeslant barrier is assumed to be constant. The area which is influenced with the current closure reliability of the Maeslant barrier, is based on the study of HKV (2006).

A nationwide study was performed to estimate flood damages from dike breaches. Jongejan et al. (2013) describe the method applied to estimate flood damages. The results were reported per dike ring part, i.e., a part of a dike ring where breaches result in approximately the same amount of damage (Ministry of Infrastructure and Environment, 2016). Table 3.1 provides expected flood damages for the dike ring parts affected by the Maeslant barrier.

Table 3.1: Flood damages and costs to raise dikes at dike ring parts significantly affected by closure reliability of the Maeslant barrier.

Dike ring part name	Code	Flood damage (2011) [M€]	Costs to raise safety level with factor 10 [M€]
Zuid-Holland	14-2	12000	132
	14-3	1700	89
Krimpenerwaard	15-2	19000	180
Alblasserwaard	16-2	12000	371
IJsselmonde	17-1	780	119
	17-2	2600	153
	17-3	11000	24
Pernis	18-1	240	10
Rozenburg	19-1	1100	91
Voorne-Putten	20-3	5300	89
Hoekse Waard	21-1	1000	100
Eiland van Dordrecht	22-2	5300	226
Total		**72020**	**1584**

The following parameters are applied for the extreme water level distribution: a yearly exceeded water level H_A of 2.1 m and a decimal height H_B of 0.75 m. Van Dantzig also applied these values. For frequencies between 1/100 and 1/100,000 years, the distribution corresponds well to the Generalized Pareto Distribution, which Deltares (2013) currently proposes to apply in flood risk assessments.

3.3.2 Reduced discount rate

The reduced discount rate consists of four elements: interest, economic growth, and sea level rise. For the development of flood safety standards in the Netherlands, an interest rate of 5.5% and an economic growth of 2% were applied (Kind, 2014), which are applied to this case as well. For sea level rise, the SSP2-4.5 scenario of the KNMI (2021) is used, which is the middle of the three sea level projections presented. Linear regression is applied to describe the rate of sea level rise:

$$r_{SLR} = 4.4 \cdot 10^{-5} \cdot (t + t_r) + 4.6 \cdot 10^{-3} \quad (14),$$

in which t is the year number and t_r is a correction for the year of investment relative to the year of the sea level projection. As the sea level projection starts in 2005, while the price level of flood damages originates from 2011, a correction of six years is applied (t_r=6).

3.3.3 Storm surge barrier

The Maeslant barrier probability of non-closure estimate is based on an extensive risk analysis using fault trees. A fault tree is a graphical model with logic gates that displays the various combinations of equipment failures, dependent failures, and human failures. Boolean algebra is used to quantify the probability of the top event (Henley and Kumamoto, 1981). The probability of non-closure of the Maeslant barrier is approximately 1/100 per request.

Currently, no cost function is available for improvements with respect to this probability of non-closure. Therefore, a cost function is proposed, using the existing Maeslant barrier as a reference. With respect to this reference, one major down- and upgrade is taken: a barrier without redundant systems and a redundant barrier, respectively. A simplified fault tree of the Maeslant barrier is used to estimate the probabilities of non-closure. Figure 3.7 shows the fault tree for this storm surge barrier. All base systems are assumed to have the same failure probability: 1/100 per request. All backup systems are two times more likely to fail (1/50 per request). With this fault tree, probabilities of non-closure can be calculated in a simple manner with the use of two assumptions. First, the basic events are assumed to be independent. With an AND-gate, failure probabilities of basic events can then be multiplied to find the failure probability. Second, with OR-gates, as failure probabilities of the basic events are sufficiently small, the probability can be summed to estimate the failure probability. As a result, a single barrier with redundant systems has a probability of non-closure of 1/100 per request, similar to the existing Maeslant barrier. The barrier without redundancies has a probability of non-closure of 1/25 requests. The double barrier is about 10 times as reliable as the single barrier (see appendix B).

For the cost of these three arrangements, actual construction cost and annual maintenance cost are used. The construction cost was retrieved from Mooyaart and Jonkman (2017) and corrected for the price level of 2011 (640 M€). Aerts et al. (2013) provided the maintenance cost: 15 M€/year. Both the construction as the maintenance cost of the improvements of the power supply, control, and decision system is set at 10% of these costs, as generally, the costs of these systems are smaller than the cost of the storm surge barrier gate. A redundant barrier is assumed to have the same construction and maintenance cost as the initial barrier.

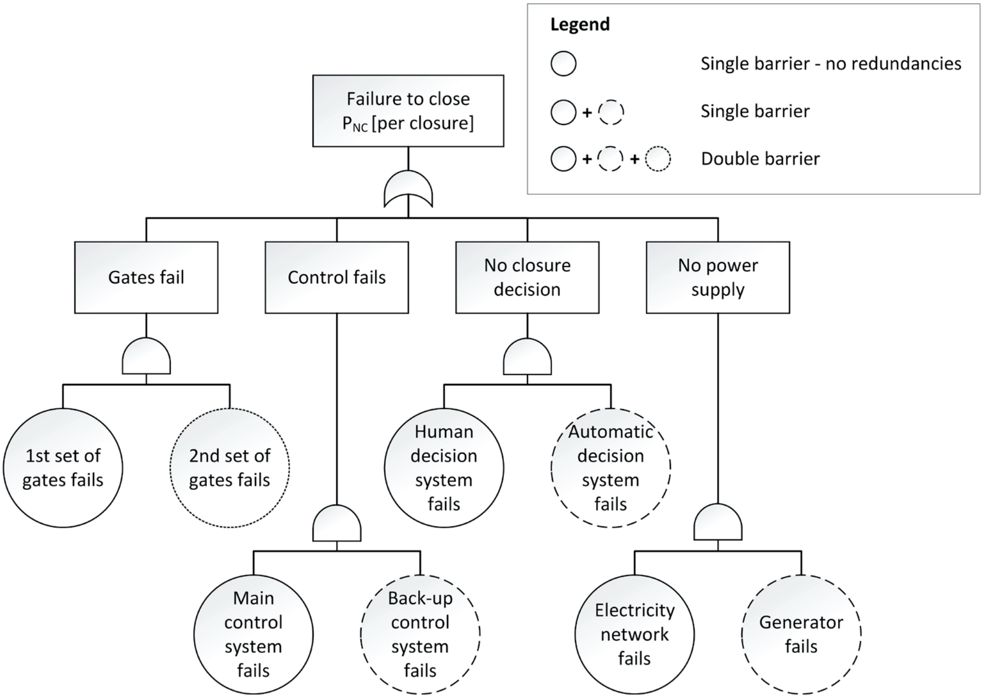

Figure 3.7: Simplified fault tree proposed for Maeslant barrier case. Basic events belonging to all storm surge barrier arrangements are indicated with solid borders. Basic events corresponding to a single and double barrier have dashed borders. The double barrier has an added basic event with a dotted border.

Table 3.2 shows the failure probabilities of the storm surge barrier systems and their redundancies. Table 3.3 presents the results of the fault tree analysis for the three storm surge barrier arrangements.

Table 3.2: Probabilities of basic events leading to failure of subsystems [on demand] of simplified fault tree for Maeslant barrier.

Item	Main system	Backup system	Combined
Gate	$1 \cdot 10^{-2}$	$2 \cdot 10^{-2}$	$2 \cdot 10^{-4}$
Power supply	$1 \cdot 10^{-2}$	$2 \cdot 10^{-2}$	$2 \cdot 10^{-4}$
Control	$1 \cdot 10^{-2}$	$2 \cdot 10^{-2}$	$2 \cdot 10^{-4}$
Decision	$1 \cdot 10^{-2}$	$2 \cdot 10^{-2}$	$2 \cdot 10^{-4}$

Table 3.3: Maeslant barrier closure reliability improvement cost relation

#	Storm surge barrier arrangement	Cost [M€]	Probability of non-closure P_{NC} [per request]
0	No barrier	0	1
1	Single barrier – no redundancies	810	$4.0 \cdot 10^{-2}$
2	Single barrier	900	$1.1 \cdot 10^{-2}$
3	Double barrier	1800	$8.0 \cdot 10^{-4}$

3.3.4 Dike raise

Dikes along the inner basin of the Maeslant barrier vary in height and strength. Some dikes were already raised to resist sea water levels without a storm surge barrier and are, therefore, over-dimensioned up to about 2 meters. On the other hand, many dikes such as those in the city center of Rotterdam and Dordrecht proved difficult to raise, motivating the construction of a storm surge barrier. The existing dike in the city center of Rotterdam is expected to breach with water levels higher than MSL + 3.6 meter (Janssen and Jorissen, 1992). On average, this water level is expected to be exceeded once every 100 years without a storm surge barrier, corresponding with the exponential distribution proposed. For this case, this level is used as the initial dike critical water level of all dike ring parts considered. Furthermore, all dike ring parts are assumed to fail if the critical water level is exceeded. Moreover, only dike raise of all the dike ring parts combined is explored.

For the study on flood safety standards, linear dike raise costs were reported (The Ministry of Infrastructure and Environment, 2016). The dike raise cost mentioned is the cost to lower the probability of dike failure with a factor 10 (corresponding to the product of dike raise cost per meter and decimal height: $k_D \cdot H_B$). Table 3.1 presents the cost per dike ring part.

No fixed cost is applied in this case. The Ministry of Infrastructure and Environment (2016) does not report any fixed cost. Moreover, Lenk et al. (2017) did not find any data to support fixed dike raise cost. Current dike raise optimization models often use other approaches to avoid small yearly raises. Brekelmans et al. (2012) assumed that dike raises are designed for a period of at least 40 years. In the results they present, the minimal dike raise is 25 centimeters. Van Dantzig (1956) used a minimal dike raise of one meter. In the result section, the relevance of estimating fixed cost is reflected upon.

3.4 Results

Before addressing the improvements, the risk without any measure is reflected upon. Appendix C presents the present value calculation of flood damages, showing that the present value of all 100 years ($(\hat{D}\Sigma(1+d')^{t})$) amounts to $4.2{\cdot}10^{6}$ M€. Without any measure, the expected damage is $4.2{\cdot}10^{4}$ M€ (see Figure 3.8). This is a factor 100 lower as the dike breaches every 100 years on average.

Then, the optimization method is used to select solutions. First, the optimal amount of dike raise is found without storm surge barrier closure reliability improvements. This is 1.4 meter (equation 10), corresponding to a flood frequency of 1/6000 per year (equation 11). Second, with equations 12 and 13, the amount of dike raises with closure reliability improvements are determined: 0.3, -0.1 and -1.0 meter. The minimal dike raise is 0 meter, as there is no fixed cost (see equation 14). Only the single barrier without redundancies has a (positive) dike raise. Hence, for the final step, six solutions were selected: no measure, three closure reliability improvements, a dike raise of

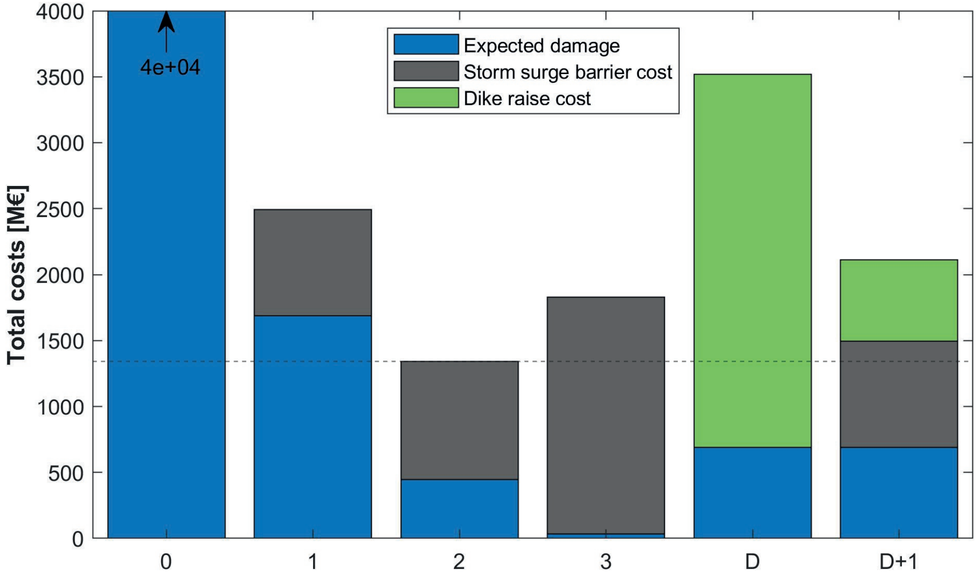

Figure 3.8: Total costs for selected solutions of Maeslant barrier case. The blue, grey, and green costs correspond with the risk, storm surge barrier costs, and dike raise costs, respectively. With a dashed line, the minimum total costs are indicated. The selected solutions are: 0) no measure, 1) single barrier without redundancies, 2) single barrier with redundancies, 3) double barrier, D) 1.4 meter dike raise and D+1) 0.3 meter dike raise with a single barrier without redundancies.

1.4 meter and a storm surge barrier without redundancies together with a dike raise of 0.3 meter.

Figure 3.8 presents the total cost of the optimal possible solutions. Of the six remaining solutions, the single barrier has the lowest total cost (1,300 M€), followed by the double barrier (1,700 M€). Dike raise is almost three times as expensive as a single barrier (3,500 M€). The single barrier without redundancies has a total cost of 2,450 M€. Including dike raise with this closure reliability improvement, lowers the total cost with 300 M€.

3.4.1 Sensitivity sea level rise

In this section, the sensitivity of the results is explored with respect to sea level rise. It is assumed that with an average rise in sea level, extreme water levels rise at the same pace. Hence, a 0.4 meter average sea level rise raises the 1/100 year exceeded water level from MSL + 3.6m to MSL + 4.0m. Using this approach, the distribution parameter

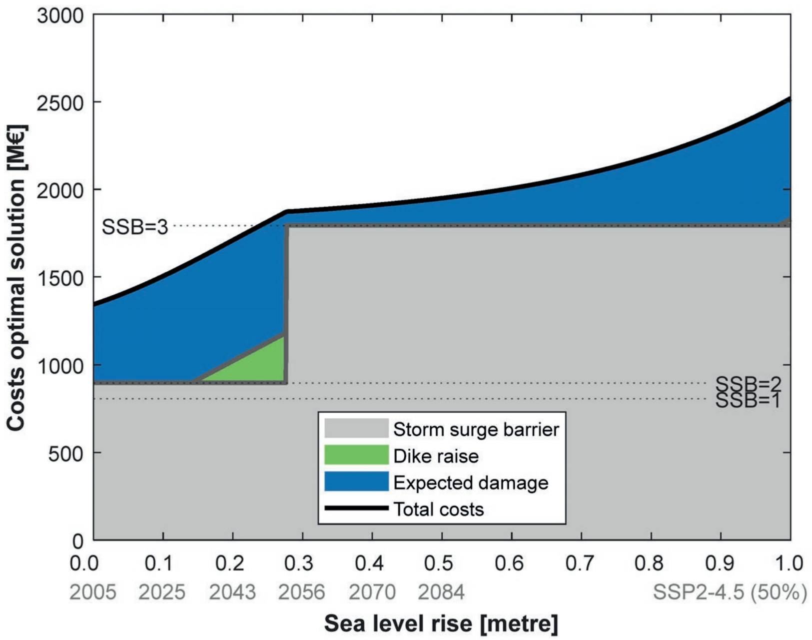

Figure 3.9: Total costs of optimal solutions with increasing sea level rise. The grey, green, and blue hatched areas indicate the storm surge barrier improvement costs, dike raise, and expected flood damage, respectively. The costs of the three storm surge barrier improvements are indicated with a dotted line. At the horizontal axis, the year corresponding to the amount of sea level rise according to scenario SSP2-4.5 (50%) is mentioned.

H_A of the exponential distribution changes with sea level rise SLR. For sea level rises until 1.0 meter, optimal solutions were derived.

Figure 3.9 presents the total cost of the optimal solution. Until a sea level rise of approximately 0.15 meters, a single barrier without dike raise is optimal. Beyond approximately 0.25m, a double barrier is the solution with the least total cost. Between these sea level rises, a single barrier including a small amount of dike raise (0 – 0.2m) is found to be optimal. This latter result is surprising, as normally these small amounts of dike raise are uneconomical. The model produces this result for two reasons: 1) no fixed cost or minimal lifetime of dike raise are assumed and 2) there are no closure reliability improvements in between a single and double barrier.

Figure 3.10 presents the flood frequency of the optimal solution. If only storm surge barrier improvements are optimal, the optimal flood frequency varies, due to the

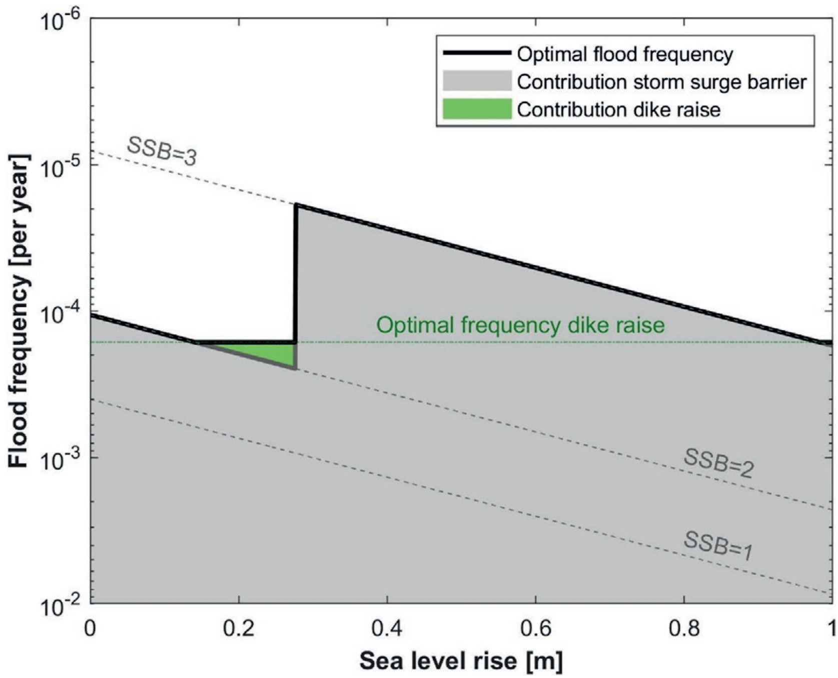

Figure 3.10: Optimal flood frequencies with increasing sea level rise. The grey and green hatched areas indicate which part of the optimal flood frequency can be contributed to storm surge barrier improvements and dike raise, respectively. A green dashed line indicates the optimal flood probability with dike raise alone. The flood frequency for the three investigated storm surge barrier improvements is indicated with a dotted line. These flood frequencies increase, because the initial dike height stays constant while extreme water levels become more frequent with sea level rise.

discrete nature of the improvements. When storm surge barrier improvements are combined with dike raise, the optimal flood frequency is constant and equal to the optimal flood frequency of dikes. Because there is no fixed dike raise cost in this case, optimal solutions with storm surge barrier improvements always have a lower flood frequency than the dike raise optimal flood frequency.

From the results, an optimal strategy can be deducted with respect to sea level rise. Until a sea level rise of 0.15 meter, the current situation is economically optimal. Beyond this sea level rise, small dike raises or a double barrier can be considered.

3.5 Discussion

This section discusses the case study's results and the model's broader applicability. The case study motivates the construction of the Maeslant barrier. Although with respect to the dikes behind the barrier, some highly simplified approaches were taken such as ignoring spatial variability of dike heights and ignoring the fragility of dikes, these assumptions are not expected to greatly affect the result.

The sensitivity analysis indicated that substantial investments such as a double barrier might become feasible with a sea level rise even smaller than the 0.15 to 0.25 meter which the sensitivity analysis indicated.

Rijkswaterstaat (2023) researched the economic feasibility of a redundant barrier, but found less promising results. Based on more advanced hydraulic model calculations, they found that the length of interior flood defenses affected by improving closure reliability is smaller than in the case study of this chapter, which agrees with earlier research findings (Slootjes et al., 2011). The dike raise costs to reduce the flood frequency by a factor 10 are then 400 instead of 1580 M€, making dike raise more effective than a double barrier. Furthermore, their economic model assumes that every storm surge barrier improvement also requires dike raise, only reducing the extend of this dike raise. This assumption seems unrealistic as at some locations the additional barrier lowers the flood frequency with a factor 50. It is hard to imagine that with such a flood risk reduction, the need for dike raise can still be motivated as there have been many dike raises which had a lower flood frequency reduction. Although the result could not be reproduced, this assumption seems to be the main reason why the effect of the double barrier on avoided dike raise costs was merely 100 M€.

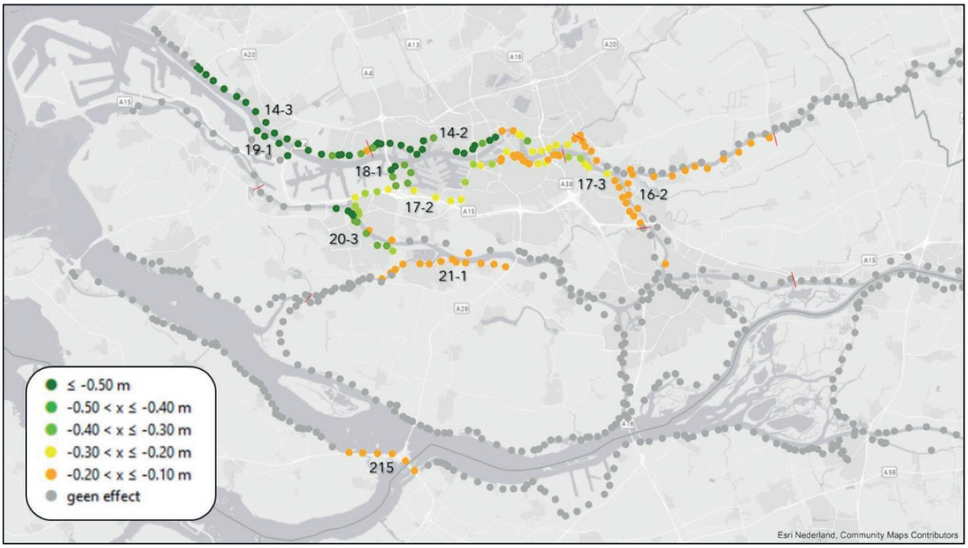

Figure 3.11: Effect of double barrier on extreme water level maxima with a frequency corresponding to legislated flood frequencies of interior flood defenses (Rijkswaterstaat, 2023)

The Rijkswaterstaat study (2023) also indicated that the benefits of a double barrier would be larger if the sluicing capacity at the Haringvliet sluices is increased. Currently, the extreme water levels around Dordrecht are mainly determined by events with high Rhine flows (Q>8000 m^3/s) together with a North Sea with a water level maximum with a 10-year return period. In the future, extreme Rhine flows are expected to increase, making these scenarios even more important. A higher sluicing capacity lowers the extreme water level maxima in these situations. As a result, situations with a failed Maeslant barrier become more important. In that case, the assumed area of influence assumed in this case study is more realistic.

Both this case study and Rijkswaterstaat (2023) did not include substantial investments in between a single and double barrier with an intermediate effect on flood risk. Based on the results of the case study, such intermediate closure reliability improvements seem most promising. Examples of such improvements are: more reliable equipment, optimized test procedures, or (even) better trained staff. Based on the results of this study, a better understanding of the costs and benefit of these type of improvements is most important to come to an economic optimal solution.

In addition, most model variables have considerable uncertainty. Probably most important are climate change effects and discount rates. In this case, only mild projections with respect to sea level rises were considered. If more extreme sea level rise projections are considered, larger investments become economic. On the other hand, there are also uncertainties with respect to interest rate and economic growth, which might motivate to await larger investments. To account for these and other uncertainties, the robustness of the measures needs to be tested.

Although for the Maeslant barrier the model seems applicable for short term economic decision due to the current dominance of the non-closure risk, other risks and effects are to be considered for long-term decision making and a wider applicability of the model.

3.6 Concluding remarks

This research aimed to develop a method to effectively optimize coastal flood defense systems with a storm surge barrier. Closure reliability was identified as an important parameter for economic optimization. A model was developed to show how closure reliability affects economic decision-making, balancing coastal flood risk with investments in closure reliability and dike raise.

The model was applied at the region protected by the Maeslant barrier. The model results substantiated the decision to construct the Maeslant barrier. Moreover, it was demonstrated that large investments into closure reliability can already be relevant with a few decimeters of sea level rise.

Based on our experience with this case, it is expected that the proposed model can support many studies. Storm surge barrier managers can apply the model to support large maintenance investments. Regional flood authorities can balance storm surge barrier improvements with local measures to protect the area behind the barrier. The model can be used at feasibility studies of new storm surge barriers such as New York, Goteborg, Galveston, and Shanghai. Finally, the model can assist in finding appropriate strategies to compensate for sea level rise and other effects raising coastal flood risk.

3.7 References

Aerts, J., Botzen, W., and Moel, H. D. (2013). Cost Estimates for Flood Resilience and Protection Strategies in New York City. Technical report.

Aerts, J. C. (2018). A review of cost estimates for flood adaptation. *Water (Switzerland)*, 10(11).

Aerts, J. C., Botzen, W. J., Emanuel, K., Lin, N., De Moel, H., and Michel-Kerjan, E. O. (2014). Climate adaptation: Evaluating flood resilience strategies for coastal megacities. *Science*, 344(6183):473–475.

Arns, A., Wahl, T., Haigh, I. D., Jensen, J., and Pattiaratchi, C. (2013). Estimating extreme water level probabilities: A comparison of the direct methods and recommendations for best practice. *Coastal Engineering*, 81:51–66.

Brekelmans, R., den Hertog, D., Roos, K., and Eijgenraam, C. (2012). Safe Dike Heights at Minimal Costs: The Nonhomogeneous Case. *Operations Research*, 60(6):1342–1355.

Calafat, F. M., Wahl, T., Tadesse, M. G., and Sparrow, S. N. (2022). Trends in Europe storm surge extremes match the rate of sea-level rise. *Nature*, 603(7903):841–845.

Ceres, R. L., Forest, C. E., and Keller, K. (2019). Optimization of multiple storm surge risk mitigation strategies for an island City On a Wedge. *Environmental Modelling and Software*, 119(April):341–353.

Ceres, R. L., Forest, C. E., and Keller, K. (2022). Trade-offs and synergies in managing coastal flood risk: A case study for New York City. *Journal of Flood Risk Management*, 15(1):1–12.

CPB Netherlands Bureau for Economic Policy Analysis (2013). Economic optimal safety at the IJssel Lake area (Dutch: Economisch optimale waterveiligheid in het IJsselmeergebied). Technical report, CPB.

Deltares (2013). Representative values coastal waters and large rivers (Dutch: Kenmerkende waarden kustwateren en grote rivieren). Technical report, Deltares.

Dupuits, E. J., Schweckendiek, T., and Kok, M. (2017). Economic optimization of coastal flood defense systems. *Reliability Engineering and System Safety*, 159(October 2016):143–152.

Eijgenraam, C., Brekelmans, R., Den Hertog, D., and Roos, K. (2017). Optimal strategies for flood prevention. *Management Science*.

Eijgenraam, C., Kind, J., Bak, C., Brekelmans, R., Den Hertog, D., Duits, M., Roos, K., Vermeer, P., and Kuijken, W. (2014). Economically efficient standards to protect the netherlands against flooding. *Interfaces*.

Groves, D. G. and Sharon, C. (2013). Planning Tool to Support Planning the Future of Coastal Lousiana. *Journal of Coastal Research*, 67:147–161.

Haasnoot, M., Kwakkel, J. H., and Walker, W. E. (2013). Dynamic adaptive policy pathways: A method for crafting robust decisions for a deeply uncertain world. *Global Environmental Change*, 23(2):485–498.

Hallegatte, S., Green, C., Nicholls, R. J., and Corfee-Morlot, J. (2013). Future flood losses in major coastal cities. *Nature Climate Change*, 3(9):802– 806.

Henley, E. J. and Kumamoto, H. (1981). *Reliability engineering and risk assessment*. Preston Hall, Englewood Cliffs, N.J.

HKV (2006). Achterlandstudie Maeslantkering, Hydra-B. Technical report.

Janssen, J. P. and Jorissen, R. E. (1992). Integrating forecast effects and operational behaviour in designing the Rotterdam storm surge barrier. In *Floods and Flood Management. Fluid Mechanics and its Applications*, number January.

Jongejan, R., Maaskant, B., Horst, W. T., Havinga, F., Roode, N., and Stefess, H. (2013). The VNK2-project: A fully probabilistic risk analysis for all major levee systems in the Netherlands. *IAHS-AISH Publication*, 357:75–85.

Jonkman, S. N., Hillen, M. M., Nicholls, R. J., Kanning, W., and van Ledden,M. (2013). Costs of Adapting Coastal Defences to Sea-Level Rise— New Estimates and Their Implications. *Journal of Coastal Research*, 290:1212– 1226.

Jonkman, S. N., Kok, M., Van Ledden, M., and Vrijling, J. K. (2009). Riskbased design of flood defence systems: A preliminary analysis of the optimal protection level for the New Orleans metropolitan area. *Journal of Flood Risk Management*.

Kim, M. J., Nicholls, R. J., Preston, J. M., and de Almeida, G. A. (2019). An assessment of the optimum timing of coastal flood adaptation given sealevel rise using real options analysis. *Journal of Flood Risk Management*, 12:1–28.

Kind, J. M. (2014). Economically efficient flood protection standards for the Netherlands. *Journal of Flood Risk Management*.

KNMI (2021). Klimaatsignaal'21. Technical report.

Lendering, K., Jonkman, S., van Ledden, M., and Vrijling, J. (2020). Defend or raise? Optimising flood risk reduction strategies. *Journal of Flood Risk Management*.

Lendering, K., Schweckendiek, T., and Kok, M. (2018). Quantifying the failure probability of a canal levee. *Georisk*, 9518:1–15.

Lendering, K. T., Jonkman, S. N., Van Gelder, P. H., and Peters, D. J. (2015). Risk-based optimization of land reclamation. *Reliability Engineering and System Safety*, 144(August 2015):193–203.

Lenk, S., Rybski, D., Heidrich, O., Dawson, R. J., and Kropp, J. P. (2017). Costs of sea dikes-regressions and uncertainty estimates. *Natural Hazards and Earth System Sciences*, 17(5):765–779.

Lewin, J., Ballard, G., and Bowles, D. S. (2003). Spillway gate reliability in context of overall dam failure risk. In *USSD Annual Lecture*, pages 1–17. Charleston, South Carolina.

Ministry of Infrastructure and Environment (2016). Factsheets flood safety standards primary flood defences (Dutch: Factsheets normering primaire waterkeringen). Technical report.

Mooyaart, L. F. and Jonkman, S. N. (2017). Overview and Design Considerations of Storm Surge Barriers. *Journal of Waterway, Port, Coastal, and Ocean Engineering*, 143(4):06017001.

Rijkswaterstaat (2002). Project note / EIA Ramspol barrier, Hydraulic boundary conditions (Dutch: Projectnota / MER keersluis Ramspol, Hydraulische randvoorwaarden). Technical report.

Rijkswaterstaat (2008). Performance levels Eastern Scheldt, continuation (Dutch: Prestatiepeilen Oosterschelde, vervolg). Technical report.

Rijkswaterstaat (2023). Investigation resolution Grinwis, 'Holland barrier' (Dutch: Onderzoek Motie Grinwis c.s., 'Hollandkering'). Technical report.

Ruig, L. T. D., Barnard, P. L., Botzen, W. J. W., Grifman, P., Finzi, J., Moel, H. D., Sadrpour, N., and Aerts, J. C. J. H. (2019). Science of the Total Environment An economic evaluation of adaptation pathways in coastal mega cities : An illustration for Los Angeles. *Science of the Total Environment*, 678:647–659.

Slootjes N., T. Botterhuis, A. Jeuken, Q. Gao, 2011. Resultaten MHW berekeningen t.b.v. probleemanalyse en verkenning hoekpunten. Voor het Deltaprogramma RijnmondDrechtsteden. Projectnummer 1202134-016. HKV/Deltares, Delft.

Vader, H., Bakker, A. M., Jonkman, S. N., van den Boomen, M., van Baaren, E., and Diermanse, F. L. (2022). A framework for assessing the remaining life of storm surge barriers [Manuscript submitted for publication].

van Berchum, E. C., Mobley, W., Jonkman, S. N., Timmermans, J. S., Kwakkel, J. H., and Brody, S. D. (2019). Evaluation of flood risk reduction strategies through combinations of interventions. *Journal of Flood Risk Management*, 12(October 2018):1–17.

van Berchum, E. C., van Ledden, M., Timmermans, J. S., Kwakkel, J. H., and Jonkman, S. N. (2020). Rapid flood risk screening model for compound flood events in Beira, Mozambique. *Natural Hazards and Earth System Sciences*, 20(10):2633–2646.

van Dantzig, D. (1956). Economic decision problems for flood protection. *Econometrica*, 24(3):276–287.

van der Pol, T., Hinkel, J., Merkens, J., MacPherson, L., Vafeidis, A. T., Arns, A., and Dangendorf, S. (2021). Regional economic analysis of flood defence heights at the German Baltic Sea coast: A multi-method cost-benefit approach for flood prevention. *Climate Risk Management*, 32(February).

Van Manen, S., Brandt, E., Van Ekris, J., and Geurts, W. (2015). TOPAAS: An alternative approach to software reliability quantification. *Quality and Reliability Engineering International*, 31(2):183–191.

Vezér, M., Bakker, A., Keller, K., and Tuana, N. (2018). Epistemic and ethical trade-offs in decision analytical modelling: A case study of flood risk management in New Orleans. *Climatic Change*, 147(1-2):1–10.

Wemelsfelder, P. (1939). Wetmatigheden in het optreden van stormvloeden. *De Ingenieur*, 54(9):31–35.

Wing, O. E., Pinter, N., Bates, P. D., and Kousky, C. (2020). New insights into US flood vulnerability revealed from flood insurance big data. *Nature Communications*, 11(1):1–10.

4

A screening method to identify promising performance improvements[6]

6 This chapter is largely based on Mooyaart, L. F., Bakker, A. M. R., van den Bogaard, J. A., van den Boomen, M. & Jonkman, B. (2024). A screening method to identify promising performance improvements of storm surge barriers: a case study in the Netherlands – Submitted to Journal of Reliability Engineering & System Safety.

The second chapter identified a failure to close a dominant failure mechanism, yet little is known about how to improve it. The previous chapter demonstrated that closure reliability requirements become more stringent with increasing flood risk. Moreover, it was found that the degree to which requirements become more stringent depends on the costs and risk reduction of closure reliability improvements. Thus, it is important to gain more systematic insight into these options to reduce the probability of a failure to close.

Therefore, this chapter presents a list of principal performance improvements and a three-stage screening process to determine the most effective options to lower the probability of a failed closure.

Section 4.1 discusses current methods for identifying performance improvements. Section 4.2 offers theories on analytical tools to detect performance killers (i.e. items in the reliability and availability analysis which greatly contribute to the overall result). Section 4.3 explains how the list of principal performance improvements was established. Section 4.4 describes the three-stage screening process. This method is applied to a case study in Section 4.5, which is discussed in Section 4.6. Section 4.7 concludes the chapter.

4.1 Introduction

In the Netherlands, the probability of a failure to close is typically estimated with a *reliability and availability analysis* (RA analysis), which uses fault and event trees that contain a thousand to ten thousand failure scenarios. In this paper, we define a failure scenario as a group of failure events resulting in failure of the analyzed object. In other industries, RA analyses are referred to as probabilistic safety assessments, quantitative risk analyses or other combinations of these words. RA analyses are applied to various technological objects (nuclear plants, airplanes, space missions, chemical facilities) to analyze events with low probabilities and large consequences, where data to quantify risk are sparse (Bier & Cox Jr., 2007).

Rijkswaterstaat - the executive agency of the Ministry of Infrastructure and Water Management responsible for the maintenance and operation of Dutch storm surge barriers - has been challenged for several decades with exploring most relevant performance improvements. After a thorough RA analysis of the Maeslant storm surge barrier (NRG, 2003), several performance improvements were implemented. In a review by Horvat and Partners (2006), five additional performance improvements were suggested: removing RA-model conservatism based on a storm closure, partial testing of subsystems, starting closure procedure earlier, redesigning of operating mechanism and redesigning of control system. In the following decades, many performance improvements were considered of which some were implemented. However, the process was unsystematic, and it remained difficult to establish whether all relevant performance improvements were considered.

The current practice at Rijkswaterstaat and in reliability engineering in general (Henley & Kumamoto, 1981; Pate-Cornell, 2002; Aven, 2017) is to mitigate risk by searching for performance killers in the RA analysis. *Performance killers* refer to either a single event or group of events that greatly contribute to overall unreliability, unavailability, and/or probability of failure on demand, the influence of which could be lowered by a single performance improvement. The identified performance killers are subsequently used to find performance improvements by *putting yourself into a creative mode*, as Haimes et al. (2002) nicely phrase.

To illustrate that finding performance killers can be difficult in fault and event trees, we use a fault tree of a relatively simple object (Figure 4.1). The fault tree contains AND- and OR-gates. AND-gates indicate that all underlying failure events have to occur for the upper event to occur. OR-gates are used when only one underlying failure event has to occur for the upper event to occur. The fault tree represents an object that

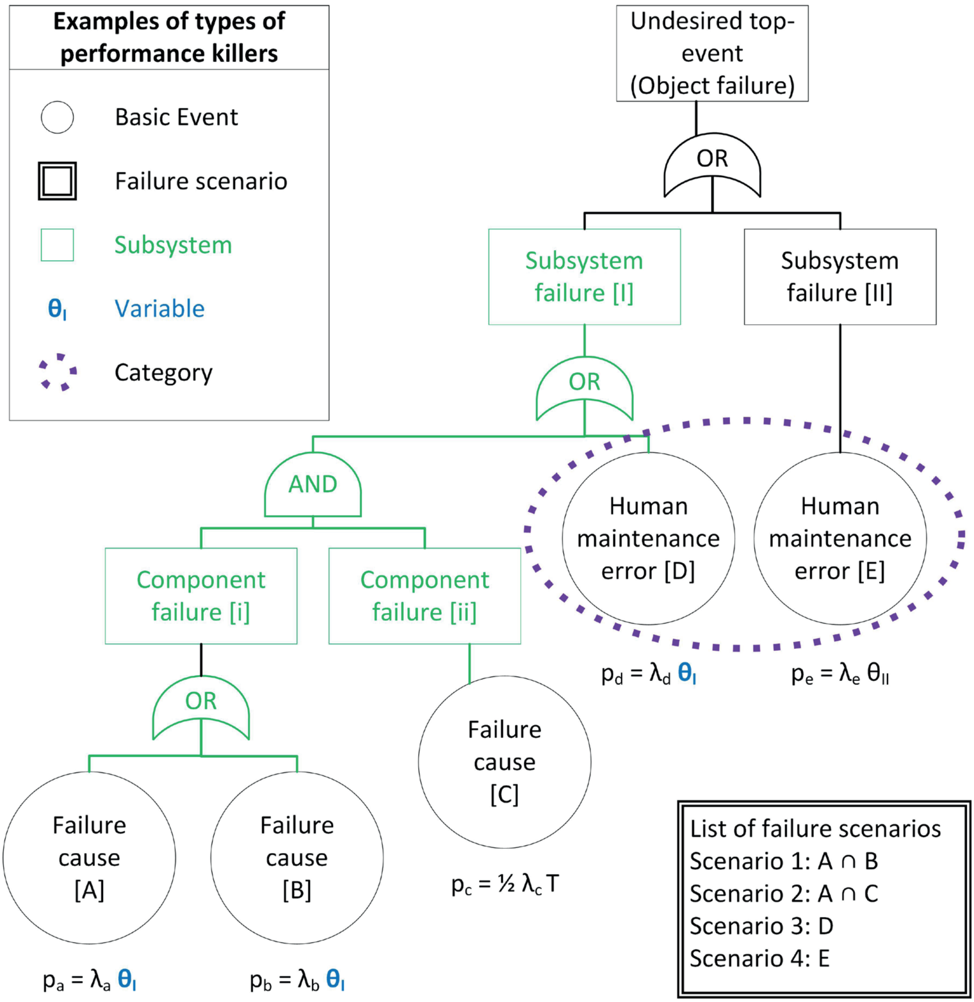

Figure 4.1: Example fault tree of an object with two subsystems of which one has two components. The fault tree aims to illustrate that even for a relatively simple system, there are many performance killers of which five examples are highlighted: any basic event, any failure scenario, subsystem A, repair time θ_I and human maintenance errors.

consists of two subsystems, of which one has two components. Customary formulas {Schüller et al. (1997), pages 9.30 to 9.40} are used to determine the unavailability of technical components.

Already, for this half-page fault tree (note that the RA model of the Maeslant barrier is over 1,200 pages), many potential performance killers can be identified, depending on how failure events are grouped and ranked. Five of these methods are presented in Figure 4.1. They are also used to discuss current approaches and their limitations in identifying performance killers. First, basic failure events and failure scenarios can be identified that kill performance. Then, subsystems containing multiple failure events already require grouping of failure events. Other useful grouping options include variables affecting multiple failure events, such as repair times for multiple components, and failure events belonging to a specific category, such as human maintenance errors.

Rijkswaterstaat guidelines (Rijkswaterstaat, 2011, 2018a) propose to rank failure scenarios - in fault tree analysis referred to as minimal cut-sets - according to their contribution to the object's unreliability and/or unavailability. Failure scenarios have occasionally been grouped into subsystems (Horvat and Partners, 2006; Rijneveld, 2008). However, this approach can easily overlook basic failure events which affect multiple failure scenarios.

Alternatively, the importance measures of Fussell-Vesely (Vesely et al., 1983) and Birnbaum (1969) are well-known analytical tools for identifying basic event performance killers. The Fussell-Vesely importance measure indicates the extent to which a basic event affects object performance. The Birnbaum importance measure compares the object's performance in the case of success and failure of basic events. Rijkswaterstaat has occasionally applied these importance measures to prioritize the importance of basic events. Many authors (Borgonovo &Apostolakis, 2001; Dutuit & Rauzy, 2015; Xu et al., 2020; Zhang et al., 2022; Chen et al., 2023; Liu et al., 2023a,b; Rusnak et al., 2024) extend upon these importance measures to find new ways to rank failure events. With this approach, however, grouping of failure events can be overlooked.

Therefore, Cheok et al. (1998) describe how to use importance measures for groups of basic events. They suggest defining groups for (sub)systems and components and evaluating them based on the size and constituency of these groups. The prevailing nuclear industry guideline (Nuclear Energy Institute, 2018) still includes their recommendation. Moreover, several authors (Borgonovo & Apostolakis, 2001; Dutuit & Rauzy, 2015) acknowledge the possibility of importance measures to group events, but do not discuss how to group failure events.

In fact, the grouping method determines which performance killers are identified. For instance, prioritizing components results in a list of the most critical components, prioritizing repair times results in a list of the most critical repair times, and so on. For simple fault trees, such as those sketched in Figure 4.1, the multidimensionality of performance killers makes it difficult to systematically identify performance improvements. For large fault trees, it is unlikely that all relevant performance improvements are identified using the discussed approaches.

Thus, in the current approach, the success of finding relevant performance killers and performance improvements is determined by the creativity and quality of reliability experts. As there are many possible performance improvements that vary in scale and type, this approach can easily overlook important performance improvements. Therefore, we do not know how to identify relevant performance killers and improvements in a systematic manner.

To overcome this issue, we researched an alternative approach to find promising performance improvements that uses 1) a checklist of principal performance improvements (PPI's) and 2) a method to screen that checklist effectively.

The remainder of this paper is structured as follows: Section 2 presents key definitions used throughout the study. Section 3 describes the research approach for developing the checklist. Section 4 introduces the three-stage screening method for applying the checklist. Section 5 demonstrates the application of the checklist and screening method to the Maeslant barrier case study. Section 6 discusses the method and section 7 concludes the paper.

4.2 Reliability and availability analysis of storm surge barriers

2.1. Definitions

This section provides some important definitions to clarify the checklist (Appendix A) and the screening method presented in this paper.

Four hierarchical levels of decomposition are defined: *object, object system, subsystem* and *component*. In this paper, the object is always the storm surge barrier. For a decomposition with more hierarchical levels than four, subsystems are ranked (i.e., subsystem level 1, subsystem level 2, etc.). Thus, components are the lowest level of detail in the object decomposition (Schüller et al., 1997).

Each element of the object decomposition provides a particular function. A failure is defined as a loss of this element's functionality (Dummer et al., 1997). A *failure criterion* is used to define how much functionality can be lost before an element is considered failed. For instance, at a storm surge barrier with multiple gates, a closure of all gates except one can still be considered a successful closure if this event does not result in a coastal flood. In this example, the term partial failure can also be used to describe that part of the element's functionality is lost.

A reliability and availability analysis (RA analysis) establishes the reliability, availability and/or probability of failure on demand of an object. For storm surge barriers, the most important result is often the probability of a failure to close, which best aligns with the term probability of failure on demand. To avoid repetition, we only use this term to describe the main result of an RA analysis - and not reliability and availability.

On the failure event level, we define four *unavailability types*: 1) dormant failure [7], 2) unavailability due to repair, 3) failure during mission and 4) failure on demand. Here, unavailability is the probability that an object is in a failed state at a stated time under a given set of conditions (Van Der Weide & Pandey, 2015; Li et al., 2024).

Based on guidelines for the nuclear industry (IAEA, 1992) and storm surge barriers (Rijkswaterstaat, 2018a), we define five *failure categories*: 1) hardware failure, 2) external events, 3) common cause failure, 4) human error and 5) software error. Thus, hardware failures are all inherent failures of physical objects except for failures due to external events and common cause failure.

2.2. Set-up RA model

An RA model is part of an RA analysis that 1) illustrates how combinations of events result in undesired outcomes and 2) is used to quantify the probability and/or frequency of those outcomes. An RA model consists of three elements:

- A *logic model structure*, for instance, a fault or an event tree.
- A *failure event model structure*, for instance, the equations shown below the basic event in Figure 4.1.
- *Model variables*, for instance, the failure rate λ, the repair time θ and the test interval *T* in Figure 4.1.

Failure event model structures can contain a model parameter, that is, a calibrated and/or validated value specifically belonging to that model. For instance, in the TOPAAS-model - a model specifically developed to determine the probability of software error at storm surge barriers (Van Manen et al., 2015) - the maximum

7 Dormant failure refers to a failure which was undetected during normal conditions.

probability of software error of 10^{-5} is such a model parameter. In contrast to model variables such as the development and test quality of software, the model validity is lost when the maximum probability is adjusted. Thus, adapting a model parameter is considered a change of the failure event model structure.

The logic model establishes failure scenarios, which contain one or multiple failure events (*A*,*B*,...). When failure scenario probabilities P_i are low and independent from each other, the probability of failure on demand P_f can be approximated with:

$$P_f = 1 - \prod_i^n (1 - P_i) \approx \sum_i^n P_i \quad (1).$$

2.3. Fussell-Vesely Importance Measure

To effectively screen principal performance improvements (PPI's), the Fussell Vesely Importance Measure I_{FV} is used to establish the maximum effect a PPI has on the probability of failure on demand.

Here, the RA model in Figure 4.1 is used to demonstrate how the Fussell-Vesely Importance Measure I_{FV} is determined for a basic event, groups of events and variables. This model has four failure scenarios, which have the following probabilities:

$$P_1 = P(A \cap B) = \lambda_a \cdot \theta_I \cdot \tfrac{1}{2} \cdot \lambda_c \cdot T$$

$$P_2 = P(A \cap C) = \lambda_b \cdot \theta_I \cdot \tfrac{1}{2} \cdot \lambda_c \cdot T$$

$$P_3 = P(D) = \lambda_d \cdot \theta_I$$

$$P_4 = P(E) = \lambda_e \cdot \theta_{II}$$

In which λ are failure rates of components or human error [per hour], θ the repair time [hour], and *T* the test interval [hour], relevant for dormant failures. Indices correspond to components and subsystems where failure rates, repair times, and test intervals that failure events belong to (see Figure 4.1). With equation 1, the probability of failure on demand for this object is found:

$$P_f = \frac{1}{2} \cdot (\lambda_a + \lambda_b) \cdot \theta_I \cdot \lambda_c \cdot T + \lambda_d \cdot \theta_I + \lambda_e \cdot \theta_{II}$$

For basic events, the Fussell-Vesely Importance Measure I_{FV} is the sum of all failure scenarios that contain that event relative to the probability of failure on demand. For failure event *A* in Figure 4.1, the Fussell-Vesely Importance Measure I_{FV} is

$$I_{FV}(A) = \frac{P_1}{P_f} = \frac{\frac{1}{2} \cdot \lambda_a \cdot \lambda_c \cdot \theta_I \cdot T}{P_f} \quad (2).$$

For group of failure events, the Fussell-Vesely Importance Measure I_{FV} is the sum of all failure scenarios that contain at least one of the failure events relative to the probability of failure on demand. The Fussell-Vesely Importance Measure I_{FV} of human maintenance errors ($D \cup E$) is, thus,

$$I_{FV}(D \cup E) = \frac{P_3 + P_4}{P_f} = \frac{\lambda_d \cdot \theta_I + \lambda_e \cdot \theta_{II}}{P_f} \quad (3).$$

For variables affecting multiple events, the Fussell-Vesely Importance Measure I_{FV} is calculated in an opposite manner. For the variable (in the example of Figure 4.1, repair time θ_I), the probability of failure on demand without the influence of this variable ($\theta_I = 0$) is determined. This value $P_f(\theta_I = 0)$ is then used to attain its Fussell Vesely Importance Measure $I_{FV}(\theta_I)$ in the following manner:

$$I_{FV}(\theta_I) = 1 - \frac{P_f(\theta_I = 0)}{P_f} = 1 - \frac{\lambda_e \cdot \theta_{II}}{P_f} \quad (4).$$

In the hypothetical case that each failure scenario has the same probability ($P_1 = P_2 = P_3 = P_4 = 25\% P_f$), multiple performance killers can be identified. Failure cause *C* and the failure category human maintenance errors are included in half of the failure scenarios, resulting in a Fussell-Vesely value I_{FV} of 50%. Subsystem *I* and its repair time θ_I affect three failure scenarios and, thus, their maximum effect I_{FV} is 75%. This hypothetical case illustrates that even a simple object can have multiple performance killers, depending on how it is analyzed.

4.3 Development of a checklist

The checklist was developed in three steps:

1. Literature study
2. Dialogues
3. Systematic structuring

The checklist was revised after the case study (see section 5.4). The final version is presented in appendix D.

3.1. Literature study

The literature only reveals a few structured lists to enhance the performance of safety-critical infrastructure. We discovered lists for defending against common cause failures (Paula et al., 1990; Parry, 1991) and best practices for the reliability of spillway gates of dams (Lewin et al., 2003), which resulted in an initial list of 32 PPI's. Due to the scarcity of performance improvement lists, the literature study was extended.

We studied model variables of human reliability models (Swain & Guttmann, 1983; Barnes et al., 2000; US Nuclear Regulatory Commission, 2006; NUREG, 2004; Heslinga, 2004), software reliability models (Van Manen et al., 2015; Rijkswaterstaat, 2018b), external event screening methods (Knochenhauer & Louko, 2003), a repair model (Kiel et al., 2023) and a guideline on CCF modeling (International Electrotechnical Commission, 2021). For these variables, corresponding PPI's were proposed. For example, software reliability models (United States Nuclear Regulatory Commission, 2011; Van Manen et al., 2015) consider the development process as a factor influencing the probability of software errors. Subsequently, we added 'redeveloping software' as a PPI to our checklist. Excluding human reliability performance improvements, this step resulted in an additional 22 PPI's.

The literature study into human reliability models highlighted the need to cluster PPI's for practical use. The OPSCHEP human reliability model, used for storm surge barriers, has 36 variables (Heslinga, 2004). While these variables stem from nuclear industry studies (e.g. Barnes et al., 2000), different models often employ slightly different variables. Moreover, these studies present lists of best practices and important considerations, some of which may not be included in the model itself. Attempting to comprehensively cover all these variables and aspects would result in an unwieldy list of over a hundred PPI's for human reliability alone, many of which would be closely related. Based on this insight, PPI's of human reliability and other categories were clustered, which resulted in a list of approximately fifty PPI's.

3.2. Dialogues

The initial checklist, based on the academic literature review only, was found incomplete, lacking crucial PPI's implemented at Dutch storm surge barriers. This highlighted a gap between academic literature and real-world practice in storm surge barrier management.

To address this gap, dialogues were conducted with co-authors and reliability experts of Rijkswaterstaat. An important example was that high software probability errors could be resolved by human recovery. This revealed that performance killers in a certain category could be addressed by solutions from another category. Based on this insight, six PPI's were added (e.g. hardware improvements for software, software improvements for human error, etc.). In this stage, operational performance improvements such as preventive closure of the barrier in case of malfunctioning were identified as well, resulting in five more PPI's.

Finally, the option to adapt the RA model was mentioned. Based on this suggestion, we studied options to reduce conservatism in RA analyses, which Aven (2016) convincingly argues is desirable. We found three PPI's of this type: using less conservative model variables (Hegseth et al., 2021), less conservative model structures (Gomes & Beck, 2021) and less strict failure criteria (dialogues with co-authors). These principles can be applied to the models of each failure category (human, software, hardware, external event, CCF) and, thus, resulted in fifteen PPI's.

3.3. Systematic structuring

The literature study and dialogues resulted in about eighty PPI's. To validate whether this long-list was near complete, we defined three key *improvement dimensions* (see Figure 4.2), which are the result of a combination of literature study and scientific reasoning:

- Improvement types: model, system properties, maintenance, and operation
- Failure categories: hardware, common-cause-failure, external events, human reliability, and software reliability
- Hierarchical levels: object, object system, subsystem, and component

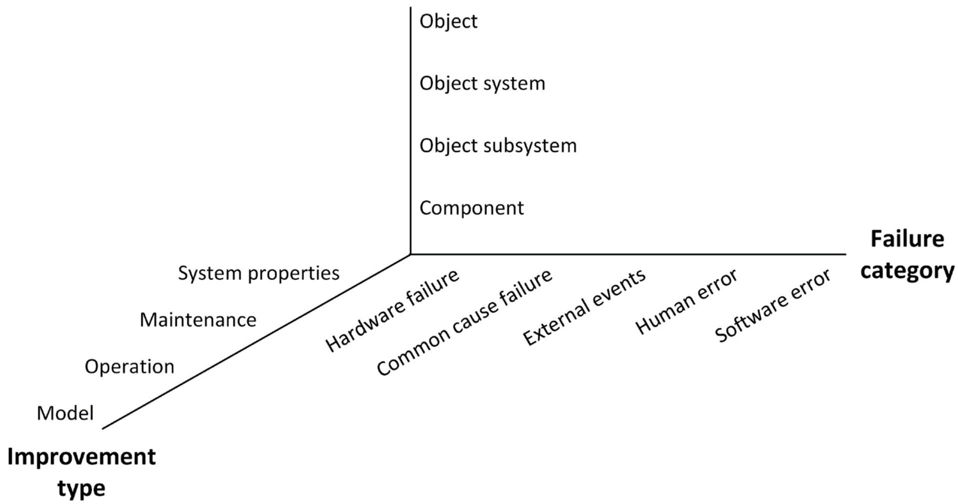

Figure 4.2: Three dimensions of improvement that were used to structure the checklist

We utilized the hierarchical levels to incorporate PPI's across the checklist. For example, we included PPI's such as testing at different hierarchical levels and implementing more reliable equipment at each level.

Although the key dimensions nicely illustrate the large number of possible performance improvements, we found it difficult to use to identify relevant performance improvements. Therefore, we returned to the use of the checklist and structured it into eight categories based on these key improvement dimensions:

1. Reducing model conservatism
2. Hardware
3. Common-cause-failure
4. External events
5. Human reliability
6. Software reliability
7. Maintenance
8. Operation

4.4 Three-stage screening method

This section describes the developed method to screen the checklist for most promising performance improvements. The method is inspired by three well-known methods in reliability and availability analyses: HAZOP (International Electrotechnical Commission, 2016) for the general set-up, external events screening (Knochenhauer & Louko, 2003) for efficient selection from a long-list and FMECA (International Electrotechnical Commission, 2018) for prioritizing improvements.

The method consists of three-stages (see Figure 4.3), which are:

- Stage 1: Analyze importance aiming to remove PPI's with no or only a marginal effect and supporting the subsequent screening stages.
- Stage 2: Select performance improvements with expert evaluation.
- Stage 3: Rank performance improvements with expert scores.

Expert sessions are included in the method as assessing the feasibility of PPI's and case-specific performance improvements requires object knowledge and expertise from different disciplines. For instance, adding redundancy can be applied to both mechanical and electrical systems, thus requiring multidisciplinary knowledge. Object knowledge was assumed to be essential to assess the costs and feasibility of a performance improvement.

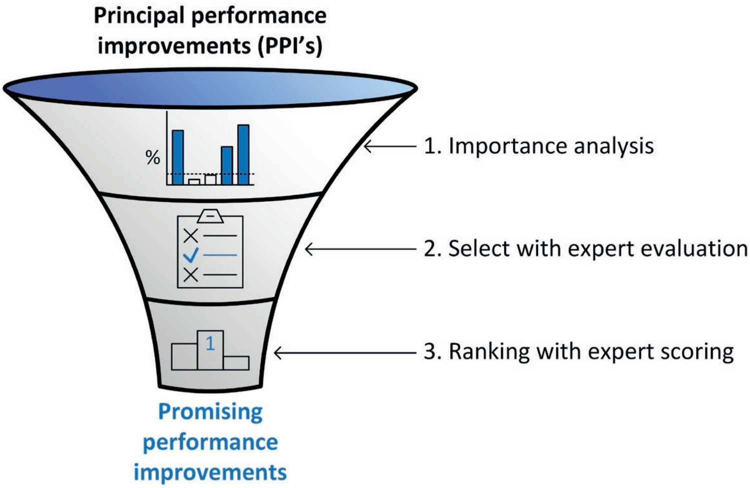

Figure 4.3: Schematic of the three-stage screening method

4.1. Screening stage 1: Importance analysis

The first aim of the importance analysis is to remove PPI's which do not or only marginally affect the probability of failure on demand for the case considered. Generically applicable PPI's do not need to have an effect on a specific case. For example, the RA analysis of the considered case might assume a constant failure rate in all hardware failure models. Hence, PPI's that reduce aging do not have any effect.

Screening criteria are set to exclude PPI's that only have a small effect on the probability of failure on demand. Nuclear Energy Institute (2018) prescribes that screening criteria depend on size and constituency of the group of events. They mention criteria of 1% and 5% as typical examples for components and subsystems, respectively. Both these screening criteria are used in the case study.

A secondary aim of the importance analysis is to support decision-making in subsequent screening stages. For this purpose, performance killers are identified by determining the Fussell-Vesely Importance Measure of the following (groups of) failure events and/or variables:

- Basic events - equation 2
- Failure categories - equation 3
- Unavailability types - equation 4
- The object decomposition - equation 3
- Combinations the object decomposition and failure categories – equation 3

- Combinations the object decomposition and unavailability types - equation 3 & 4
- Variables affecting multiple basic events - equation 4

The results of the importance analysis are described in a report, which is shared with and reviewed by the team of experts.

4.2. Screening stage 2: Select performance improvements

The main objective of this step is to select performance improvements. In an expert session, the session leader, together with the experts, uses four *screening questions* to assess PPI's:

1. Is the PPI applicable to the case considered?
2. Is the PPI expected to have a substantial effect on reliability, availability and/or probability of failure on demand?
3. Does the PPI impede other functions of the object in an unacceptable manner?
4. Are there any other reasons why the PPI is unpromising?

The PPI is only selected for the next screening stage when the answers to the first two questions are positive, and the last two are negative. The last question can be used to rule out performance improvements that are already known to be worse than others. For example, replacing the entire storm surge barrier is more costly and less effective than adding a redundant one. Important motivations to rule out PPI's - especially in the case of the final question - are noted.

The second task of this session is to make PPI's case-specific, which is achieved in two ways: 1) per PPI, experts are asked to provide case-specific examples and 2) per category, experts check whether important performance improvements were missed.

The prepared information on performance killers, that is, the Fussell-Vesely Importance Measures for all (groups of) events and variables, is used in two manners. First, for those PPI's that just passed the screening criterion, it can be judged whether the PPI is likely to have a substantial effect on performance. Second, the most critical object systems, object subsystems and components are defined to find case-specific examples.

The results of the session are reported and shared with the experts for verification.

4.3. Screening stage 3: Ranking

The third screening stage is designed to narrow down a relatively long list of performance improvements to a top selection of five. This top 5 then needs to be worked out in finer detail.

This second expert session ranks remaining performance improvements, using *scoring criteria*. Each scoring criterion is scored from 1 (lowest) to 5 (highest). The performance improvements that greatly improve performance at low cost, score highest.

Four screening criteria are applied:

1. Maximum theoretical effect
2. Effectiveness
3. Costs
4. Feasibility

The first screening criterion establishes the theoretical maximum effect of a performance improvement. Generally, this directly results from the importance analysis using the Fussell-Vesely importance measure. In some cases, experts can comment on the chosen maximum effect. For instance, experts can argue that a PPI only reduces long - and not short - repair times. In that case, only the Fussell-Vesely importance measures of long repair times need to be considered rather than all unavailability due to repair.

The second screening criterion - effectiveness - is used to judge the improvement percentage given the maximum effect on the probability of failure on demand. For instance, a software replacement affects a set of the minimal cut-sets which together determine 30% of the probability of failure on demand (criterion 1). Experts expect that the software replacement reduces this contribution by about 50% (criterion 2). They use the value of 50% to score the second criterion.

The third screening criterion is cost. These costs are life cycle costs relative to the current situation. The cost classes should be distinctive and are, therefore, case-dependent. The leader proposes initial values for scoring cost based on performance improvements defined in the first session (screening step 2), which is then verified by the experts.

The final screening criterion is feasibility. This criterion aims to capture aspects not included in the other criteria. For example, a performance improvement can take a long time to implement, be politically difficult or have a negative effect on another function of the object. More important than with other criteria is that these considerations are noted.

The total score is the product of the scores per criterion. The results of the session and the entire process are reported and checked by experts.

Table 4.1 shows the values for the scoring criteria that were applied in the case study. With respect to the first two criteria, it is - generally - expected that most performance improvements only affect a portion of minimal cut-sets while sometimes having a large effect on them. Therefore, the highest score for maximum effect is already achieved with percentages higher than 40%, while improvement percentages need to be higher than 90% to achieve the highest score.

Table 4.1: Classes used for scoring criteria in case study

Criterion	Class 1	Class 2	Class 3	Class 4	Class 5
Maximum effect	< 5%	5% - 10%	10% - 20%	20% - 40%	> 40%
Effectiveness	< 10%	10% - 30%	30% - 60%	60% - 90%	> 90%
Cost [M€]	> 25	5 - 25	1 - 5	0.1 - 15	< 0.1
Feasibility	Very diff.	Difficult	Normal	Easy	Very easy

4.5 Case study: Maeslant barrier

The Maeslant barrier is a storm surge barrier in the Netherlands that protects Rotterdam and Dordrecht against coastal floods. The barrier consists of two floating sector gates that, in their closed position, span over the 360-meterwide navigation canal: the New Waterway.

The floating sector gates are operated as follows (see Figure 4.4). In normal conditions, the gates are located in a dry dock. When a storm surge is expected the dry dock and gate are prepared to close by jacking up the ball joint, filling the dock, and opening the dock door. The closure commences when the sector gates are - horizontally -

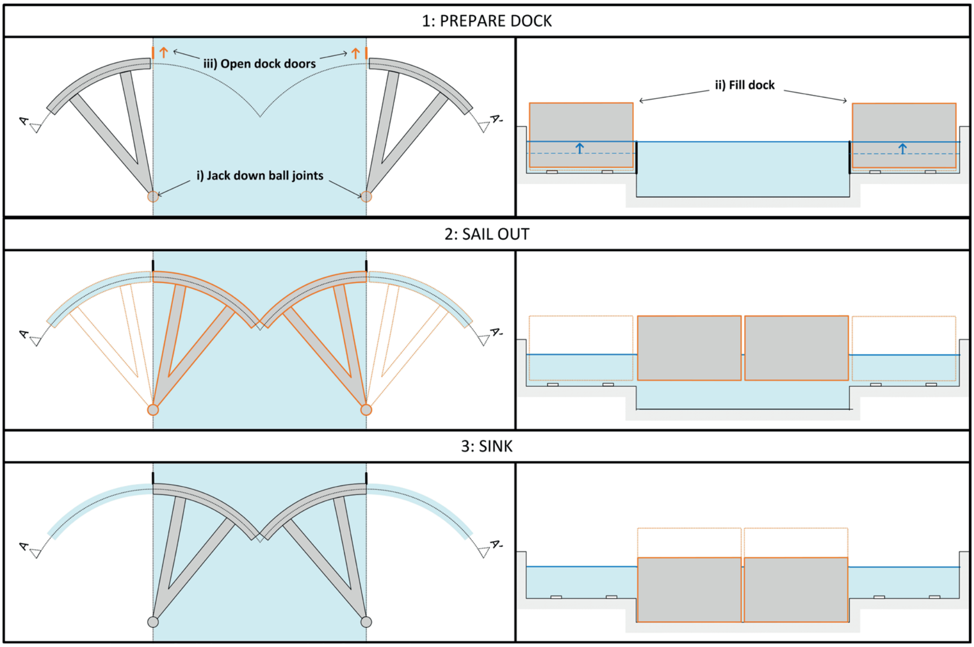

Figure 4.4: Schematic top view (left) and cross-section (right) of floating sector arms during three main closure procedure steps. Orange solid lines highlight gate parts which have moved during a main closure step, orange dotted lines indicate where the gate part was positioned in the previous step.

positioned in the New Waterway. The closure is realized by sinking the gates onto a sill. To achieve high reliability, the barrier closes automatically but can be operated by staff in the event of a malfunction.

In this case study, we aim to reduce the probability of a failure to close. Mooyaart et al. (2025) showed that this failure mechanism is dominant. Moreover, the Maeslant barrier has been struggling to meet the design and later legal requirements for this probability of failure to close. The original design requirement was 1/1000 on demand. Quickly after delivery of the barrier to Rijkswaterstaat, reliability experts started to doubt whether the required design probability was achieved. Between 2003 and 2008, the probability of a failed closure estimate was reassessed and ultimately determined to be 1 in 100 per request, which was deemed acceptable at the time. Meeting this lower requirement has remained a struggle, resulting in several performance improvements and many model adjustments (Rijkswaterstaat, 2023).

Initially, a case was preferred to best reflect the current situation. In that manner, sensible performance improvements could be suggested to improve the Maeslant barrier. However, two difficulties were encountered. First, due to confidentiality issues, it was uncertain whether study results could be published. Second, more importantly, it proved impossible to understand the current RA analysis, including all the model adjustments made over the last few decades, as the underlying documentation had not been updated.

Therefore, a historic RA analysis of 2005 was selected for the case study. Although this RA analysis also had quality issues, for instance, the name of a component in the system analysis report could be inconsistent with the fault tree report and the fault tree model, this analysis had the highest available quality. An independent consultant reviewed this RA analysis (Horvat and Partners, 2006) and deemed it the ″best available.″

Using a historical case also had an important advantage. Making use of a historical case enables comparison with current approaches. The implemented performance improvements can be compared with those proposed by the method. Moreover, if the method identifies other performance improvements, this could also lead to valuable insights for the barrier.

For the case study, only the fault tree model of the RA analysis was used. The 2005 RA analysis consisted of a fault tree model and a separate database with failure scenarios to model human recovery actions. The database is difficult to use, and there is no report on it. As the human recovery actions were excluded from the fault tree model, it was practically impossible to determine Fussell-Vesely importance measures of them. Therefore, the fault tree model was used which finds a probability of a failure to close of 4/100 on demand.

Several aspects were taken into consideration when selecting the experts. First, the experts needed to have a multidisciplinary technological background, including civil, mechanical, and electrical engineering. Moreover, expertise in both the design and the operation & maintenance stages was needed. This requirement limited the options for selecting experts. To minimize potential bias due to the historical nature of the case, one expert was included who was not involved in the RA analysis during the period of 2003–2008. Finally, given the study's objective and budget, a group size of more than six was deemed undesirable. These considerations resulted in a selection of six experts, of whom five were able to attend.

5.1. Screening stage 1: Importance analysis

The initial phase of the screening process involved sharing a comprehensive report with the expert panel. This report contained:

1. The study's primary objective: identifying performance improvements to achieve the original design requirement of 1/1000 on demand
2. Eight detailed tables presenting importance analyses of:

- Failure rates
- Failures on demand
- Repair times
- Test intervals and mission times
- Single events
- Failure scenarios
- Object decomposition
- Top 5 per hierarchical level

Figures 4.5 and 4.6 along with Table 4.2 summarize this information. Here, Table 4.2 describes the top 3 critical items, for which the Fussell-Vesely Importance Measure is shown in Figure 4.6. For example, the failure rate belonging to "object system 1: measurements" has a Fussell-Vesely Importance Measure of just over 6%.

Based on this analysis, two screening criteria were applied. For larger groups of failure events (e.g., object systems, failure categories, unavailability types), a screening criterion of 5% was applied. For smaller groups of failure events (e.g., components, repair times), a criterion of 1% was used. The first criterion excluded all PPI's related to human reliability and external events from the subsequent screening stage (see Figure 4.5). The second criterion rejected four other PPI's for further evaluation. This approach ensured that only the PPI's that potentially substantially affect the probability of failure on demand progress to the next stage.

Many categories, unavailability types, variables and elements (e.g. object systems, subsystems and components) remained relevant to consider for the next stage. Figure 4.5 shows that hardware, software and CCF all contributed highly to the probability of failure on demand. Although failures on demand and unavailability due to repair dominate, test intervals and mission times also substantially affect the result. Figure 4.6 illustrates that all top 5 object systems remained above the 5% screening criterion and all other top 5 items above the 1% screening criterion.

5.2. Screening stage 2: Select performance improvements

In this stage, an expert session was conducted to systematically evaluate the remaining PPI's of the checklist. The session involved a multidisciplinary team of five experts. The session leader guided the experts through each PPI, applying the four screening questions as outlined in the method.

From the original checklist, 38 performance improvements were selected as potentially applicable and promising based on the response to these screening questions. The experts utilized the Fussell-Vesely Importance Measures to assess the potential impact of each improvement on the barrier's probability of failure on demand.

Table 4.2: Top 3 critical items. Object systems (OS) and their sub-elements are anonymously numbered. Other abbreviations are: CCF (Common Cause Failure), SW (Software), Ex (External) and Inf (Information).

Item	1st	2nd	3rd
Failure rates	OS1: Measurements	OS1-1-1-2	OS5-1-4: CCF
Failure on demand	Dependency SW	SW type 1	SW type 2
Repair time	OS5: 24h	OS10: 168h,	OS1: 5h
Test interval/	OS1: 1 month	OS5: 4 months	
Mission time			OS1: 33h
Single events	Dependency SW1	Dependency SW2	Ex Inf 1
Failure scenarios	Ex Inf 1	Ex Inf 2	CCF Inf cable
Object systems	OS2	OS1	OS5
Subsystems	OS1-1	OS5-1	OS10-1
Components	OS5-1-4	OS3-1	OS6-1-3-1

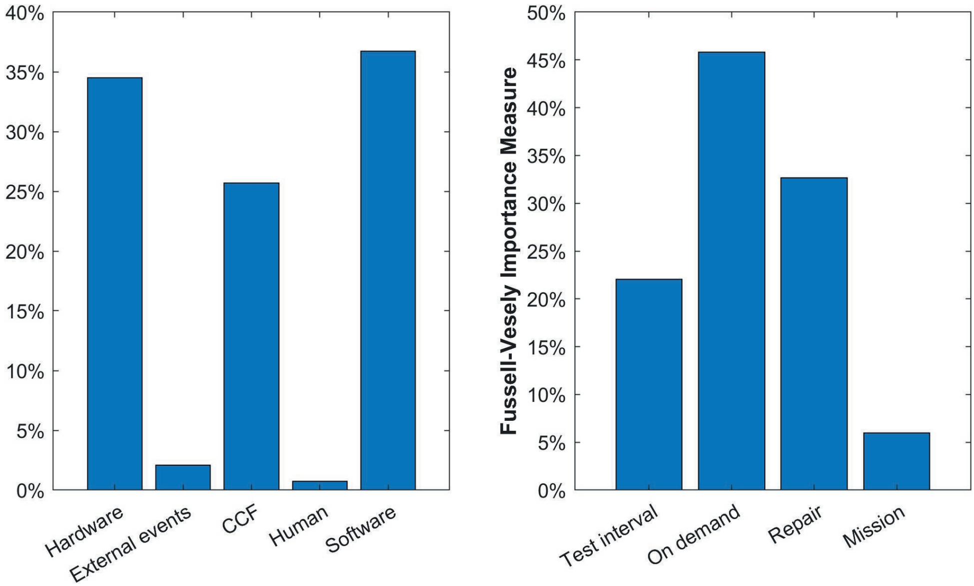

Figure 4.5: Fussell-Vesely importance of failure categories (left) and unavailability types (right) of the Maeslant barrier case study

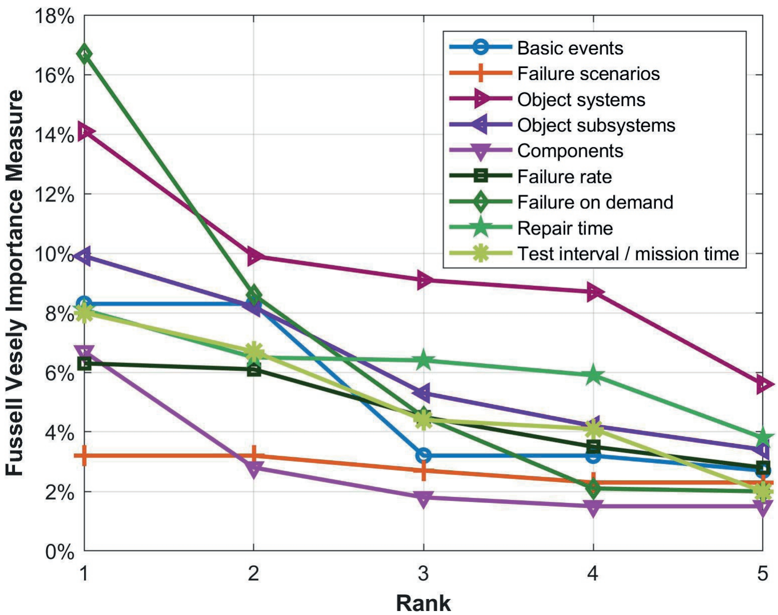

Figure 4.6: Fussell-Vesely importance of top 5 basic events, failure scenarios, elements of object decomposition and variables (failure rate, failure on demand, test interval, mission time and repair time) of the Maeslant barrier case study

For each selected PPI, the experts provided case-specific examples relevant to the Maeslant barrier. This process helped to contextualize the generically formulated improvements and ensure their applicability to the specific case study.

At the end of each category discussion, the experts were asked whether any important performance improvements had been missed. Six additional performance improvements were found in this manner.

In fact, all the newly found performance improvements were already on the checklist. However, the formulation of the PPI did not trigger the according performance improvement. For instance, continuous monitoring was found unpromising, but "making dormant failures noticeable" was identified as an additional improvement, while being essentially the same.

In total, 44 performance improvements (38 from the original checklist and six additional) were considered promising enough to progress to the next screening stage. The results of this session, including the rationale for including or excluding each improvement, were documented and shared with the experts for verification.

5.3. Screening stage 3: Ranking

In this final screening stage, the expert panel convened to score the remaining performance improvements identified in stage 2. The session followed the methodology outlined in the paper, using four scoring criteria: maximum theoretical effect, effectiveness, costs, and feasibility. Each criterion was scored on a scale from 1 to 5. Performance improvements with a large effect on the probability of failure on demand at low cost scored highest.

The experts carefully considered each performance improvement, discussing its potential impact, practicality, and associated costs. They used the Fussell-Vesely Importance Measures from the Importance Analysis to inform their judgments on the maximum theoretical effect. For effectiveness, they estimated the improvement percentage given the maximum effect. Costs were evaluated based on life cycle costs relative to the current situation, using the case-specific cost classes established in the previous session. Feasibility scores accounted for factors such as the need for specialized staff, the difficulty in defending less conservative assumptions and organizational/political acceptance.

Figure 4.7 presents the scores of the experts in a quadrant. The vertical axis shows the score for the expected effect on performance. The horizontal axis indicates costs and feasibility, where a high score represents a low cost and high feasibility. Those performance improvements that score high on both aspects receive the highest overall score and can generally be found in the top right quadrant, which is indicated in green. Other quadrants are colored orange and red to indicate medium-favorable and unfavorable performance improvements, respectively. As these quadrants do not accurately reflect the total score, isolines were included in the figure. More information on the names and scores of the performance improvements can be found in Appendix E. The scoring process resulted in the following top 5 performance improvements:

1. Implement human recovery actions for software failures.
2. Test object system 5 every month instead of every four months
3. Jack-up the ball joint earlier in the closure procedure
4. Measure and update repair times
5. Establish more realistic common-cause failure probabilities

We highlight that the performance improvements found are a result of an old RA analysis and are not applicable to the current situation of the Maeslant barrier as most performance improvements were already implemented.

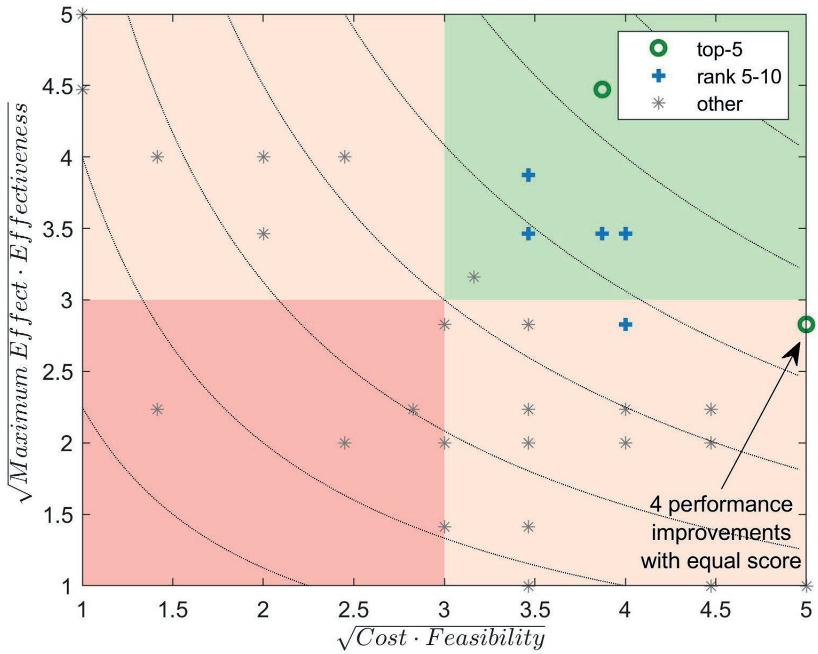

Figure 4.7: Quadrant with ranking results with top-10 in blue. Background colors indicate whether performance improvements are promising (green) or unattractive (red). Dotted lines are isolines of total scores

This set of performance improvements will not result in a probability of failure on demand to meet the original design criterion; rather, it reduces this probability by approximately a factor of three. Three approaches could be considered to come closer to the design criterion: 1) implementing performance improvements lower on the ranking, 2) a new screening procedure based on a revised RA analysis with implemented performance improvements or 3) a combination of these approaches.

Another option is to reconsider the design criterion. In 2005, this option was chosen and resulted in a criterion of a probability of failure of 1/100 on demand.

Further results of the case study are reported in Appendix E.

5.4. Adjustments to the checklist based on the case study

Based on the case study, the list of PPI's was adjusted. PPI's were clustered, especially in the common cause failure category as the applied list is fairly time demanding to navigate through without creating different performance improvements.

Some of the model conservatism reductions were repeated at the end of a category. For instance, adjusting the model variable was introduced at the maintenance sub-categories (repair time, dormant failures), as an important PPI (using more realistic repair times in the model) was almost missed. Based on this choice, we decided to move some other model conservatism reductions to another category. For instance, adjusting the model used for software was transferred to the software reliability category.

Finally, the wording of some of the PPI's was adjusted if their concept was not well understood during the expert session. Appendix D presents the final version of the checklist.

4.6 Discussion

This study aimed to develop a systematic method for identifying performance improvements. Based on the results of the case study, we claim that the proposed approach is more systematic than current approaches. The list of PPIs assists in finding performance killers in a more systematic manner than is currently undertaken. Next, the list of PPIs – including its categorization – structures discussions between experts, making it less likely that important improvement categories are missed. As the method is more systematic, it is also more efficient. The process of deriving a top 5 list of case-specific performance improvements required two expert sessions of a day, spread over a month. In contrast, the historical process of deriving these improvements involved multiple iterative steps over several years.

However, as only one case study was performed, it is impossible to make wider claims about its credibility. In the selected case study, a twenty-year old RA analysis was used, after which many performance improvements were implemented. As a result, experts might be biased about case-specific performance improvements. More case studies can give better insight into the effect of potential bias of experts.

These case studies could be used to test the set-up of expert sessions, which is crucial for the outcome (Kletz, 1992). The approach chosen in the case study highly depends on the role of the leader (Eames, 2022). Expert judgment methods such as the Delphi- (Dalkey & Helmer, 1963) and Cooke-method (Cooke, 1991) would require less from the leader, but are not necessarily better at tackling the multidisciplinary problem addressed in this study. Still, experiments with independent control groups and/or inquiries are recommended to further develop the screening method.

This study revealed a need to improve or even redevelop the RA analysis of the Maeslant barrier. The top 5 contained two model improvements and the top 30 more than ten. While preparing the case study, it turned out that the results of the current RA analysis (2025) were impossible to reproduce due to the numerous model adjustments. The older and more reproducible RA analysis of 2005 still has several weaknesses, of which the unclear object decomposition was the most salient. Moreover, the RA analysis often assumes independence of failure events with storms, which seems unrealistic given the possibility of storm surge clusters and multi-peak storms (Bakker et al., 2025). As the RA analysis of the Maeslant barrier was important for the development of other RA analyses of other Dutch barriers, we expect that these need to be improved as well.

The case study demonstrated the importance of how information is shared with experts. We provided the experts with a report containing the importance analysis and worked with a sheet as presented in Appendix B during the session. Based on our evaluation of the expert sessions, we would refine these pieces of information. An important example is that we now advise to include the most critical components, object subsystems, and object systems in the worksheet. During the expert evaluations, this information was only available in the separate report. As it proved difficult to go back and forth between the report and the worksheet, experts also suggested performance improvements on components, object subsystems and systems that were not critical, thereby reducing the efficiency of the session.

For other storm surge barriers, it is useful to analyze the effect on flood risk more directly, rather than just reducing the probability of failure to close alone. Mooyaart et al. (2025) propose examining the impact of barrier failure mechanisms on extreme water level frequencies behind the barrier. This approach is expected to be a good proxy for flood frequency and, hence, suitable for identifying effective performance improvements as well.

4.7 Conclusion

This paper proposes a method to systematically identify performance improvements for storm surge barriers using a checklist. The method consists of 3 screening stages: one desk study and two structured expert evaluations. This checklist contains 85 principal performance improvements (PPI's), which were subdivided into eight categories: Model conservatism, hardware, common-cause failure, human error, software error, maintenance, and operation. This checklist was developed based on a literature review, dialogues with co-authors and Rijkswaterstaat colleagues, systematic structuring, and the Maeslant barrier case study (in Rotterdam, the Netherlands).

The case study demonstrates that the checklist is, at the very least, nearly complete. Together with the screening method, it is effective in deriving case-specific performance improvements. No additional PPIs were identified in the case study, indicating that the steps taken to develop the checklist (literature study, dialogues, and systematic structuring) were thorough. The process of deriving a top 5 list of case-specific performance improvements required two expert sessions of a day over a period of one month. In contrast, the historical process to derive these improvements required multiple iterative steps over a period of several years.

While the checklist and its screening method were found promising for other barriers, this paper contains only one case study, and more case studies are required to improve the credibility of the method.

4.8 References

Aven, T. (2016). On the use of conservatism in risk assessments. *Reliability Engineering and System Safety*, *146*, 33–38. URL: http://dx.doi.org/10. 1016/j.ress.2015.10.011. doi:10.1016/j.ress.2015.10.011.

Aven, T. (2017). Improving the foundation and practice of reliability engineering. *Proceedings of the Institution of Mechanical Engineers, Part O: Journal of Risk and Reliability*, *231*, 295–305. doi:10.1177/1748006X17699478.

Bakker, A. M., Rovers, D. L., & Mooyaart, L. F. (2025). Storm Surge Clusters, Multi-Peak Storms and Their Effect on the Performance of the Maeslant Storm Surge Barrier (The Netherlands). *Journal of Marine Science and Engineering*, *13*. doi:10.3390/jmse13020298.

Barnes, M. J., Bley, D., & Cooper, S. (2000). *Technical basis and implementation guidelines for a technique for human event analysis (ATHEANA)*. Technical Report. URL: http://scholar.google.com/scholar?hl=en&btnG=Search&q=intitle:Technical+Basis+and+Implementation+Guidelines+for+A+Technique+for+Human+Event+Analysis#0.

Bier, V. M., & Cox Jr., L. A. (2007). Probabilistic Risk Analysis for Engineered Systems. In *Advances in Decision Analysis, from foundations to applications*. Cambridge University Press. (1st ed.).

Birnbaum, Z. (1969). On the importance of different components in a multicomponent system. In P.R. Kreshnaiah (Ed.), *Multivariate analyses II* (pp. 581–592). New York: Academic Press.

Borgonovo, E., & Apostolakis, G. E. (2001). A new importance measure for risk-informed decision making. *Reliability Engineering and System Safety*, *72*, 193–212. doi:10.1016/S0951-8320(00)00108-3.

Chen, R., Zhang, C., Wang, S., Zio, E., Dui, H., & Zhang, Y. (2023).

Importance measures for critical components in complex system based on Copula Hierarchical Bayesian Network. *Reliability Engineering and System Safety*, *230*, 108883. URL: https://doi.org/10.1016/j.ress.2022. 108883. doi:10.1016/j.ress.2022.108883.

Cheok, M. C., Parry, G. W., & Sherry, R. R. (1998). Use of importance measures in risk-informed regulatory applications. *Reliability Engineering and System Safety*, *60*, 213–226. doi:10.1016/S0951-8320(97)00144-0.

Cooke, R. (1991). *Experts in uncertainty: opinions and subjective probability in science*. Oxford University Press.

Dalkey, N., & Helmer, O. (1963). An Experimental Application of the DELPHI Method to the Use of Experts. *Management Science*, *9*. doi:10.1287/mnsc. 9.3.458.

Dummer, G., Tooley, M., & Winton, R. (1997). *An Elementary Guide To Reliability*. (Fifth edit ed.). doi:10.1016/B978-0-7506-3553-0.50003-X.

Dutuit, Y., & Rauzy, A. (2015). On the extension of Importance Measures to complex components. *Reliability Engineering and System Safety*, *142*, 161–168. URL: http://dx.doi.org/10.1016/j.ress.2015.04.016. doi:10.1016/j.ress.2015.04.016.

Eames, P. (2022). *The HAZOP Leader's Handbook*. Elsevier. doi:10.1016/ C2021-0-01014-2.

Gomes, W. J. d. S., & Beck, A. T. (2021). A conservatism index based on structural reliability and model errors. *Reliability Engineering and System Safety*, *209*. doi:10.1016/j.ress.2021.107456.

Haimes, Y. Y., Kaplan, S., & Lambert, J. H. (2002). Risk filtering, ranking, and management framework using hierarchical holographic modeling. *Risk Analysis*, *22*, 383–397. doi:10.1111/0272-4332.00020.

Hallegatte, S., Green, C., Nicholls, R. J., & Corfee-Morlot, J. (2013). Future flood losses in major coastal cities. *Nature Climate Change*, *3*, 802–806. URL: http://www.nature.com/doifinder/10.1038/nclimate1979. doi:10.1038/nclimate1979.

Hegseth, J. M., Bachynski, E. E., & Leira, B. J. (2021). Effect of environmental modelling and inspection strategy on the optimal design of floating wind turbines. *Reliability Engineering and System Safety*, *214*, 107706. URL: http://dx.doi.org/10.1016/j.ress.2021.107706. doi:10.1016/j. ress.2021.107706.

Henley, E. J., & Kumamoto, H. (1981). *Reliability engineering and risk assessment*. Englewood Cliffs, N.J.: Preston Hall.

Heslinga, G. (2004). *Report failure probability model human error (Dutch: Rapport faalkansmodel menselijke fouten), ref: OKE-2005-258-T*. Technical Report KEMA Arnhem.

Horvat and Partners (2006). *Second Opinion Failure Probability Maeslant barrier (Dutch: Second opinion Faalkans Maeslantkering)*. Technical Report Rotterdam.

IAEA (1992). *Procedures for Conducting Common Cause Failure Analysis in Probabilistic Safety Assessment: IAEA TECDOC Series No. 648*. Technical Report.

International Electrotechnical Commission (2016). *Hazard and operability studies (HAZOP studies)- Application guide (IEC 61882)*. Technical Report.

International Electrotechnical Commission (2018). *Failure modes and effects analysis (FMEA and FMECA) (IEC 60812)*. Technical Report.

International Electrotechnical Commission (2021). *Safety of machinery - functional safety of safety-related control systems (IEC Standard no. 62061)*. Technical Report. URL: https://www.nen.nl/ nen-en-iec-62061-2021-en-fr-285780.

Kiel, E. S., Catrinu-Renstrøm, M. D., & Kjølle, G. H. (2023). A Transformer Outage Duration Model with Application to Asset Management Decision Support. In *ESREL 2023* (pp. 2215–2222). doi:10.3850/978-981-18-8071-1_ p078-cd.

Kletz, T. (1992). *Hazop and hazan*. (3rd ed.). Rugby, Warwickshire, UK: Institution of Chemical Engineers.

Knochenhauer, M., & Louko, P. (2003). *Guidance for External Events Analysis*. Technical Report February Swedish Nuclear Inspectorate (SKI). doi:10.1007/ 978-0-85729-410-4_241.

Lewin, J., Ballard, G., & Bowles, D. S. (2003). Spillway gate reliability in context of overall dam failure risk. In *USSD Annual Lecture* (pp. 1–17). Charleston, South Carolina.

Li, Y., Zhang, W., Liu, B., & Wang, X. (2024). Availability and maintenance strategy under time-varying environments for redundant repairable systems with PH distributions. *Reliability Engineering and System Safety*, *246*, 110073. URL: https://doi.org/10.1016/j.ress.2024. 110073. doi:10.1016/j.ress.2024.110073.

Liu, M., Wang, D., & Si, S. (2023a). Mixed reliability importance-based solving algorithm design for the cost-constrained reliability optimization model. *Reliability Engineering and System Safety*, *237*, 109363. URL: https://doi. org/10.1016/j.ress.2023.109363. doi:10.1016/j. ress.2023.109363.

Liu, M., Wang, D., & Si, S. (2023b). Solving algorithm design for the cost minimization reliability optimization model driven by a novel costbased importance measure. *Reliability Engineering and System Safety System Safety*, *244*, 109907. URL: https://doi.org/10.1016/j. ress.2023. 109907. doi:10.1016/j.ress.2023.109907.

Mooyaart, L. F., Bakker, A. M., van den Bogaard, J. A., Jorissen, R. E., Rijcken, T., & Jonkman, S. N. (2025). Storm surge barrier performance—The effect of barrier failures on extreme water level frequencies. *Journal of Flood Risk Management*, *18*, 1–17. doi:10.1111/jfr3.13048.

Mooyaart, L. F., Bakker, A. M. R., van den Bogaard, J. A., Rijcken, T., & Jonkman, B. (2023). Economic optimization of coastal flood defence systems including storm surge barrier closure reliability. *Journal of Flood Risk Management*, *16*. URL: https://onlinelibrary.wiley.com/doi/10. 1111/jfr3.12904. doi:10.1111/jfr3.12904.

Mooyaart, L. F., & Jonkman, S. N. (2017). Overview and Design Considerations of Storm Surge Barriers. *Journal of Waterway, Port, Coastal, and Ocean Engineering*, *143*, 06017001. doi:10.1061/(asce)ww.1943-5460.0000383.

NRG (2003). *Reliability analysis OKE (Dutch: Betrouwbaarheidsanalyse OKE)*. Technical Report Arnhem.

Nuclear Energy Institute (2018). *NUMARC 93-01 revision F, Industry guideline for monitoring the effectiveness of maintenance at nuclear power plants*. Technical Report. URL: https://www.nrc.gov/docs/ML1812/ML18120A069.pdf.

NUREG (2004). *Good Practices for Implementing Human Reliability Analysis (HRA)*. Technical Report. URL: https://citeseerx.ist.psu.edu/ viewdoc/ download?doi=10.1.1.194.8511&rep=rep1&type=pdf.

Parry, G. W. (1991). Common cause failure analysis: A critique and some suggestions. *Reliability Engineering and System Safety*, *34*, 309–326. doi:10. 1016/0951-8320(91)90106-H.

Pat´e-Cornell, E. (2002). Finding and fixing systems weaknesses: Probabilistic methods and applications of engineering risk analysis. *Risk Analysis*, *22*, 319–334. doi:10.1111/0272-4332.00025.

Paula, H., Campbell, D., Parry, G., Mitchell, D., & Rasmuson, D. (1990). *A cause-defense approach to the understanding and analysis of common cause failures, NUREG/CR-5460*. Technical Report NUREG Springfield. URL: http://inis.iaea.org/search/search.aspx?orig_q=RN:34002229.

Rijkswaterstaat (2011). *Leidraad Risicogestuurd Beheer en Onderhoud (conform de ProBo werkwijze)*. Technical Report. URL: https://puc.overheid.nl/ rijkswaterstaat/doc/PUC_143949_31/.

Rijkswaterstaat (2018a). *Handreiking prestatiegestuurde risicoanalyses (PRA)*. Technical Report. URL: https://www.leidraadse.nl/assets/files/ latestversion/Downloads/RWS/RAMS/1_ Handreiking_PRA/LeidraadPRA_ vigerend.pdf.

Rijkswaterstaat (2018b). *TOPAAS: Deel 1 Handleiding (Kader)*. Technical Report.

Rijkswaterstaat (2023). *Investigation resolution Grinwis, "Holland barrier" (Dutch: Onderzoek Motie Grinwis c.s., 'Hollandkering')*. Technical Report november.

Rijneveld, B. (2008). *A study into failure probability reducing measures at the Maeslant barrier (Dutch: Een studie naar faalkansreducerende maatregelen voor de Maeslantkering)*. Technical Report Delft University of Technology Delft.

Rusnak, P., Zaitseva, E., Levashenko, V., Bolvashenkov, I., & Kammermann, J. (2024). Importance analysis of a system based on survival signature by structural importance measures. *Reliability Engineering and System Safety*, *243*, 109814. doi:10.1016/j.ress.2023.109814.

Schüller, J., Brinkman, J., van Gestel, P., & van Otterloo, R. (1997). *Methods for determining and processing probabilities. 'Red Book'*. Technical Report Committee for the Prevention of Disasters Arnhem.

Swain, D., & Guttmann, H. E. (1983). *Handbook of reliability analysis with emphasis on nuclear plant applications*. Technical Report August.

United States Nuclear Regulatory Commission (2011). *Development of Quantitative Software Reliability Models for Digital Protection Systems of Nuclear Power Plants*. May.

US Nuclear Regulatory Commission (2006). *Evaluation of Human Reliability Analysis Methods Against Good Practices (NUREG-1842)*. Technical Report. URL: https://www.nrc.gov/docs/ML0632/ML063200058.pdf.

Van Der Weide, J. A., & Pandey, M. D. (2015). A stochastic alternating renewal process model for unavailability analysis of standby safety equipment. *Reliability Engineering and System Safety*, *139*, 97–104. URL: http://dx.doi. org/10.1016/j.ress.2015.03.005. doi:10.1016/j.ress.2015.03.005.

Van Manen, S., Brandt, E., Van Ekris, J., & Geurts, W. (2015). TOPAAS: An alternative approach to software reliability quantification. *Quality and Reliability Engineering International*, *31*, 183–191. doi:10.1002/qre.1570.

Vesely, W. E., Davis Thomas, C., Denning, R. S., & Saltos, N. (1983). *Measures of Risk Importance and Their Applications, NUREG/CR-3385, BMI-2103*. Technical Report May.

Xu, Z., Ramirez-Marquez, J. E., Liu, Y., & Xiahou, T. (2020). A new resiliencebased component importance measure for multi-state networks. *Reliability Engineering and System Safety*, *193*, 106591. URL: https://doi.org/10.1016/j.ress.2019.106591. doi:10.1016/j.ress.2019.106591.

Zhang, C., Chen, R., Wang, S., Dui, H., & Zhang, Y. (2022). Resilience efficiency importance measure for the selection of a component maintenance strategy to improve system performance recovery. *Reliability Engineering and System Safety*, *217*, 108070. URL: https://doi.org/10.1016/j.ress.2021.108070. doi:10.1016/j.ress.2021.108070.

5

Optimal model refinements of reliability and availability analyses

The previous chapter proposed a method to systematically identify the top five options for reducing the probability of failure to close. To assess their effect, the reliability and availability analysis - used to determine the probability of failure to close – needs to be adapted. Effectively adapting this model is not always straightforward. Therefore, this chapter examines ways to refine reliability and availability models.

Section 5.1 presents current literature on model refinements. Section 5.2 classifies model refinements based on how reliability and availability analyses are set up. Section 5.3 quantifies the value of model refinements, while Section 5.4 presents how to evaluate them. Section 5.5 applies the method to the Maeslant barrier. Sections 5.6 and 5.7 discuss and conclude the chapter, respectively.

5.1 Introduction

Due to the increasing risk of coastal flooding, storm surge barriers need to improve their performance. At the Maeslant barrier, the probability of a failure to close is the dominant failure mechanism (Chapter 2). From an economic perspective, reliability requirements should be more stringent as flood risks rise (Chapter 3). Therefore, the Maeslant barrier must reduce its probability of a failure to close.

In the Netherlands, the probability of a failure to close is typically determined with a reliability and availability analysis (RA analysis) using fault and event trees. In other industries, RA analyses are also referred to as probabilistic safety assessments, quantitative risk analyses, or various combinations of these terms. RA analyses are applied to a variety of technological objects, including nuclear plants (NUREG, 1975), airplanes (Sachon and Paté-Cornell, 2000), space missions (Paté-Cornell, 2002; Apostolakis, 2004), and chemical facilities (Van Sciver, 1990) to analyze events with low probability and large consequences, where data needed to quantify risk are sparse (Bier and Cox Jr., 2007).

Chapter 4 presents a method to systematically find options to reduce the probability of failure to close through RA analysis. This method starts with a checklist of 85 principal performance improvements and then narrows them down to a top five. The method was applied to (a historic case of) the Maeslant barrier and resulted in the following five performance improvements: 1) implement human recovery actions for software failures, 2) test object system 5 every month instead of every four months, 3) jack-up the ball joint earlier in the closure procedure, 4) measure and update repair times, 5) establish more realistic common cause failure probabilities

Implementing these performance improvements often requires refining of the reliability and availability model (RA model). For instance, the first performance improvement involves adding human recovery actions to the model. As RA models of storm surge barriers can become large and complex (the fault tree of the Maeslant barrier must be printed on over a thousand pages to be readable), it is not always obvious how and how far to refine the model.

Model refinements are adjustments to the reliability and availability model that aim at increasing solution space and/or lowering the model output uncertainty. These adjustments can either be extensions of the model structure or better-supported input values. By increasing solution space, the effect of new performance improvements on the model outcome can be included. Model output uncertainty is uncertainty about the model error. The model error is the difference between the RA model outcome and the true value (Aven and Zio, 2013). By lowering the model output uncertainty, performance improvements can be implemented with more confidence.

For example, at the Maeslant barrier, the TDT model was initially used to determine software failure probabilities (NRG, 2003). This model was required as the Maeslant barrier closes automatically. Therefore, its operation heavily relies on the quality of the software. The TDT model is a non-validated model containing only three variables. Given the importance of software reliability for the Maeslant barrier, the TOPAAS model was developed. This model was validated through an expert judgment session and includes 14 variables (Van Manen et al., 2015). In this example, the improved validation reduces the uncertainty, and the higher number of variables increases the solution space.

The project management aspects cost, time, and quality can be used to describe the disadvantages of model refinements. Obviously, a model refinement has costs and requires time. However, it can also improve and reduce the quality of the RA analysis.

Establishing the quality of RA analyses is fundamentally challenging. The definition of quality in RA analyses is already a matter of debate (Aven & Zio, 2018). Furthermore, even those actively involved in reliability science dispute the quality of RA analyses. Aven and Renn (2009) show that it can be questioned whether RA analyses satisfy any scientific criteria for reliability and validity. Before Rae et al. (2014) introduce their method to determine the quality of RA analyses, they argue that the quality of RA analyses can never truly be established. Goerlandt et al. (2017) present an overview of methods to validate RA analyses and discuss the limitations of these methods. In this chapter, the quality of an RA analysis is considered high when it is both usable and as credible as reasonably possible.

Refining an RA model can make it even more difficult to assess its quality. A finer model has more details, and this more detailed model is less amenable to reproducibility and scrutiny and more susceptible to non-transparency (Vézer et al., 2018). Hence, a model refinement could result in reduced usability of the model and credibility of the result. In that case, the quality of the RA analysis is lower.

The quality of an RA analysis can be related to its model output uncertainty. Generally, RA analyses with a lower quality have a higher model output uncertainty and vice versa.

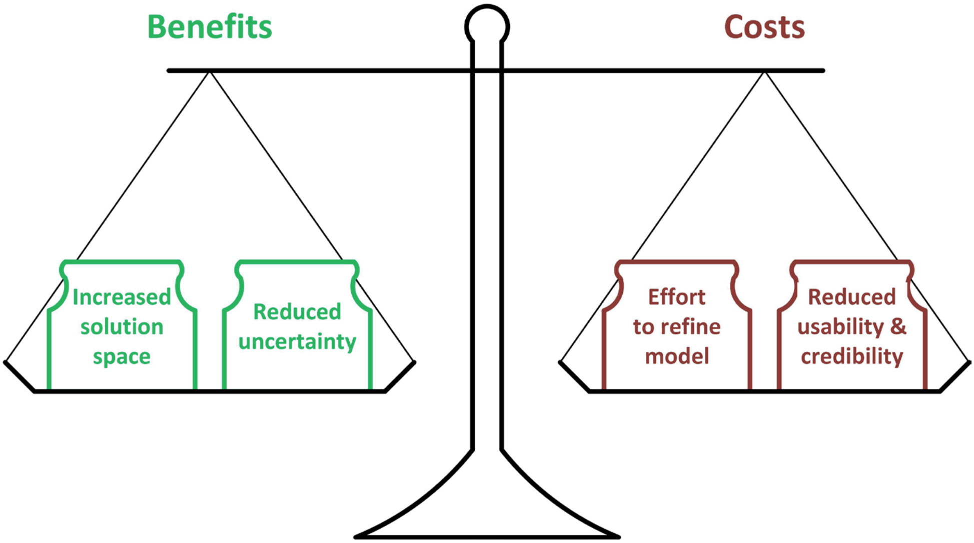

Figure 5.1: Balance of benefits and costs of model refinements.

The question is then how to trade off the potential benefits of model refinements with the cost and their effect on the quality of RA analyses (see Figure 5.1).

Surprisingly little literature was found to determine when a model is sufficiently refined for its study purpose. Moubray (1997) is most specific, stating that highly refined models easily result in "analysis paralysis", that is, a situation where overthinking leads to indecision. On the other hand, too simplified models are more likely to overlook significant failure modes. Although Moubray (1997) highlights the importance of this issue, his book focuses on maintenance and relies solely on qualitative analyses (FMEA). Thus, it remains unclear whether his approach is applicable for quantitative RA analyses and a broader range of performance improvements beyond maintenance alone.

RA analyses guidelines (NUREG, 1983; Schüller et al., 1997; IAEA, 2010) and one article (Apostolakis and Lee, 1977) present considerations regarding the appropriate level of detail. In summary, these documents indicate that the level of detail depends on 1) the scope and objectives of the analysis and 2) the availability of data to quantify failure events. The process is described as iterative and investigative, depending on the preferences of the risk analyst.

The availability of data to quantify failure events is not as clear of a criterion as it initially seems. RA guidelines differ on whether these failure data should originate from the analyzed object itself (NUREG, 1983), its industry (IAEA, 2010) or can even come from other industries (Schüller et al., 1997). Moreover, failure data are collected based on the need of RA analyses (NUREG, 1983; NVvB, 1993), which suggests that the level of refinement is again found with an iterative approach. Thus, the question remains how to determine whether a model refinement is desirable, given the objective to find performance improvements at storm surge barriers to lower coastal flood risk.

This chapter presents a systematic method to optimally select model refinements for adapting RA analyses of storm surge barriers. Section 5.2 describes the general process of an RA analysis described to classify model refinements. Section 5.3 presents a method to quantify the value of model refinements. Section 5.4 shows how to balance costs and benefits of these model refinements. This method is then applied to a case study with the Maeslant barrier to illustrate the method (section 5.5). Section 5.6 discusses the method and the case study. Section 5.7 concludes the chapter.

5.2 Refining RA analyses

5.2.1 General set-up of a RA analysis

Primarily based on the IAEA (2010), Rijkswaterstaat (2018), and RA analyses of Dutch storm surge barriers, eight main steps were identified for conducting an RA analysis (see Figure 5.2).

An RA analysis begins by defining the scope and objectives of an RA analysis. A typical example of an objective is to meet a legislated requirement. Defining the scope includes establishing the object boundaries and identifying the team involved in the RA analysis along with their roles.

After defining the scope and objectives, information about the technological object is gathered. Typically, design specifications, drawings, procedures, and operational experiences/data are collected.

Based on this information, the system is defined by a) decomposing the object and b) splitting operation and maintenance in tasks. There is little literature on decomposing

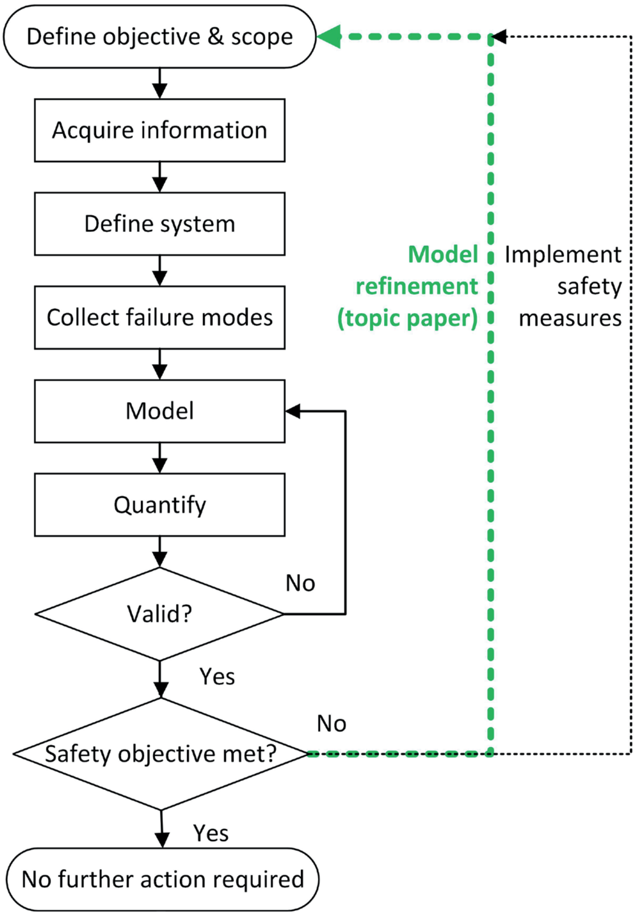

Figure 5.2: Workflow diagram of method to develop optimal level of detail in an RA analysis

an object, while it is an important aspect for model refinement. Therefore, the next section elaborates on this step.

This system definition is then used to collect failure modes. A comprehensive RA analysis identifies hardware, external events, common cause failures, software, and human failures. Common cause failures refer to instances where two or more similar elements fail during a single mission. Lightning and ship collisions are critical external events for storm surge barriers. HAZOP and FMEA (International Electrotechnical Commission, 2016, 2018) are well-known, standardized methods to identify hardware failures.

Based on the collected failure modes, a model is established. This model links failure modes to undesired outcomes. Fault and event trees are predominantly used in RA analyses. Paté-Cornell (1984) provides clear descriptions of these two models. The method to develop a fault tree is standardized (IEC 61025).

The probability or frequency of failure events is typically estimated based on failure data and/or expert judgment. For Dutch storm surge barriers, failure data is favored over expert judgment (Rijkswaterstaat, 2011). Data from the object itself is preferred, then from a supplier, and finally from international databases (Rijkswaterstaat, 2017). Subsequently, the reliability model is used to determine the frequencies and/or probabilities of the undesirable outcomes.

The analysis is validated, possibly supported by importance, sensitivity, uncertainty analyses and a comparison with accident frequencies (if available). Goerlandt et al. (2017) present a recent overview of methods to validate an RA analysis. If validation proves inadequate, the model and/or its quantification are adapted.

In the final step, the result is evaluated. If it is unsatisfactory either the model can be refined, or safety measures can be recommended.

This process of setting-up a RA analysis is iterative rather than linear. A model refinement, for example, could directly be implemented in the model or require a team expansion of a reliability expert specifically related to that model refinement (objective & scope stage). Moreover, a model refinement could require additional information, an adjustment of the system definition or another way to divide the risk into failure modes (see Figure 5.2).

5.2.2 Decomposing an object

An object decomposition is hierarchical. In this thesis, it is ordered as follows: object, object systems, object subsystems, and components. If there are more than four hierarchical levels, the object subsystems are numbered (i.e., object subsystem level 1, level 2, etc.). Figure 5.3 presents an example of an object decomposition.

An object's decomposition tends to grow exponentially when it is refined. For every element, there are multiple sub-elements, and for each sub-element, there are multiple sub-sub-elements, and so on. In storm surge barriers, there are often repetitive elements. For instance, the Eastern Scheldt barrier has 62 gates, each equipped with two hydraulic cylinders, which also have redundancies at lower levels.

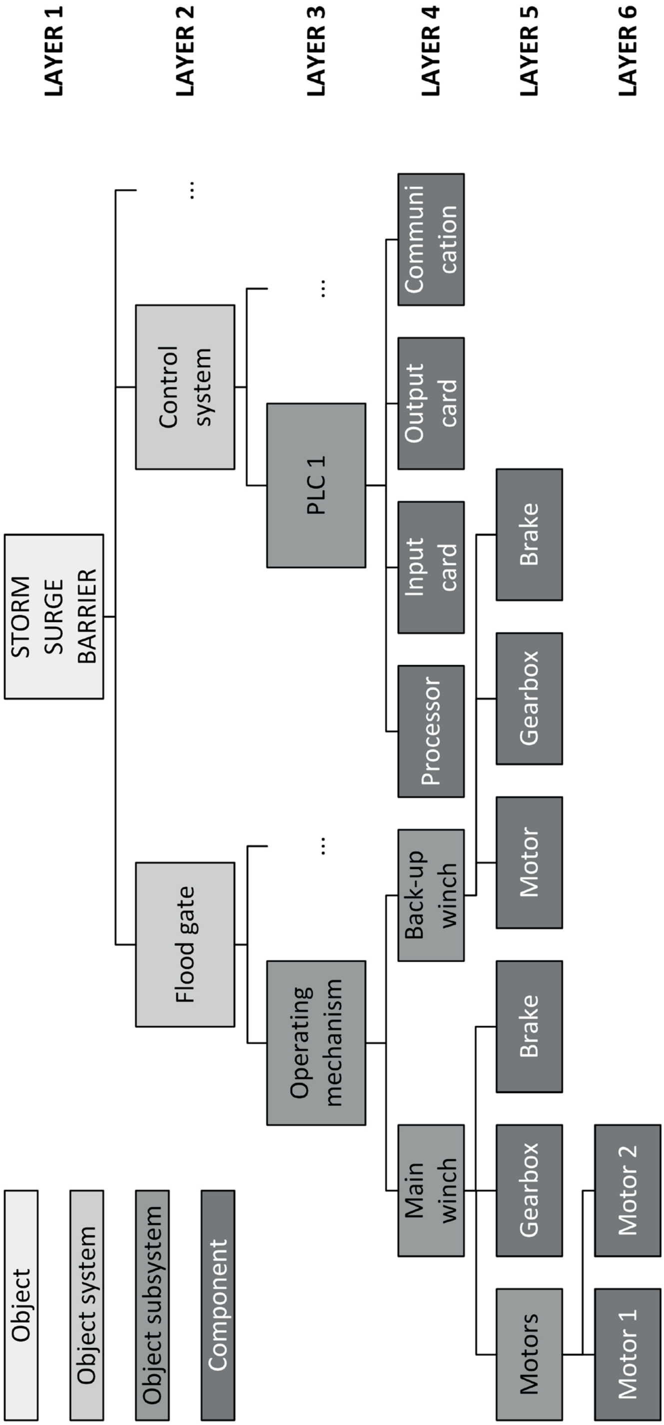

Figure 5.3: Example of object decomposition of a flood gate.

Therefore, the size of an object's decomposition can become substantial with a high level of detail.

For each element, criteria are set to define functional, failed, and any other relevant states (Shooman, 1990). Preferably, these criteria are quantitative. For instance, a floodgate may only be considered failed if its closure takes longer than 2 hours. This latter value serves as the failure criterion.

This failure criterion is especially useful for higher hierarchical levels as it helps determine whether all sub-elements are necessary or serve as backup in case of malfunction. At lower hierarchical levels, the failure criterion can be excluded. For instance, for a power supply a critical amount of power can serve as a failure criterion. Based on this criterion, it can be determined whether lower-level elements like switches and cables are redundant or crucial in for the power supply to function.

Decomposing an object allows to acquire more failure data. For instance, the Eastern Scheldt barrier consists of 62 gates. Each gate has two hydraulic cylinders and each hydraulic cylinder has multiple valves and pumps. Operational data can be collected at the "barrier level" (1), the "gate-level" (62), the "cylinder level" (124) and the "valves & pumps level" (a certain factor times 124). This example illustrates that with a finer decomposition, more operational data becomes available.

5.2.3 Types of model refinements

Based on the RA analysis procedure, three main types of model refinement are defined: 1) refining the system definition, 2) adding model complexity, and 3) refining model input. The system definition can become more precise by refining the decomposition, tasks, and failure criteria. Model complexity can be added by including more failure modes, refining the logic, or the failure event model. Here, an extreme example of refining the model logic would be to change a fault into an event tree, where an event tree has the possibility to consider more (scenarios of) undesired outcomes. Model input can be refined by acquiring more failure data, obtaining more representative failure data, or conducting more advanced expert judgment, such as employing the Cooke (Cooke, 1991) or Delphi methods (Dalkey and Helmer, 1963). In the next section, the value of these different types of model refinements is quantified.

5.3 Value of model refinements

This section establishes the value of model refinements *before* they are implemented and, thus, the outcome of the model refinement is yet uncertain. The presented approach from the value of information theory, described by Faber (2007). A recent review by Zhang (2021) was used to understand the latest developments in this theory.

The method looks at the effect of model refinements on safety target optimization. It is assumed that a storm surge barrier has to meet a certain safety target and that costly measures are needed to meet this safety target. The model refinement can assist in safety target optimization in two manners. First, the model refinement can find alternative measures to meet the safety target. This type of benefit is referred to as “adding solution space”. Second, the model refinement can show that the risk was initially overestimated and that the original costly safety measures are not needed anymore or, at least, not all. This type of benefit is referred to as “reducing uncertainty”. The next sections elaborate on these two types of benefits.

5.3.1 Adding solution space

Model refinements add solution space when they include new variables. For example, the model is refined by including a human recovery model in the reliability and availability model. This human recovery model includes several variables, such as the level of training and the time available to recover. These variables can be optimized, for instance, by raising the level of training.

Figure 5.4 shows a decision diagram of this example. The first decision is whether to add the human recovery model. If this model is not added, a certain set of safety measures is required to meet the safety target. If it is added, there are two possibilities: either the set of safety measures originally anticipated can be chosen or a new set which was defined using the human recovery model. Naturally, it makes sense to choose this more affordable option.

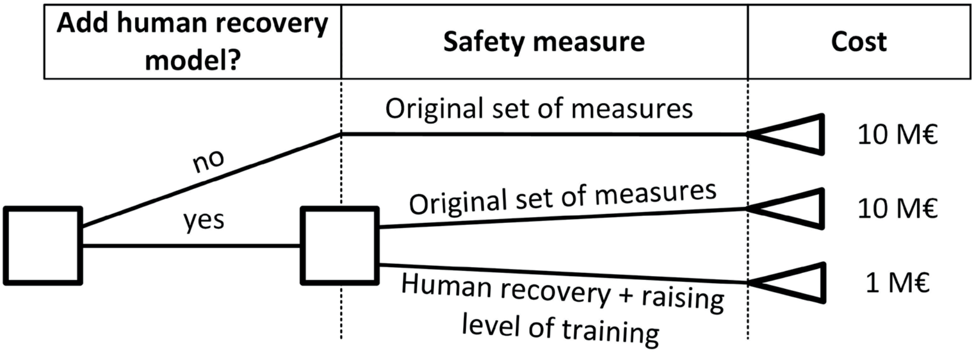

Figure 5.4: Decision tree of model refinement "human recovery model" and its effects on the cost for safety target optimization.

Thus, with more solution space, the costs of safety measures to attain the safety target can become lower. This difference ΔC_{sm} is used to quantify the value of adding solution space V_{ss}:

$$V_{ss} = \Delta C_{sm} = C_{sm_1} - C_{sm_2} \quad (1).$$

In which C_{sm1} are the costs of the safety measures required to attain the safety target before and C_{sm2} after solution space is added, both expressed as a present value. When determining the present value, the annual (maintenance) costs of the safety measures can be included. In the example of Figure 5.4, the value of adding solution space is (10 – 1 =) 9 M€.

In the previous example, it might be difficult to establish the costs of the original set of measures. Here, it could be easier to use lower and upper bounds of cost estimates. For instance, the original set of measures might be to raise interior flood defences. Establishing an accurate cost figure for this measure can be a large and expensive study. Using the lower bound of a rough estimate (somewhere between 10 and 100 M€) can then be sufficient to support implementing the model refinement.

5.3.2 Reducing uncertainty

Treatment of uncertainties at storm surge barriers

In the RA analyses of storm surge barriers, the probability of failure to close is based on a combination of expected and conservative values. For instance, often 95% upper confidence bounds of failure rates are applied for electrical and mechanical equipment (conservative), while in other cases, best estimates (expected values), such as mission time, are employed. In some cases, it is not sure whether a conservative or expected value is applied, for instance, with common-cause failure rates. Therefore, the value of model refinements is determined for both conservative (section 3.2.2) and expected values (section 3.2.3).

Remove conservatism

Removing conservatism results in a lower probability of a failed closure. Hence, safety measures might not be necessary to meet the safety target. The value of removing conservatism V_{rc} can then be calculated in the same manner as equation 1.

As an example, the fourth performance improvement is considered: "measure and update repair times". Assumed repair times in the RA model were expected to be relatively long compared to the current situation. By measuring and updating the repair times, the probability of a failure to close was expected to become lower. Due to this lower failure probability, less measures are needed to meet the safety target. This difference is considered the value of this model refinement.

Better support for best estimate

Here, model refinements are considered which better support a best estimate. This better support can come from introducing more data, more representative data or more advanced expert judgement. These model refinements are referred to as model input refinements.

A model input refinement has three potential outcomes: a much higher, a much lower and a similar probability of failure. In the first case, additional measures are necessary, while with a much lower estimate no safety measures might be needed at all. If the probability of failure remains approximately the same, the same safety measures are needed as before implementation of the model refinement (see Figure 5.5).

To quantify the value of a model input refinement, the possibility of a much higher estimate – with consequently more safety measures – is ignored. If this approach is not taken, the value of a model refinement would become zero or even negative and no model input refinement can be justified. By ignoring this less favorable possibility, the value of a model refinement is naturally overestimated and must be seen as an upper bound of the value. The discussion contains suggestions to more accurately determine the value of a model refinement.

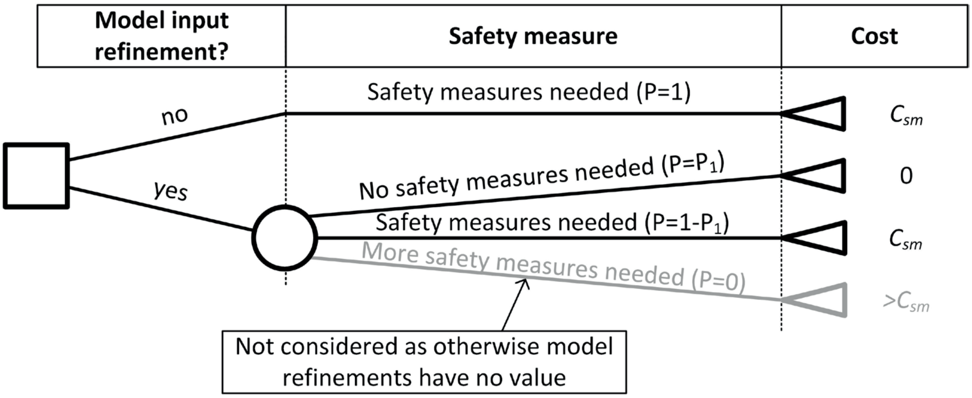

Figure 5.5: Decision tree of a model input refinement and its effects on the cost for safety target optimization. Costs of safety measures are described by the symbol C_{sm}, the probability that the model input refinement will reveal that no safety measures are needed P_1.

The value of a model input refinement is then the probability that this refinement will result in a low probability of failure *P1* where no safety measures are needed or, at least, less safety measures than currently anticipated Δ*Csm*:

$$V_{nb} = P_1 \cdot \Delta C_{sm} \tag{2}$$

To determine the probability P_1, the failure probabilities are described by a probabilistic distribution which best reflect the uncertainty around the failure probability. For Dutch storm surge barriers, the current approach is to use a single value to describe failure probabilities at storm surge barriers. For example, the Maeslant barrier has an expected probability of a failure to close of 1/100 on demand. With the proposed approach here, this failure to close is described by a probabilistic distribution, for instance, a log-normal distribution with 2.5% and 97.5% confidence bounds of 1/1000 and 1/10 on demand (see Figure 5.6).

The probabilistic distribution can now be used to establish the probability that no safety measures are needed. The value P_1 is equal to the cumulative probability below the safety target (see Figure 5.7).

However, after a model input refinement, uncertainty about the failure to close will remain. If the initial estimate of the uncertainty was incorrect, this refinement could even indicate that the true uncertainty is larger than originally anticipated. Moreover,

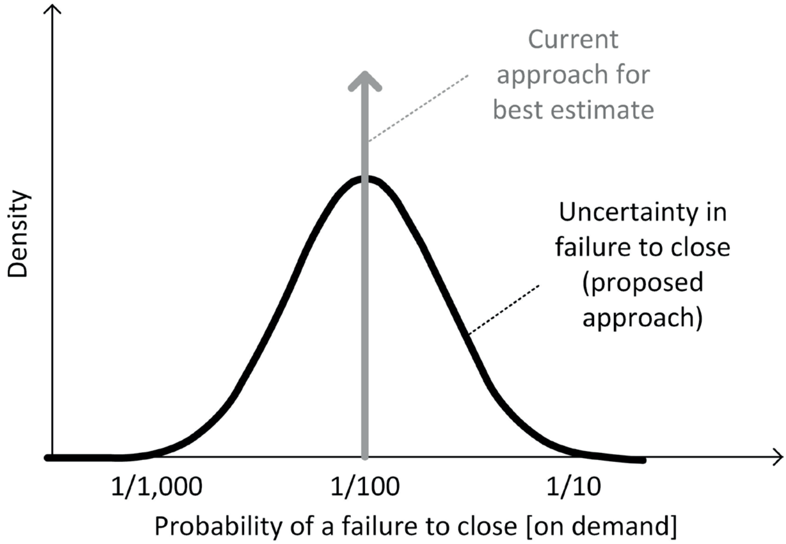

Figure 5.6: Current approach to describe failure probabilities at storm surge barrier and probabilistic distribution describing the uncertainty around the probability of a failure to close.

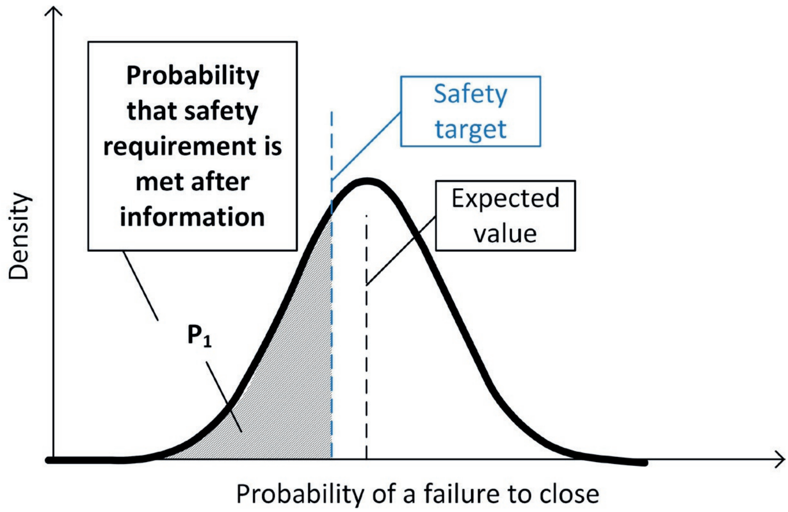

Figure 5.7: The probability that the safety target is met and no safety measures are, thus, needed given the uncertainty around the probability of a failure to close

the true value might be higher than the safety target; however, the model input refinement indicates it is lower. The true value could also be lower than the safety target but not identified by the model input refinement.

To account for the remaining uncertainty, a correction is applied. The correction is based on a narrower probabilistic distribution with the same expected value. At this stage, there is no argumentation to deviate from this expected value as the original estimate is a best estimate. It is reasonable to narrow the bandwidth as two sources of information are combined: the information supporting the original estimate and the new information of the model input refinement. The probability density below the safety target, $P_{2,}$ is then determined for this distribution (see Figure 5.8). As the probabilistic distribution is narrower, this value P_2 is always lower than P_1. Including this correction results in the following the value of a model (input) refinement:

$$V_{nb} = (P_1 - P_2) \cdot \Delta C_{sm} \quad (3).$$

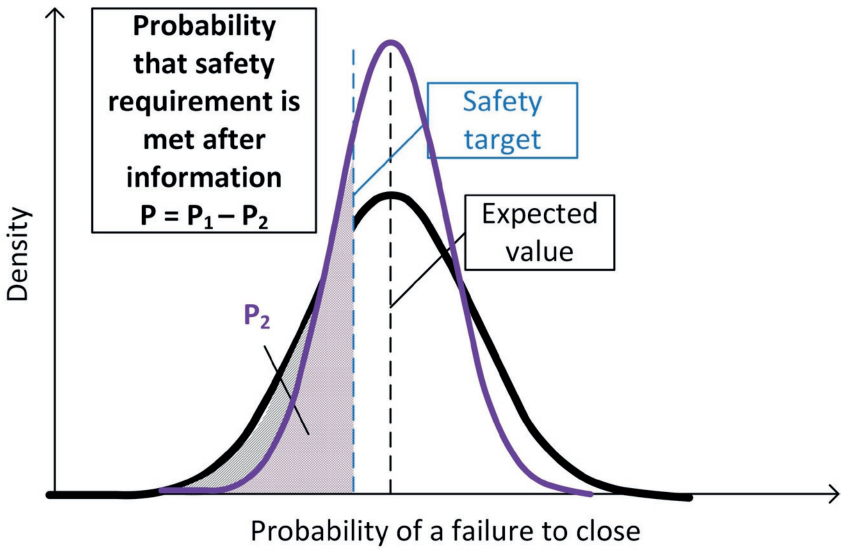

Figure 5.8: Proposed correction P_2 for remaining uncertainty after implementation of the model refinement. The uncertainty around the probability of a failure to close before and after reducing uncertainty is described by a (normal) probabilistic distribution. The remaining uncertainty is described by a narrower distribution with the same expected value.

5.3.3 Total value

The total value of the model refinement V_{tot} is then the sum of the value of adding solution space V_{ss}, removing conservatism V_{rc} and narrower bandwidths V_{nb}:

$$V_{tot} = V_{ss} + V_{rc} + V_{nb} \quad (4)$$

5.4 Evaluating model refinements

5.4.1 Screening criteria

This section proposes how to compare the value with costs. To evaluate model refinements effectively, a screening process is proposed for model refinements. The screening process consists of three steps. Here, the first step is quick and requires little information. Subsequent screening steps are "finer" and require more information before filtering out the model refinement.

The first screening criterion is that a model refinement needs to have value ($V_{tot} \geq 0$). Therefore, it needs to either reduce uncertainty or add solution space. If the model refinement does neither, it should not be implemented.

Second, the value needs to exceed the cost. Thus, the analysis costs C_a need to be lower than the total value of information ($C_a < V_{tot}$).

Third, qualitative trade-off aspects are considered: time (*T*) & quality (*Q*). With respect to time, the question can be raised whether there is sufficient time to implement the model refinement. With respect to quality, the credibility and usability of the model are considered. If the trade-off is negative, that is the costs, time and effect on quality $f(C_a, T, Q)$ are lower than its added value, the model refinement is not implemented. Table 5.1 presents these screening criteria.

Table 5.1: Screening criteria model refinements

#	Question	Screening criterion
1	Added value?	$V_{tot} > 0$
2	Added value > costs?	$V_{tot} > C_a$
3	Net added value?	$V_{tot} > f(C_a, T, Q)$

5.4.2 Trade-off matrix

When multiple model refinements meet the criteria, a trade-off matrix is used to determine which one is most favorable. All trade-off aspects are scored ranging from very low (−−) to very high (++). Classes for these scores are defined based on the added value of the model refinements.

The disadvantages of model refinements are scored per project management aspect: cost, time, and quality. Next to the analysis costs, also life cycle costs of the model refinement are considered when establishing the cost. For instance, the ease at which the model can be adapted later. Depending on the case study, weights can be assigned to the scores of these aspects.

Table 5.2 presents an example of such a trade-off matrix. The mentioned considerations and scores are hypothetical and aim to illustrate its use. In this matrix, a model input refinement is compared with a model refinement that adapts the system definition and one that accounts for human recovery actions. The model input refinement uses failure data from other storm surge barriers, improving the quality of the analysis. The costs of acquiring data (option 1) are relatively small, but the model refinement takes a lot of time as barrier managers need to be contacted and convinced of this undertaking. Adjusting the system definition is expected to be relatively costly and difficult. Adapting the model to account for human recovery is favorable on most aspects, but is expected to lower the quality. There are many human recovery actions which will make the model larger and more difficult to use. Moreover, it is difficult to establish credible failure probabilities of human recovery actions as these are rarely needed and are performed in circumstances which are difficult to simulate. Based on the scores, it seems favorable to implement two of the three model refinements: 1) using of failure data from storm surge barriers and 2) accounting for human recovery.

Table 5.2: Example of trade-off matrix of model refinements

Trade-off aspect	1: Model input refinement – use failure data from storm surge barriers	2: Adapt system definition – develop a less stringent failure criterion	3: Adapt model - Account for human recovery
Value	+	+	++
Costs	+	-	++
Time	-	0	+
Quality	++	-	--

5.5 Case study

5.5.1 Ballast system of the Maeslant barrier

The case study is the Maeslant barrier, which protects Rotterdam and Dordrecht (Netherlands) against coastal floods. The barrier consists of two floating sector arms, which in normal conditions are positioned in a dry dock. When an extreme storm surge is expected, the floating sector arms are positioned into the New Waterway, a canal that runs from Rotterdam to the North Sea. As the sill of the dry dock is eight meters higher than the sill of the New Waterway, the floating sector arms need to be ballasted to sink on the sill.

Due to rising flood risk, the barrier needs to be upgraded (see Chapter 3). The case study extends upon the case study of the previous chapter. Here, a top five performance improvements was established for (a historic case of) the Maeslant barrier. As the first four the model refinements are fairly obvious, this case study focuses on the fifth: Establish more realistic common cause failure probabilities. Common cause failures are failures at identical redundant components which fail because of a common cause such as a design error in both components (IAEA, 1992; Duy, 2018).

The case study focuses on the ballast system, as it contains relatively many common cause failures. The ballast system is designed to sink the floating sector gates in a stable manner, avoiding damage to the gates and undesirable translation waves in the inner basin. Therefore, each gate consists of compartments, with each compartment containing a double set of valves. Important common cause failures are the simultaneous failure of a double set of valves, their operating mechanisms and their drives.

5.5.2 Failure criterion

The failure criterion or the RA analysis of 2005 is relatively complicated. The RA model assumes that a single compartment failure can result in exceedance of critical water levels at Rotterdam, if a storm has unfavorable characteristics. To account for these "unfavorable storms", failure rates are multiplied with a certain percentage, which depend on the failure mode. For instance, if a failure mode for a single compartment failure has a probability X and storms that are unfavorable for that failure mode have a probability Y. The probability of failure which can result in exceedance of critical water levels is then XY. Second, a double compartment failure is expected to only result in a flood, if two compartments fail at one side, relative to the center of gravity of a single arm. With more than two compartments failing, the barrier fails in any case. The approach is mentioned to be conservative. An issue for adapting the failure criterion, is that the approach mentioned in the report is inconsistent with the fault tree model.

5.5.3 Failure probability

The probability of failure to close is established for common cause failures in the ballast system, using the second opinion of Horvat & Partners (2006) on the historic RA analysis of the Maeslant barrier of 2005. Without formalized human recovery actions, the total probability of a failure to close is 4/100 on demand (see also previous chapter). Horvat & Partners distribute this probability into ten parts, of which two are relevant: a) Ballast system and b) common-cause failures. These parts contribute approximately twenty percent to the total probability of a failure to close. It is estimated that about half of this failure probability is not related to common-cause failures or the ballast system (10%). Hence, a probability of a failure to close of 4/1000 on demand is used to account for common cause failures in the ballast system.

This probability was established based on failure data of aggregates and valves from other industries. The binomial failure rate model was used to establish common cause failure rates. For clarity and illustrative purposes of this case study, the input failure probabilities are assumed to be expected values (rather than a mixture of conservative and expected values).

5.5.4 Failure probability distribution

For the case study, a failure probability distribution is proposed to describe the uncertainty with respect to the probability estimate for failure to close. The RA analysis does not report on the uncertainty of the estimate. Moreover, the failure probabilities reported in the historic RA analysis were assumed to be a best estimate. Therefore, the following argumentation for a probabilistic distribution was applied: Common cause failure probabilities are highly uncertain and often highly dependent on the maintenance and operation quality of staff of the specific object. Therefore, a probabilistic distribution was selected, accounting for : 1) the initial estimate to be highly uncertain as the estimate relies on values used in other industries and 2) the initial estimate to be extremely skewed, failure probability that are ten times as low are still likely.

A beta distribution is used to model uncertainty around these estimated failure probabilities. A beta distribution is continuous within the interval [0, 1] described by two distribution parameters (α, β). In Bayesian interference, the beta distribution is commonly applied as a prior when the likelihood function is binomial. This feature makes the beta distribution particularly suitable for determining the failure on demand (Kelly and Siu, 1998), also when using the binomial failure rate model (Atwood, 1986).

The beta distribution can take several shapes, two of which are important to describe the uncertainty of a failure probability on demand. Failure probabilities are typically low, that is, smaller than 1/100 on demand. The ratio between distribution parameters α/β is then smaller than 1/100 as well. With this ratio, beta distributions have a shape similar to an exponential distribution ("reverse J-shaped") for α ≤ 1 and else a positively skewed shape (see Figure 5.9). Reverse J-shaped distribution reflect more uncertain estimates of failure probabilities than positively skewed shaped distributions.

Based on these considerations a beta distribution with parameters α = 0.5 and β = 125 was chosen (see blue line in Figure 5.10).

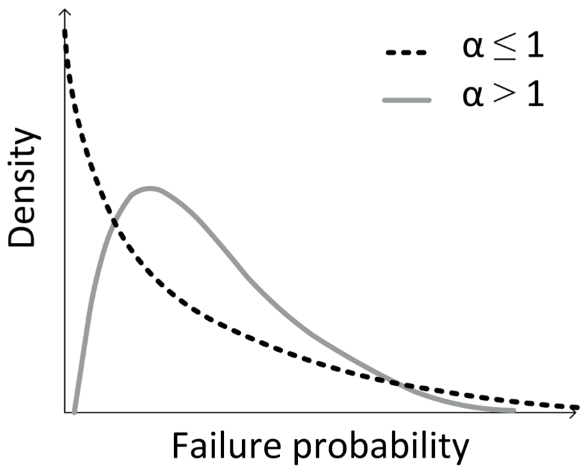

Figure 5.9: Shapes of a beta distribution for describing uncertainties around failure probability estimates. Here, the β distribution parameter is more than a hundred times larger than the α distribution parameter as expected failure probabilities are low.

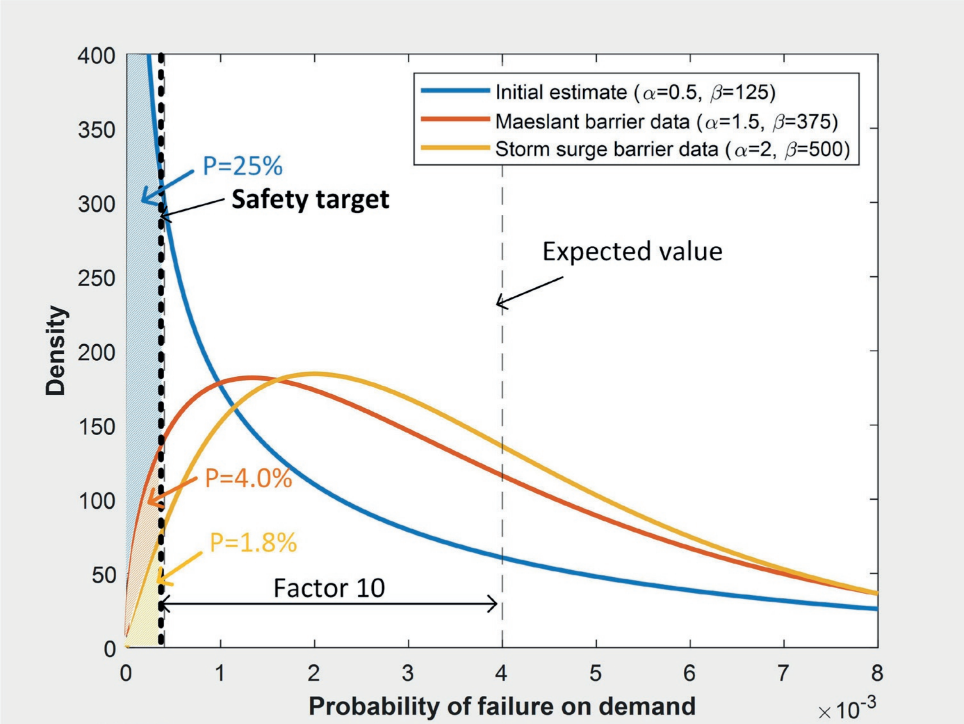

Figure 5.10: The probability distributions describing the uncertainty around the probability of a failure to close estimate for 1) initial estimate, 2) using Maeslant barrier data, and 3) using data from more storm surge barriers. The hatched areas indicate probabilities that the model input refinement reveals that the safety target is met.

5.5.5 Model refinements

Three model refinements are considered to establish more realistic common cause failure probabilities for the ballast system: 1) supporting the estimate with failure data from the Maeslant barrier, 2) supporting the estimate with data from other barriers and 3) adapting the failure criterion [8]. The costs of these model refinements are 25, 50 and 100 k€, respectively.

The data studies are assumed to result in a narrower bandwidth. Beta distributions with high α distribution parameters and a similar ratio between the α and β distribution parameters have narrower bandwidths. With Bayesian interference (Kelly and Siu, 1998), the α distribution parameter can be raised with the number

8 Initially a fourth model refinement was considered: adapting the way common cause failure events are modeled and related to the top event. However, due to quality issues with the current model, this raised too many questions.

of representative failures found in the data and β with the number of operations. Based on the expected probability of failure (4/1000 on demand), the number of operational years (28 years), and monthly testing (12 per year), it is assumed that one representative common cause failure will be found in the data (4/1000 x 28 x 12 ~ 1). Hence, the original α-distribution parameter value (0.5) is raised with 1, resulting in a α-distribution parameter of 1.5.

When using data from other storm surge barriers, the variability between barriers needs to be accounted for. Hierarchical Bayes is typically used to account for variability between nuclear power plants (Kelly and Siu, 1998). In any case, the α-distribution parameter is raised because operational data is added. However, the operational years of other barriers with floating gates (St. Petersburg, barge gates around New Orleans) are shorter and less representative. Therefore, it is expected that the α-distribution parameter is raised with only 0.5, resulting in a value of 2.0.

Adapting the failure criterion is a relatively extensive study. The current failure criterion already has been discussed with experts. Therefore, more than merely expert judgement is required. First, more insight is needed in the effect of failing compartments on the degree of closure. With these partial closures, more water will pass the barrier. If there is only a small opening, a coastal flood occurs only with an extremely severe storm. With larger openings, also less severe storms can result in too high water levels in the inner basin. A study into the hydraulic behavior of the inner basin related to partial openings is, thus, needed to refine the failure criterion. At this stage, it is uncertain how much conservatism can be removed by this study. To explore whether such an undertaking is feasible, it is assumed that the probability of a common cause failure of the ballast system is reduced by a factor of 3.

5.5.6 Results

The value of model refinements is determined in a way which reflects the results of the case study of the previous chapter. In the top 30 (see appendix E), there were also many other model refinements that substantially reduced the probability of failure to close (from 1% to 10%) at a low cost (under 100 k€). Next, there were approximately 10 performance improvements, costing between 100 and 1000 k€, which lowered the probability of failure to close with 2 to 15%. The top 30 included a few options which considerably improved performance (around 20%) at a cost ranging from 1 to 5 M€. Given the large number of safety measures, a cost function could be developed. The method to determine the value of model refinements would have to be refined to include this cost function. However, to illustrate the selection method, a simple discrete assumption is used which is based on this data: When the probability of failure to close - of common cause failures in the ballast system - is lowered by a factor 10, the reduced cost in safety measures is 500 k€. In that way, this model refinement removes the need for one of the more costly measures between 100 and 1000 k€.

Based on this assumption, the value of the model refinements is determined. Figure 5.10 is used to establish the probability that the model input refinement reveals that the probability of a failure to close is a factor 10 lower.

With the use of Figure 5.10 and equations 1 and 3, the value of the model refinements is determined. No value is found for adapting the failure criterion. The assumption is that there is only value, if the model refinement results in a ten times lower probability of a failure to close than the initial estimate. Adapting the failure criterion only results in a factor three lower probability of a failure to close and, therefore, has no value using this (discrete) approach.

The next screening criterion compares (present) costs with their value. Adding data from the other storm surge barriers costs more than its value and, hence, is not feasible. At this stage, using Maeslant barrier data is the only model refinement which passed the first two criteria.

The third screening criterion includes qualitative considerations with respect to time and quality. Using data from the Maeslant barrier is not expected to require much time. The credibility of the model is expected to improve, while the usability is not affected. Possibly, the failure data could be used to simplify the model, improving the usability. Thus, this model refinement is recommended, when including these qualitative considerations.

As only one model refinement passed the screening criteria, no trade-off between model refinements is necessary (see table 5.3).

Table 5.3: Use of three screening criteria (1. Added value? 2. Value > costs? 3. Net added value?) for model refinements of Maeslant barrier, ballast system case study. P_1- P_2 is the (corrected) probability that the safety target is met (see equation 3). ΔC_{sm} are the reduced safety measure costs.

Model refinement	Costs [k€]	P_1-P_2	ΔC_{sm}	Value [k€]	1. Added value?	2. Value> costs?	3. Net added value?
Maeslant barrier data	25	21%	500	105	Yes	Yes	Yes
Storm surge barrier data	50	2.2%	500	11	Yes	No	-
Adapt failure criterion	100	N/A	0	0	No	-	-

5.6 Discussion

The proposed method for selecting model refinements is straightforward, organized, and clear. Screening criteria and a trade-off matrix are proposed to determine whether model refinements should be implemented. The case study illustrated the method's simplicity and applicability.

Still, the method can be optimized to better select model refinements. A discrete approach was selected which only assigned value to a model refinement if it has the potential to meet the safety target. In reality, it will often be necessary to implement a set of model refinements (and safety measures) to meet the safety target. Using a cost function for failure probability reduction could assist with this issue.

Another aspect is that screening and trading off model refinements relies on qualitative judgement. An attempt could be made to quantify the value of time and quality aspects, which would make the selection of model refinements more objective.

The method overvalues model input refinements which are based on a best estimate. The quantification method only considers scenarios where less safety measures are needed and ignores those scenarios where more are needed. As a result, model refinements could be selected with too high costs for its benefits or model input refinements can wrongfully be preferred over those refinements which reduce conservatism. In those cases, the value of model input refinements could be more exactly determined by applying economic instead of safety target optimization. With economic optimization (see chapter 3), costs of safety measures and risks are balanced to find the lowest total cost (= cost + risk). A model input refinement has the potential to reveal an economic need for more safety measures, which cannot be identified without this refinement. The value of the model refinement is then the difference between the expected total costs with and without the model refinement.

This economic optimization perspective on the value of model refinements, also brings an important insight into finding performance improvements in a more general sense. For this process, it is not only important to analyze failure scenarios with high expected values but also those that could be critical considering the uncertainty around their expected value.

Experienced reliability analysts might argue that the presented method is not new. In the current practice, model refinements are only implemented if their benefit outweighs their cost. However, in storm surge barrier practice, it is often observed that model refinements are implemented without arguing why this refinement was best, or even why it was implemented at all. For instance, storm surge barrier RA analyses often contain a highly detailed decomposition for a (sub)system which is not critical for the analyzed function. Moreover, currently, model refinements are selected based on preferences of the risk analyst. The method presented in this chapter makes choices with respect to model refinements transparent, making it more likely for other experts and decision-makers to intervene if the model is unnecessarily refined.

While this method is developed to refine existing RA models, it could be useful for developing new RA models. Difficulties encountered with highly detailed models such as "analysis paralysis" are expected to be prevented by using criteria and trade-off matrices as described in this method. Moreover, the possibility to intervene is likely to result in more homogeneous RA analyses of a higher quality. However, if every model refinement is evaluated, the level of detail of the analysis could become too low, with subsequent difficulty to find performance improvements. Therefore, it is recommended to investigate the optimal balance between evaluating model refinements and implementing them.

The method and case study can also be used to more precisely define an acceptable level of conservatism. Currently, Aven (2016) eloquently argues that conservatism should not be used, while others (Jamali, 2015; Gomes et al., 2021) claim that a small amount of conservatism is acceptable. Based on this method and case study, the following criteria could be applied for conservatism: 1) the risk reduction achieved by removing the conservatism must be greater than its costs, considering the effects on time and quality, and 2) no other model refinements should be preferred over removing this conservatism.

The case study revealed the potential for a storm surge barrier failure database, because the model refinement to develop a failure database for the ballast system of the Maeslant barrier was most promising. The Maeslant barrier RA analysis was developed about twenty years ago and had to rely on failure data that originate from other industries. This practice has likely resulted in an undesired focus on barrier elements that are critical in other industries and not necessarily for storm surge barriers. The Maeslant barrier RA analysis was also important for RA analyses of other Dutch storm surge barriers. Since then, there are more operational years and more storm surge barriers. This experience can be used to develop a failure database for these structures specifically, which would lower the uncertainty about current estimates.

This chapter developed an explicit and quantifiable method to value the effect of reducing uncertainty. However, the value of uncertainty also depends on personal preferences, thus making it important that risk experts and higher-level decision-makers understand how large uncertainty is. Making use of explicit probability distributions can assist in making decisions with respect to this uncertainty.

5.7 Conclusions

This chapter presents a method to balance the costs and benefits of implementing model refinements. The method first uses screening criteria to establish whether a model refinement is sufficiently valuable, followed by a trade-off matrix to determine which model refinement should be implemented first.

This chapter progressed on the case study of the previous chapter by analyzing model refinements needed for one of the identified performance improvements: Establish more realistic common cause failure probabilities. One barrier system (Ballast system) was analyzed, which has a relatively high influence on the total probability of common-cause failures. Three model refinements were evaluated. Refining the model (input) by using failure data from the Maeslant barrier was revealed to be most favorable, because it was expected to lower uncertainty greatly at low costs. The two other model input refinements (a more general storm surge barrier database & an adapted failure criterion) had too high costs compared to its benefits. Therefore, these model input refinements were not recommended. As such it was demonstrated that the method can be used to identify promising model refinements.

This method can assist in improving RA analyses of storm surge barriers. With these improved RA analyses, the decisions for additional safety measures at existing storm surge barriers are more effectively supported. Consequently, the method can help reduce coastal flood risk at these critical safety structures. Furthermore, it could be applied to other safety-critical technological systems aiming to improve their performance.

5.8 References

Apostolakis, G. E. (2004). How useful is quantitative risk assessment? *Risk Analysis*, 24(3):515–520.

Apostolakis, G. E. and Lee, Y. T. (1977). Methods for the estimation of confidence bounds for the top-event unavailability of fault trees. *Nuclear Engineering and Design1*, 41:411–419.

Atwood, C. L. (1986). The binomial failure rate common cause model. *Technometrics*, 28(2):139–148.

Aven, T. and Renn, O. (2009). On risk defined as an event where the outcome is uncertain. *Journal of Risk Research*, 12(1):1–11.

Aven, T. and Zio, E. (2013). Model output uncertainty in risk assessment. *International Journal of Performability Engineering*, 9(5):475–486.

Aven, T. (2016). On the use of conservatism in risk assessments. *Journal of Reliability Engineering and System Safety*, 146:33–38.

Bier, V. M. and Cox Jr., L. A. (2007). Probabilistic Risk Analysis for Engineered Systems. In *Advances in Decision Analysis, from foundations to applications*. Cambridge University Press, 1st edition.

Cooke, R. (1991). *Experts in uncertainty: opinions and subjective probability in science*. Oxford University Press.

Dalkey, N. and Helmer, O. (1963). An Experimental Application of the DELPHI Method to the Use of Experts. *Management Science*, 9(3).

Goerlandt, F., Khakzad, N., and Reniers, G. (2017). Validity and validation of safety-related quantitative risk analysis: A review. *Safety Science*, 99:127–139.

Horvat and Partners (2006). Second Opinion Failure Probability Maeslant barrier (Dutch: Second opinion Faalkans Maeslantkering). Technical Report, Rotterdam.

IAEA (2010). Development and Application of Level 1 Probabilistic Safety Assessment for Nuclear Power Plants. Technical report.

International Electrotechnical Commission (2016). Hazard and operability studies (HAZOP studies)- Application guide (IEC 61882). Technical report.

International Electrotechnical Commission (2018). Failure modes and effects analysis (FMEA and FMECA) (IEC 60812). Technical report.

Kelly, D. L. and Siu, N. O. (1998). Bayesian parameter estimation in probabilistic risk assessment. *Reliability Engineering and System Safety*, 62(12):89–116.

Moubray, J. (1997). *Reliability-centred Maintenance*. Biddles LtD, Guildford & King's Lynn, 2nd edition.

NUREG (1975). Reactor safety study – an assessment of accident risks in U.S. Commercial Nuclear Power Plants, WASH 1400, NUREG 75/014.

Technical report.

NUREG (1983). PRA Procedure Guide. Technical report.

NRG (2003). Reliability analysis OKE (Dutch: Betrouwbaarheidsanalyse OKE). Technical report, Arnhem.

NVvB (1993). *Business continuity data (Dutch: Bedrijfszekerheidsgegevens)*. Kluwer Technische Boeken, Deventer, 1st edition.

Paté-Cornell, E. (2002). Finding and fixing systems weaknesses: Probabilistic methods and applications of engineering risk analysis. *Risk Analysis*, 22(2):319–334.

Paté-Cornell, M. E. (1996). Uncertainties in risk analysis: Six levels of treatment. *Reliability Engineering and System Safety*, 54(2-3):95–111.

Paté-Cornell, E. (1984). Fault Trees vs. Event Trees in Reliability Analysis. *Risk Analysis*, 4(3):177–186.

Rae, A., Alexander, R., and McDermid, J. (2014). Fixing the cracks in the crystal ball: A maturity model for quantitative risk assessment. *Reliability Engineering and System Safety*, 125:67–81.

Rijkswaterstaat (2011). Guideline Probabilistic Operation & Maintenance (Dutch: Leidraad ProBo). Technical report.

Rijkswaterstaat (2017). Guidance verification Reliability and Availability (Dutch: Handreiking Verificatiemethode Betrouwbaarheid en Beschikbaarheid). Technical report.

Rijkswaterstaat (2018). Manual performance-driven risk analyses PRA (Dutch: Handreiking prestatiegestuurde risicoanalyses). Technical report.

Sachon, M. and Paté-Cornell, E. (2000). Delays and safety in airline maintenance. *Reliability Engineering and System Safety*, 67(3):301–309.

Schüller, J., Brinkman, J., van Gestel, P., and van Otterloo, R. (1997). Methods for determining and processing probabilities. 'Red Book'. Technical report, Committee for the Prevention of Disasters, Arnhem.

Shooman, M. L. (1990). *Probabilistic reliability: an engineering approach*. Robert E. Krieger Publishing Company, Inc., Malabar, Florida, second edition.

Van Manen, S., Brandt, E., Van Ekris, J., and Geurts, W. (2015). TOPAAS: An alternative approach to software reliability quantification. *Quality and Reliability Engineering International*, 31(2):183–191.

Van Sciver, G. R. (1990). Quantitative risk analysis in the chemical process industry. *Reliability Engineering and System Safety*, 29(1):55–68.

Vézer, M., Bakker, A., Keller, K., and Tuana, N. (2018). Epistemic and ethical trade-offs in decision analytical modelling: A case study of flood risk management in New Orleans. *Climatic Change*, 147(1-2):1–10.

6

Conclusions and Recommendations

6.1 Motivation for and focus of study

Sea level rise and coastal urbanization increase the risk of coastal floods. Coastal flood protection needs to be enhanced to compensate for this risk increase. Storm surge barriers are critical elements of coastal flood protection and, thus, need to be improved. However, compared to other coastal structures, it is less obvious how to enhance storm surge barriers effectively.

This thesis developed four methods to more efficiently find effective storm surge barrier performance improvements. Methods are considered more efficient when they identify and assess barrier improvements in a faster or more transparent manner. Storm surge barrier performance improvements are considered to be effective when the risk they mitigate surpasses their cost.

This thesis focuses on improving closure reliability, specifically increasing the frequency with which the barrier successfully closes under severe storm conditions. Given that the lack of closure reliability is the dominant failure mechanism for the Maeslant barrier, this barrier was used for each method as a case study.

6.2 Conclusions

The conclusions are presented for each sub-question, followed by a discussion of the main research question.

> *Sub-question 1:* ***How to determine the importance of closure reliability relative to other main failure mechanisms (structural failure and hydraulic overload) for storm surge barriers?***

A general method was introduced to examine how barrier failure mechanisms - namely, operational failure, structural failure, and hydraulic overload - affect the critical level exceedance frequency in the inner basin, serving as a proxy for the flood frequency. The method identified which failure mechanisms contribute most to flood frequency and, therefore, which ones hold promise for improvement. It was extended to determine the frequency of a larger range of extreme water levels than the critical levels, accounting for the variability of interior flood defenses such as elevated land and dikes. This method was applied at the Maeslant barrier, demonstrating that the probability of failure to close the barrier accounts for more than 70% of the flood frequency in Rotterdam. Other significant failure mechanisms for the Maeslant barrier include river discharge accumulation behind the barrier (15%) and the decision not to close due to a water forecast error (10%).

> ***Sub-question 2:*** ***How to determine an economically optimal requirement for closure reliability?***

An economic optimization model was proposed that enhances a renowned optimization model for dikes (Van Dantzig, 1956) by incorporating improvements in closure reliability. The model and case study showed that the costs at which closure reliability can be adjusted are essential for setting economically optimal closure reliability requirements. The Maeslant barrier case study illustrated that even a minor increase in risk (a factor of 2 to 3, corresponding to a sea level rise of 2 to 3 decimeters) could lead to economically optimal requirements for a failure to close becoming a factor of 10 more stringent.

> ***Sub-question 3:*** ***How to find and select closure reliability improvements without overlooking important ones?***

A method was proposed involving a three-stage screening method to select the top five of performance improvements from a checklist of 85 principal performance enhancements. The first stage is a desk study that aims to identify only the principal performance improvements that could significantly impact the probability of a failure to close. The second and third stages consist of expert sessions intended to eliminate and rank the principal performance improvements, respectively. The method was applied to a historical risk assessment analysis of the Maeslant barrier and found important implemented performance improvements (formalizing human recovery) and new ones (exploring common-cause failures, specifically failures of identical components due to a shared cause). The process to compile a top five list of case-specific performance improvements required two full-day expert sessions over the course of a month. In contrast, the historical process involved multiple iterative steps spread over several years.

> ***Sub-question 4:*** ***How can the RA analysis be refined to address identified improvements in closure reliability?***

This thesis presents a method to balance the costs of model refinements with their value. The value of model refinements is quantified by examining their impact on achieving a safety target for the probability of failure to close. A screening procedure is proposed to determine whether the value of a model refinement outweighs its costs, taking into account the effects on time and quality as well. To select the best model refinements, a trade-off matrix is introduced. The case study investigates how to refine common-cause modelling, specifically for the ballast system, which is part of the Maeslant barrier that contains many identical components. Analyzing test data of ballast system components is identified as a first step to modifying the RA analysis.

Combined, the methods of the thesis constitute to a single method for finding and selecting closure reliability improvements and determining their effect on flood risk reduction, thereby answering the main research question. As such, it can be applied by asset managers of storm surge barriers to combat rising flood risk when the lack of closure reliability is the dominant failure mechanism. Moreover, the third and fourth parts could also be useful for managers of other high-performance and safety-critical objects to find effective reliability improvements and model refinements.

The thesis also demonstrated that improvements in closure reliability are feasible at the Maeslant barrier. Already a redundant barrier, that is a second Maeslant barrier which could close in case the current one fails, has a similar cost-benefit ratio as raising interior flood defenses. Smaller closure reliability improvements are expected to be more feasible as this redundant barrier. This thesis developed a method to investigate these smaller enhancements and applied it to a historical case of the Maeslant barrier. While the results are not directly applicable, the simplified analysis in this thesis revealed that a large number of closure reliability improvements can be implemented at relatively low costs. This indicates that even in the current situation, many closure reliability improvements are economically feasible.

6.3 Recommendations

This study has also revealed that scientific research into storm surge barriers is in its early stages. Little to no scientific studies were available at the start of this dissertation. Unsurprisingly, there are a lot of options to further research and, hence, it becomes more a question which aspect to emphasize. Here, the recommendations are focused on improving the methodology for enhancing storm surge barrier performance overall and for specifically improving the performance of the Maeslant barrier. Based on this focus, the following three recommendations are presented:

1. Advance the reliability and availability analysis for storm surge barriers in general, with a specific focus on the Maeslant barrier. Current analyses are over twenty years old and have relied on failure databases from other structures, such as nuclear power plants. Since storm surge barriers operate differently than other objects

(low-frequent use in hazardous conditions, unlike aerospace repairable systems), the use of this data has likely resulted in an undesired focus on elements critical to other structures, which may not be relevant to storm surge barriers and vice versa. As the Maeslant barrier has been operational for over 25 years and more storm surge barriers have been constructed since then, more data on failures and successes are now available. Insight into these operational experiences, ideally quantified as failure data, determines how a reliability analysis (RA) model is established (NVvB, 1993). Furthermore, because the RA model for the Maeslant barrier is large (>1200 pages of fault tree analysis and>7000 lines in database format) and inconsistent with its report, it is difficult to adapt. Given all these challenges, it is recommended to develop a new RA analysis practice specifically for storm surge barriers and to redevelop the RA analysis for the Maeslant barrier. As part of this, it is recommended to create a database of failures and incidents based on the 25 years of Maeslant barrier operations.

2. Extend the method to include other barrier failure mechanisms. This thesis only investigated how to improve closure reliability. At other barriers, other failure mechanisms than failure to close are dominant. For instance, at Ramspol (Zikidou, 2023) and the Eastern Scheldt barrier (Rijkswaterstaat, 2022a), failure to close is not the most probable scenario to result in a coastal flood. In these cases, the lack of a closure decision or a delayed closure is more significant in contributing to flood risk. These risks could be managed by adapting the closure strategy. To develop a methodology for improving storm surge barriers, a strategy is necessary to effectively evaluate and enhance these and other failure mechanisms.
3. Develop a new legal framework for coastal areas protected by storm surge barriers. Current legal requirements assume that storm surge barrier performance is more difficult to improve than raising interior flood defenses. This thesis demonstrates that closure reliability improvements are likely achievable and often cost-effective, making it relevant to include in a legal framework. This new legal framework is expected to result in more stringent requirements for closure reliability of storm surge barriers and less stringent requirements for interior flood defenses.

6.4 Other applications of this thesis

Although not directly related to the main aim of this thesis, three communities can benefit from the acquired knowledge in this thesis:

- Storm surge barrier designers: Currently, storm surge barriers are being planned in Belgium, Houston/Galveston, New York, New Jersey and Denmark. This thesis focuses on adapting existing structures, but the methods can also be applied to modify storm surge barrier designs. These methods may be even more suitable at this stage, as there is more flexibility to adapt the design.

- Asset managers of other hydraulic structures: This thesis has referred to storm surge barriers but can also be applied to smaller floodgates. Moreover, the approach might apply to other hydraulic structures (sluices and locks) to reduce the probability of failures to close and possibly to other types of operational failures, such as failures to open.
- Asset managers of other high-performance and safety-critical objects: The last two parts of the thesis (chapters 4 and 5) were formulated in a way that allows application to more technological objects beyond storm surge barriers. As such, they can assist in setting up a reliability and availability analysis and its validation.

6.5 References

NVvB (1993). *Business continuity data (Dutch: Bedrijfszekerheidsgegevens)*. Kluwer Technische Boeken, Deventer, 1st edition.

Rijkswaterstaat (2022a). Legal assessment trajectory 218, Eastern Scheldt barrier [Dutch: Wettelijke beoordeling traject 218, Oosterscheldekering]. Technical report.

Rijkswaterstaat (2022b). Legislated assessment Europoort barrier (Dutch: Wettelijke beoordeling Europoortkering I Dijktraject 208). Technical report.

Zikidou, Z. (2023). Assessment method of multiple flood protection improvements in a water system governed by a storm surge barrier: The case of Ramspol Barrier (MSc thesis). Technical report.

DANKWOORD

Het schrijven van een proefschrift wordt toegekend aan een persoon, zo ook dit proefschrift. Echter, de inhoud van dit proefschrift is in hoge mate gestuurd door mijn begeleiders, soms meer dan ze zelf beseft hebben en voor die bijdrage wil ik hen danken.

Professor Jonkmans (Bas) bijdrage begint eigenlijk al voor de start van dit proefschrift. Wij vonden elkaar bij de organisatie van een symposium bijna twintig jaar geleden. Sindsdien heeft hij een bepalende rol gehad in mijn loopbaan. Beginnend met een studentenassistentschap over getij-energie, daarna een stage en later een baan bij Royal Haskoning, een deeltijdbaan bij de TU Delft, deze promotie en ook mijn huidige functie als postdoc. Door deze voorgeschiedenis was hij de enige professor waarbij ik het risicovolle project van een promotie aandurfde. Gedurende het promotietraject stuurde hij op een tijdige afronding, bijvoorbeeld door mij een overzicht van hoofdstukken met voortgangspercentages te laten maken en andere begeleiders erop aan te spreken dat een bepaald extra deel van het onderzoek niet meer mogelijk was.

Qua inhoud van het proefschrift heeft Bas er met name aan bijgedragen om de nieuw ontwikkelde kennis duidelijk en scherp op te schrijven. Bas heeft op deze wijze een nadrukkelijke rol gehad in de totstandkoming van het tweede hoofdstuk, waarvan ik dacht dat dit algemeen beschikbare kennis was, maar door Bas' doorvragen bleek dat hier eigenlijk weinig over opgeschreven stond.

Dr. Bakker (Alexander) heeft de grootste rol gehad in mijn begeleiding en daarmee ook op de inhoud van dit proefschrift. Wij leerden elkaar kennen via deze promotie en hadden al snel een klik. Vanwege de coronamaatregelen hebben wij met name in het eerste jaar uren telefonisch gefilosofeerd en gediscussieerd over de invulling van dit proefschrift. Deze discussies zijn met name gegaan over de definitie van stormvloedkeringprestatie (hfst. 2), de eisen aan stormvloedkeringen (hfst. 3) en de zoektocht hoe om te gaan met de weinig toegankelijke beschikbaarheids- en betrouwbaarheidsmodellen (hfst. 5). Doordat hij goed op de hoogte was van de inhoud van mijn thesis, heeft hij meerdere malen een sturende rol gehad als ikzelf er met de andere begeleiders niet uitkwam.

Dr. Van den Bogaard (Johan) heeft een grote rol gehad in de totstandkoming van hoofdstuk 4. Deze nieuwe methode, die naar mijn beeld de kern is van vernieuwing in dit proefschrift, hebben Johan en ik samen ontwikkeld. Daarbij vulden wij elkaar goed aan: Johan met een nadruk op het maken van de lijst met verbeteringen, ik met een nadruk op het gebruik van de RA analyse.

Verder kon Johan mij op de meest begrijpelijke wijze uitleggen welke rol beschikbaarheids- en betrouwbaarheidsmodellen zouden moeten hebben in het beheer en onderhoud van stormvloedkeringen. Ook heeft Johan bij elk hoofdstuk in een laatste slag de door vele commentaarrondes murw geslagen tekst weer aangescherpt.

De samenwerking met Dr. Rijcken (Ties) is per toeval ontstaan en bewust uitgebouwd. Daardoor heb ik kunnen bijdragen aan de ontwikkeling van het concept van de "Hollandkering". Met name de behandeling van de in de Tweede Kamer aangenomen motie Grinwis door Rijkswaterstaat heeft mij inzicht verstrekt in de huidige kennisleemtes, die daarmee de basis vormde voor het tweede hoofdstuk. Verder heeft Ties rol als publicist, innovator en "nieuwsgierigheids-prikkelaar" mij geholpen om scherpte in de hoofdstukken aan te brengen. Via Ties ben ik in contact gekomen met zijn compagnon Vincent de Gooijer (Vins) die de cover van dit proefschrift heeft ontwikkeld! Ten slotte hebben Ties & Vins geholpen met verspreiden van de ontwikkelde kennis van dit proefschrift middels een website, film en artikel.

Ir. Jorissen (Richard) en Dr. van den Boomen (Martine) hebben respectievelijk hoofdstuk 2 en hoofdstuk 4 mede-ontwikkeld en meerdere malen eerdere versies van hoofdstukken van commentaar voorzien. Douwe Oppewal heeft van een ruwe versie van dit document een mooi leesbaar boek gemaakt.

Ir. Nederend (Hans) en Ir. van Akkeren (Koos) hebben mij noodzakelijke informatie verstrekt over de Maeslantkering. Met Hans Nederend heb ik daarnaast leuke discussies gevoerd via de mail, waarbij we op elkaar reageerden met steeds een andere kleur. Onze meest levendige discussie is tot zeven kleuren gekomen. De gesprekken met Koos hebben met name geholpen om inzicht te krijgen in hoe de – voor dit proefschrift belangrijke - periode direct na de bouw (1997) tot de start van risicogestuurd beheer en onderhoud (~2007, ProBo) zijn verlopen. Deze informatie heeft een plek gekregen in de inleiding van dit proefschrift.

Voor mijn onderzoek was het belangrijk om contact te kunnen hebben met de praktijk van stormvloedkeringbeheer en onderhoud. Jaco van Voorst (Maeslantkering), Nick Zegers (Oosterscheldekering) en Rens van Maarschalkerweerd (Ramspol) hebben dat voor mij mogelijk gemaakt voor Nederlandse stormvloedkeringen. Marc Walraven en Elja Huibregtse hebben via hun rol in de internationale netwerkorganisatie I-storm dit mogelijk gemaakt voor Engelse en Amerikaanse stormvloedkeringen. Here I will shortly switch to English: For my trip to the USA – the highlight of my PhD research – I thank Bradley Drouant and Sean Brunet (USACE) for their role in the preparation of this trip. De gesprekken met Maarten Kluijver hebben mij geholpen om de Amerikaanse context rondom (haalbaarheidsstudies van) stormvloedkeringen beter te begrijpen.

Drs. Busnach (Tycho) heeft een belangrijke rol gehad in de totstandkoming van hoofdstuk 4. Het experiment uitgevoerd in het kader van dit onderzoek had de inhuur van externe experts nodig en hij heeft deze mogelijk gemaakt. Verder heeft hij ook bijgedragen aan het artikel over dit proefschrift.

De studenten die ik heb mogen begeleiden, hebben mij geholpen het hun onderzoek, hun gedachten en uitwerkingen. Dank Vyasa, Zoi, Jelle, Meno, Derby, Youri, Joep, Noor en Wout.

Naast bovengenoemden hebben er veel personen bijgedragen wier namen ik niet allemaal kan noemen, alleen al omdat sommigen van hen anoniem zijn. Voor diegene wil ik vermelden dat ik mij altijd erg ondersteund voelde in mijn onderzoek en daarvoor dank.

Een proefschrift zoals dit kan alleen geschreven worden met een stabiele thuisbasis. De verantwoordelijkheid die ik voor mijn kinderen Pieter & Max had, heeft ervoor gezorgd dat ik mij niet verloor in dit prachtige onderzoeksonderwerp. Ook heeft het enthousiasme van Pieter & Max voor stormvloedkeringen, treinen en bouwen mij geïnspireerd voor het onderzoek. Zonder de steun van mijn vrouw was dit onderzoek niet mogelijk geweest. Verder heeft zij mij moeten verduren in intensieve weken van verwerking van het commentaar van externe reviewers en zo ongeveer de laatste zes maanden van het promotietraject. Ten slotte is de mooie opmaak te danken aan haar. Ik mocht van haar alleen promoveren als ik mijn boekje mooi liet opmaken.

APPENDICES

A Derivation of minimal dike raise

B Calculation steps AND- and OR-gates

C Present value calculation

D Checklist of principal performance improvements

E Notes screening process

F List of definitions

A Derivation of minimal dike raise

The minimal dike raise is the smallest amount of dike raise at which dike raise can possibly be optimal:

$$\Delta H_{min} = \breve{H}_D - H_{D,0} \qquad \text{(A.1).}$$

In which $\breve{H}_D$ [meter r.t. MSL] is the optimal dike level and $H_{D,0}$ [meter r.t. MSL] the initial dike height. At minimal dike raise ΔH_{min}, costs of dike raise are equal to the risk reduction that dike raise achieves, i.e.,

$$C = \Delta R \qquad \text{(A.2).}$$

With the use of equation 8 (section 2.2) and equation 9 (section 2.3), this can be written as

$$C_{D,0} + k_D \cdot \Delta H_{min} = \Delta F \cdot \widehat{D} \cdot \sum_{0}^{100} (1 + d')^t \qquad \text{(A.3).}$$

The flood frequency difference is as a result of the minimal dike raise is

$$\Delta F = F\left(h_1 > H_{D,0}\right) - F\left(h_1 > \breve{H}_D\right) = \ldots$$

$$10^{-\frac{\breve{H}_D - \Delta H_{min} - H_A}{H_B}} - 10^{-\frac{\breve{H}_D - H_A}{H_B}} = \ldots$$

$$10^{-\frac{\breve{H}_D - H_A}{H_B}} \cdot \left(10^{-\frac{\Delta H_{min}}{H_B}} - 1\right) \qquad \text{(A.4).}$$

The optimal flood frequency for dike raise is (see equation 11, section 2.4)

$$F\left(h_1 \geq \breve{H}_D\right) = 10^{-\frac{\breve{H}_D - H_A}{H_B}} = \frac{k_D \cdot H_B}{ln(10) \cdot \widehat{D} \cdot \sum_0^{100} (1 + d')^t} \qquad \text{(A.5).}$$

With the use of equations A.4 and A.5, equation A.3 becomes

$$C_{D,0} + k_D \cdot \Delta H_{min} = \frac{k_D \cdot H_B}{ln(10)} \cdot \left(10^{-\frac{\Delta H_{min}}{H_B}} - 1\right) \qquad \text{(A.6).}$$

Then by rearranging, the following relation is found:

$$\Delta H_{min} = H_B \cdot log\left(\frac{\Delta H_{min} \cdot ln(10)}{H_B} + \frac{C_{D,0} \cdot ln(10)}{k_D \cdot H_B} + 1\right) \qquad \text{(A.7).}$$

Using iteration, the minimal dike raise can be calculated.

B Calculation steps AND- and OR-gates

Logic gates perform a logical operation based on one or more inputs resulting in one output. In this appendix, we show the calculation steps in the case of two (input) events *A* and *B* resulting in (output) event *C*. We only present two type of logic gates: the AND- and OR-gate.

With the AND-gate, both event *A* and *B* have to occur for event *C* to take place. The probabilities of these events are described by P_A, P_B, P_C, respectively. If events *A* and *B* are independent, the probability of event *C* is:

$$P_C = P_A \cdot P_B$$

With the OR-gate, either event *A* or *B* has to occur for event *C* to take place. If the events are independent and the probabilities of events *A* and *B* are small (<1/10), the probability of event *C* can be estimated by:

$$P_C = P_A + P_B$$

We apply these equations to find the probabilities of non-closure for three system arrangements:

i. Maeslant barrier with only main systems
ii. Maeslant barrier with backup systems for the power supply, control and decision system.
iii. Maeslant barrier with all backup systems including a second gate.
The probabilities of failure events of main and backup systems are presented in Table B.1. In bold, the indices are presented per system. For instance, the probability of failure of the main system of the gate is described by the symbol P_{G1} and its backup system by P_{G2}.

Table B.1: Probabilities of basic events leading to failure of subsystems [on demand] of simplified fault tree for Maeslant barrier. In bold, the indices applied are presented.

Item	Main system (1)	Backup system (2)	Combined
Gate (**G**)	$1 \cdot 10^{-2}$	$2 \cdot 10^{-2}$	$2 \cdot 10^{-4}$
Power supply (**P**)	$1 \cdot 10^{-2}$	$2 \cdot 10^{-2}$	$2 \cdot 10^{-4}$
Control (**C**)	$1 \cdot 10^{-2}$	$2 \cdot 10^{-2}$	$2 \cdot 10^{-4}$
Decision (**D**)	$1 \cdot 10^{-2}$	$2 \cdot 10^{-2}$	$2 \cdot 10^{-4}$

For the arrangement with only main systems (i), the probability of non-closure is then:

$$P_{NC,i} = P_{G1} + P_{P1} + P_{C1} + P_{D1} = \ldots$$

$$\ldots 10^{-2} + 10^{-2} + 10^{-2} + 10^{-2} = 4 \cdot 10^{-2}$$

For the arrangement with backup systems for the power supply, control and decision system (ii), the probability of non-closure is:

$$P_{NC,ii} = P_{G1} + P_{P1} \cdot P_{P2} + P_{C1} \cdot P_{C2} + P_{D1} \cdot P_{D2} = \ldots$$

$$\ldots 10^{-2} + 10^{-2} \cdot 2 \cdot 10^{-2} + 10^{-2} \cdot 2 \cdot 10^{-2} + 10^{-2} \cdot 2 \cdot 10^{-2} = 10^{-2}$$

For the arrangement with all backup systems including a second gate (iii), the probability of non-closure is:

$$P_{NC,iii} = P_{G1} \cdot P_{G2} + P_{P1} \cdot P_{P2} + P_{C1} \cdot P_{C2} + P_{D1} \cdot P_{D2} =$$

$$\ldots 10^{-2} \cdot 2 \cdot 10^{-2} + 10^{-2} \cdot 2 \cdot 10^{-2} + 10^{-2} \cdot 2 \cdot 10^{-2} + 10^{-2} \cdot 2 \cdot 10^{-2} = 8 \cdot 10^{-4}$$

C Present value calculation

Year	Year number	Discount rate	Present cost storm surge barrier [M€]	Rate of sea level rise [m/ year]	Reduced discount rate	Present value flood damage [M€]
2011	0	5,5%	6,40E+02	0,0049	2,0%	0,00E+00
2012	1	5,5%	1,42E+01	0,0049	2,0%	7,06E+04
2013	2	5,5%	1,34E+01	0,0050	2,0%	6,92E+04
2014	3	5,5%	1,27E+01	0,0050	2,0%	6,79E+04
2015	4	5,5%	1,20E+01	0,0050	2,0%	6,66E+04
2016	5	5,5%	1,13E+01	0,0051	1,9%	6,53E+04
2017	6	5,5%	1,07E+01	0,0051	1,9%	6,41E+04
2018	7	5,5%	1,01E+01	0,0052	1,9%	6,29E+04
2019	8	5,5%	9,54E+00	0,0052	1,9%	6,18E+04
2020	9	5,5%	9,02E+00	0,0053	1,9%	6,07E+04
2021	10	5,5%	8,52E+00	0,0053	1,9%	5,96E+04
2022	11	5,5%	8,05E+00	0,0053	1,9%	5,86E+04
2023	12	5,5%	7,61E+00	0,0054	1,8%	5,76E+04
2024	13	5,5%	7,19E+00	0,0054	1,8%	5,66E+04
2025	14	5,5%	6,79E+00	0,0055	1,8%	5,57E+04
2026	15	5,5%	6,42E+00	0,0055	1,8%	5,48E+04
2027	16	5,5%	6,07E+00	0,0056	1,8%	5,39E+04
2028	17	5,5%	5,73E+00	0,0056	1,8%	5,31E+04
2029	18	5,5%	5,42E+00	0,0057	1,8%	5,23E+04
2030	19	5,5%	5,12E+00	0,0057	1,8%	5,15E+04
2031	20	5,5%	4,84E+00	0,0057	1,7%	5,07E+04
2032	21	5,5%	4,57E+00	0,0058	1,7%	5,00E+04
2033	22	5,5%	4,32E+00	0,0058	1,7%	4,93E+04
2034	23	5,5%	4,08E+00	0,0059	1,7%	4,86E+04
2035	24	5,5%	3,86E+00	0,0059	1,7%	4,79E+04
2036	25	5,5%	3,65E+00	0,0060	1,7%	4,73E+04
2037	26	5,5%	3,45E+00	0,0060	1,7%	4,67E+04
2038	27	5,5%	3,26E+00	0,0061	1,6%	4,61E+04
2039	28	5,5%	3,08E+00	0,0061	1,6%	4,55E+04
2040	29	5,5%	2,91E+00	0,0061	1,6%	4,49E+04
2041	30	5,5%	2,75E+00	0,0062	1,6%	4,44E+04
2042	31	5,5%	2,60E+00	0,0062	1,6%	4,38E+04
2043	32	5,5%	2,45E+00	0,0063	1,6%	4,33E+04
2044	33	5,5%	2,32E+00	0,0063	1,6%	4,29E+04
2045	34	5,5%	2,19E+00	0,0064	1,5%	4,24E+04

Year	Year number	Discount rate	Present cost storm surge barrier [M€]	Rate of sea level rise [m/year]	Reduced discount rate	Present value flood damage [M€]
2046	35	5,5%	2,07E+00	0,0064	1,5%	4,19E+04
2047	36	5,5%	1,96E+00	0,0064	1,5%	4,15E+04
2048	37	5,5%	1,85E+00	0,0065	1,5%	4,11E+04
2049	38	5,5%	1,75E+00	0,0065	1,5%	4,07E+04
2050	39	5,5%	1,65E+00	0,0066	1,5%	4,03E+04
2051	40	5,5%	1,56E+00	0,0066	1,5%	3,99E+04
2052	41	5,5%	1,48E+00	0,0067	1,5%	3,95E+04
2053	42	5,5%	1,39E+00	0,0067	1,4%	3,92E+04
2054	43	5,5%	1,32E+00	0,0068	1,4%	3,88E+04
2055	44	5,5%	1,24E+00	0,0068	1,4%	3,85E+04
2056	45	5,5%	1,18E+00	0,0068	1,4%	3,82E+04
2057	46	5,5%	1,11E+00	0,0069	1,4%	3,79E+04
2058	47	5,5%	1,05E+00	0,0069	1,4%	3,76E+04
2059	48	5,5%	9,93E-01	0,0070	1,4%	3,74E+04
2060	49	5,5%	9,38E-01	0,0070	1,3%	3,71E+04
2061	50	5,5%	8,87E-01	0,0071	1,3%	3,68E+04
2062	51	5,5%	8,38E-01	0,0071	1,3%	3,66E+04
2063	52	5,5%	7,92E-01	0,0072	1,3%	3,64E+04
2064	53	5,5%	7,48E-01	0,0072	1,3%	3,62E+04
2065	54	5,5%	7,07E-01	0,0072	1,3%	3,60E+04
2066	55	5,5%	6,68E-01	0,0073	1,3%	3,58E+04
2067	56	5,5%	6,31E-01	0,0073	1,3%	3,56E+04
2068	57	5,5%	5,97E-01	0,0074	1,2%	3,54E+04
2069	58	5,5%	5,64E-01	0,0074	1,2%	3,53E+04
2070	59	5,5%	5,33E-01	0,0075	1,2%	3,51E+04
2071	60	5,5%	5,04E-01	0,0075	1,2%	3,50E+04
2072	61	5,5%	4,76E-01	0,0075	1,2%	3,49E+04
2073	62	5,5%	4,50E-01	0,0076	1,2%	3,47E+04
2074	63	5,5%	4,25E-01	0,0076	1,2%	3,46E+04
2075	64	5,5%	4,02E-01	0,0077	1,1%	3,45E+04
2076	65	5,5%	3,79E-01	0,0077	1,1%	3,44E+04
2077	66	5,5%	3,59E-01	0,0078	1,1%	3,44E+04
2078	67	5,5%	3,39E-01	0,0078	1,1%	3,43E+04
2079	68	5,5%	3,20E-01	0,0079	1,1%	3,42E+04
2080	69	5,5%	3,03E-01	0,0079	1,1%	3,42E+04
2081	70	5,5%	2,86E-01	0,0079	1,1%	3,41E+04
2082	71	5,5%	2,70E-01	0,0080	1,0%	3,41E+04

Year	Year number	Discount rate	Present cost storm surge barrier [M€]	Rate of sea level rise [m/year]	Reduced discount rate	Present value flood damage [M€]
2083	72	5,5%	2,55E-01	0,0080	1,0%	3,41E+04
2084	73	5,5%	2,41E-01	0,0081	1,0%	3,41E+04
2085	74	5,5%	2,28E-01	0,0081	1,0%	3,41E+04
2086	75	5,5%	2,16E-01	0,0082	1,0%	3,41E+04
2087	76	5,5%	2,04E-01	0,0082	1,0%	3,41E+04
2088	77	5,5%	1,92E-01	0,0083	1,0%	3,41E+04
2089	78	5,5%	1,82E-01	0,0083	1,0%	3,41E+04
2090	79	5,5%	1,72E-01	0,0083	0,9%	3,42E+04
2091	80	5,5%	1,62E-01	0,0084	0,9%	3,42E+04
2092	81	5,5%	1,53E-01	0,0084	0,9%	3,43E+04
2093	82	5,5%	1,45E-01	0,0085	0,9%	3,43E+04
2094	83	5,5%	1,37E-01	0,0085	0,9%	3,44E+04
2095	84	5,5%	1,30E-01	0,0086	0,9%	3,45E+04
2096	85	5,5%	1,22E-01	0,0086	0,9%	3,46E+04
2097	86	5,5%	1,16E-01	0,0086	0,8%	3,47E+04
2098	87	5,5%	1,09E-01	0,0087	0,8%	3,48E+04
2099	88	5,5%	1,03E-01	0,0087	0,8%	3,50E+04
2100	89	5,5%	9,76E-02	0,0088	0,8%	3,51E+04
2101	90	5,5%	9,22E-02	0,0088	0,8%	3,52E+04
2102	91	5,5%	8,72E-02	0,0089	0,8%	3,54E+04
2103	92	5,5%	8,24E-02	0,0089	0,8%	3,56E+04
2104	93	5,5%	7,78E-02	0,0090	0,8%	3,57E+04
2105	94	5,5%	7,36E-02	0,0090	0,7%	3,59E+04
2106	95	5,5%	6,95E-02	0,0090	0,7%	3,61E+04
2107	96	5,5%	6,57E-02	0,0091	0,7%	3,63E+04
2108	97	5,5%	6,21E-02	0,0091	0,7%	3,66E+04
2109	98	5,5%	5,87E-02	0,0092	0,7%	3,68E+04
2110	99	5,5%	5,54E-02	0,0092	0,7%	3,70E+04
2111	100	5,5%	5,24E-02	0,0093	0,7%	3,73E+04
		TOTAL	**8,97E+02**			**4,22E+06**

D Checklist of principal performance improvements

#	Principal performance improvements	Examples
1	**Reducing model conservatism**	
1.1	Adapt failure criterion - at object level	Allow longer time to fail, allow partial functioning
1.2	Adapt failure criterion - at object system level	
1.3	Adapt failure criterion - at object subsystem level	
1.4	Adapt failure criterion - at component level	
1.5	Other logic model structure	Fault tree, event tree, …
1.6	Adapt logic model structure	Raise number of events that have to occur before upper event occurs, adapt level of detail
2	**Hardware**	
2.1	Apply higher reliability element - at object level	
2.2	Apply higher reliability element - at object system level	
2.3	Apply higher reliability element - at object subsystem level	
2.4	Apply higher reliability element - at component level	
2.5	Apply simpler element - at object level	
2.6	Apply simpler element - at object system level	
2.7	Apply simpler element - at object subsystem level	
2.8	Apply simpler element - at component level	
2.9	Apply redundancy - at object level	
2.10	Apply redundancy - at object system level	
2.11	Apply redundancy - at object subsystem level	
2.12	Apply redundancy - at component level	
2.13	Backup by human recovery - on object level	
2.14	Backup by human recovery - on object system level	
2.15	Backup by human recovery - on object subsystem level	
2.16	Backup by human recovery - on component level	
2.17	Adapt hardware failure model structure	Use a different type of model. Adapt parameters/constants or include new model variables
2.18	Adapt hardware model variables	
3	**Common-cause failure (CCF)**	
3.1	Apply diversity in design	Separate cables, different technology, different physical principles
3.2	Apply temporal differences in operation	
3.3	Apply continuous monitoring (<1 min)	

#	Principal performance improvements	Examples
3.4	Perform or improve analysis of CCF's	
3.5	Improve adequateness of organizations response to CCF's	
3.6	Add redundancy	
3.7	Apply ccf defense to other decomposition level	
3.8	Human recovery	
3.9	Adapt CCF failure model structure	Use a different type of model. Adapt parameters/constants or include new model variables
3.10	Adapt CCF model variables	Bayesian update, expert judgement, other source of failure data
4	**External events**	
4.1	Increase the distance at which the external event can occur	
4.2	Check for double-counting of external events	Are external events due to fire already included in the CCF failure rate?
4.3	Strengthen element to be able to handle external event	
4.4	Improve warning	Improve warning signals for ship traffic
4.5	Add redundancy	
4.6	Apply external event defense at other decomposition level	
4.7	Adapt external event failure model structure	Use a different type of model. Adapt parameters/constants or include new model variables
4.8	Adapt external event model variables	Bayesian update, expert judgement, other source of failure data
5	**Human reliability**	
5.1	Raise competence staff	Train more frequently, train to attain more skills, hire staff
5.2	More simple or intuitive task	Fewer dependencies between tasks, less options, better written down, improve software-human interaction, reduce need for special tools
5.3	Improve working conditions	Lower stress, ergonomics, climate, accessibility, light, reduce number of extraneous alarms/outside discussions
5.4	Software to replace human operation	
5.5	Hardware to replace human operation	
5.6	Adapt human organization	
5.7	Adapt human reliability failure model structure	Use a different type of model. Adapt parameters/constants or include new model variables

#	Principal performance improvements	Examples
5.8	Adapt human reliability model variables	Bayesian update, expert judgement, other source of failure data
6	**Software reliability**	
6.1	Redevelop software	
6.2	Optimize without changing functional requirements	
6.3	Wider range of testing	
6.4	Use Field Data	
6.5	Improved hardware to run software on	
6.6	Software reliability review	
6.7	Redundant software	
6.8	Reduce number of tasks needed to execute function	
6.9	Human actions replacing or backup for software	
6.10	Hardware replacing software	
6.11	Adapt software reliability failure model structure	Use a different type of model. Adapt parameters/constants or include new model variables
6.12	Adapt software reliability model variables	Bayesian update, expert judgement, other source of failure data
7	**Maintenance**	
7a	Strategy	
7a.1	More preventive maintenance	
7a.2	More predictive maintenance	
7a.3	More periodic maintenance	
7a.4	Maintenance at other decomposition level	
7b	Dormant failures	
7b.1	Continuous failure monitoring	Making dormant failures noticeable
7b.2	Raise test frequency	
7b.3	Optimize test frequency	
7b.4	Staggered testing	
7b.5	Test a wider range of operating conditions	
7b.6	Test at other decomposition level	
7b.7	Adapt model variables test interval	Bayesian update, expert judgement, other source of failure data
7c	Unavailability due to repair	
7c.1	More spare parts and/or closer to site	
7c.2	Repair equipment closer to / faster at site	Own repair facility (Thames barrier)

#	Principal performance improvements	Examples
7c.3	Reduce repair/install time	
7c.4	Improve mobilization of staff	
7c.5	Backup in case of unavailability	Temporary sheet pile/pump
7c.6	Repair at other decomposition level	
7c.7	Adapt model variables repair time	Bayesian update, expert judgement, other source of failure data
8	**Operation**	
8.1	Close barrier faster (lower mission time)	
8.2	Close gate earlier	
8.3	Operate in less failure-prone conditions	
8.4	Adapt failure effect into fail-safe condition	
8.5	If unavailable/malfunctioning, close preventively	

E Notes screening process

#	Performance improvements	Maximum effect > 5%	1. Technically feasible?	2. Lowers failure probability substantially?	3. Other functions still possible?	4. Other reasons why unpromising?	Considerations to rule out & other notes	Examples case	Criterion A: Maximum effect	Criterion B: Improvement percentage	Criterion C: Costs	Criterion D: Feasibility	Total score	Notes
1.	**Reducing model conservatism**													
1.1	Adapt failure criterion - at object level		Yes	Yes	Yes	No	Most performance improvements were already implemented in 2005-analysis	Elongate acceptable mission time (slow closure acceptable).	1	1	5	5	25	
1.2	Adapt failure criterion - at object system level		No				Example on object level is valid for all levels. Hence no additional performance improvements are required.							
1.3	Adapt failure criterion - at object subsystem level		No											
1.4	Adapt failure criterion - at component level		No											
1.5	Adapt logic model structure (fault tree) - at object level		No											
1.6	Adapt logic model structure (fault tree) - at object system level		Yes	No			Only if incorrectly modelled, which would need to be proven.							
1.7	Adapt logic model structure (fault tree) - at object subsystem level		Yes	No			" "							
1.8	Adapt logic model structure (fault tree) - at component level		Yes	No			" "							
1.9	Adapt failure model structure (hardware)		Yes	No			There is scientific consensus on hardware modelling							
1.10	Adapt failure model structure (CCF)		Yes	No			Earlier attempts did not substantially change result.							
1.11	Adapt failure model structure (External events)	No												
1.12	Adapt failure model structure (Human Reliability)	No												
1.13	Adapt failure model structure (Software)		Yes	Yes	Yes			TOPAAS, Reliability growth-model in stead of TDT-model	4	3	4	3	144	The effect on performance of using other models is relatively uncertain.
1.14	Adapt model variable (hardware)		Yes	Yes	Yes			Measure and update repair times (originally mentioned at maintenance - repair).	4	2	5	5	200	Only the costs to adjust the model, not those of more active checking whether repair times are met.
1.15	Adapt model variable (CCF)		Yes	Yes	Yes			More research required in the safety-critical infrastructure industry to check whether this is promising*	4	2	5	5	200	

#	Performance improvements	Maximum effect > 5%	1. Technically feasible?	2. Lowers failure probability substantially?	3. Other functions still possible?	4. Other reasons why unpromising?	Considerations to rule out & other notes	Examples case	Criterion A: Maximum effect	Criterion B: Improvement percentage	Criterion C: Costs	Criterion D: Feasibility	Total score	Notes
1.16	Adapt model variable of External Events	No												
1.17	Adapt model variable of Human Reliability	No												
1.18	Adapt model variable of Software Reliability		Yes	Yes	Yes				4	1	5	4	80	Historic research into software development might be necessary to substantiate less conservative values.
1.a	Apply factors to reduce probability of failure scenarios		Yes	Yes	Yes			Failure scenarios (/minimal cut-sets) probabilities are relatively high. Reduction factors lower these probabilities to more realistic values.	4	3	5	3	180	Difficult to substantiate reduction factors
1.b	Apply different logic model		Yes	Yes	Yes			Bayesian belief network	5	1	4	3	60	Uncertain what the effect on performance is, but not likely to have a large effect.
2.	**Hardware**													
2.1	Apply higher reliability element - at object level		Yes	Yes	Yes	No	Destruction of capital	New storm surge barrier in stead of existing one						
2.2	Apply higher reliability element - at object system level		Yes	Yes	Yes			Different motor OS6-1, different type of OS10-1, other OS3.	4	3	2	2	48	This is difficult to score, depends on which example is chosen (all or some?).
2.3	Apply higher reliability element - at object subsystem level		Yes	No			No examples were found							
2.4	Apply higher reliability element - at component level		Yes	Yes	Yes			Different drive OS5-1-4. Use component-on-the-shelf (COTS)	2	2	4	4	64	COTS are less expensive over the lifetime. Thus, reduced life cycle costs
2.5	Apply simpler element - at object level		Yes	Yes	Yes	No	Destruction of capital	New storm surge barrier in stead of existing one						
2.6	Apply simpler element - at object system level		Yes	No			No examples were found							
2.7	Apply simpler element - at object subsystem level		Yes	Yes	Yes			Diesel generator with permanent energy supply, replacing all UPS'es	1	1	4	3	12	
2.8	Apply simpler element - at component level		Yes	No			No examples were found							
2.9	Apply identical redundancy - at object level		Yes	Yes	Yes		Raises the probability of non-opening	Second Maeslant barrier	5	4	1	1	20	Costs are well above 25 million euro
2.10	Apply identical redundancy - at object system level		Yes	Yes	Yes			Identical redundant OS1.	3	4	2	2	48	Only OS1: low effect low cost. OS1+OS12: high effect, high cost

#	Performance improvements	Maximum effect > 5%	1. Technically feasible?	2. Lowers failure probability substantially?	3. Other functions still possible?	4. Other reasons why unpromising?	Considerations to rule out & other notes	Examples case	Criterion A: Maximum effect	Criterion B: Improvement percentage	Criterion C: Costs	Criterion D: Feasibility	Total score	Notes
2.11	Apply identical redundancy - at object subsystem level		Yes	No			Geen voorbeelden							
2.12	Apply identical redundancy - at component level		Yes	Yes	Yes			More components OS5-1-4	1	4	3	3	36	Without adjusting OS1 & OS3
2.13	Apply non-identical redundancy - at object level		Yes	Yes	Yes			"Holland barrier" [1]	5	5	1	1	25	
2.14	Apply non-identical redundancy - at object system level		Yes	Yes	Yes			Other type OS6. Other type OS12	4	4	3	2	96	Costs of options need to be separated to determine individual feasibility of measures.
2.15	Apply non-identical redundancy - at object subsystem level		Yes	No			Geen voorbeelden							
2.16	Apply non-identical redundancy - at component level		Yes	Yes	Yes			More and different components OS5-1-4, Alternative OS5-4.	1	5	4	4	80	Score is based on sensors, which were identified as most promising.
2.17	Backup by human recovery - on object level		Yes	Yes	No		Sinking a vessel might theoretically be possible, but not promising.							
2.18	Backup by human recovery - on object system level		Yes	Yes	Yes			Human recovery for OS1, OS3, OS5 and OS6.	3	5	4	3	180	Sufficient knowledge and expertise ("craftmanship") is required for this performance improvement
2.19	Backup by human recovery - on object subsystem level		Yes	Yes	Yes			Simulation and training of alternative manual control	1	5	4	4	80	
2.20	Backup by human recovery - on		Yes	No			Geen voorbeelden							
2.a	Investigate sill more precisely on sediment and obstacles.		Yes	No										
2.b	Hydrojet installation OS10		Yes	Yes	Yes			Aims to clear sill from sediment	1	2	3	4	24	
2.c	Combine OS1 & OS3, both software and hardware.		Yes	Yes	Yes				5	1	5	4	100	Downside of this option is that there are less human recovery options.
3.	**Common-cause failure (CCF)**													
3.1	Separate / segragate information & power cables		Yes	Yes	Yes			Only possible at OS6	1	1	5	4	20	Possible has impact on other installation parts (but not included in scoring).
3.2	Separate components/sub-systems in physically separate enclosure		Yes	Yes	Yes			Only possible at OS1 & OS6	2	4	4	4	128	Scoring based on OS1, which was identified as most promising
3.3	Apply diversity in physical principles		Yes	Yes	Yes			Separate drive OS6, Alternative OS5-4	1	5	4	2	40	Alternative measurement was scored being most promising.

#	Performance improvements	Maximum effect > 5%	1. Technically feasible?	2. Lowers failure probability substantially?	3. Other functions still possible?	4. Other reasons why unpromising?	Considerations to rule out & other notes	Examples case	Criterion A: Maximum effect	Criterion B: Improvement percentage	Criterion C: Costs	Criterion D: Feasibility	Total score	Notes
3.4	Apply temporal differences in operation		Yes	No			Model is not able to fully account for this effect.							
3.5	Apply continuous monitoring (<1 min)		Yes	Yes	Yes			More measurements to support finding of CCF errors	1	4	4	3	48	Score based on single CCF-event
3.6	Apply diversity in technology		Yes	Yes	Yes			Pumps of different suppliers or different principle for OS5 [2], two systems OS6 [1]	2	4	4	3	96	Score based on OS5, excluding costs OS3. OS3 adjustion costs can stay small if included in a planned revision.
3.7	Perform or improve analysis of CCF's		Yes	No			Het example concerns a model improvement and was replaced.							
3.8	Improve adequeteness of organizations response to CCF's		Yes	Yes	Yes			Execute the check-fase in the PDCA-cycle (Deming-cycle)	4	1	4	4	64	
3.9	Remove the need for external environmental control		Yes	Yes	Yes			Adjust OS1 to less power with less need for climate control.	1	5	5	4	100	To be included in normal renovation cycle.
3.10	Limit the influence of electromagnetic interference		Yes	No			Not included in 2005-model							
3.11	Improve quality of designers with respect to CCF		No				Design was already made.							
3.12	Add redundancy		Yes	No										
3.13	Apply ccf defense to other decomposition level		Yes	Yes	Yes			defend against leakage on object system level	1	1	4	3	12	
3.14	Human recovery		Yes	Yes	Yes			OS1 and OS3	3	4	4	4	192	
3.a	Other maintenance approach		Yes	No			Not included in 2005-model							
4.	**External events**	No												
4.1	Increase the distance at which the external event can occur													
4.2	Check for double-counting of external events													
4.3	Strengthen element to be able to													
4.4	Improve warning													
4.5	Add redundancy													
4.6	Apply external event defense at other decomposition level													
	...													
5.	**Human reliability**	No												
5.1	Raise competence staff													
5.2	More simple or intuitive task													
5.3	Improve working conditions													

#	Performance improvements	Maximum effect > 5%	1. Technically feasible?	2. Lowers failure probability substantially?	3. Other functions still possible?	4. Other reasons why unpromising?	Considerations to rule out & other notes	Examples case	Criterion A: Maximum effect	Criterion B: Improvement percentage	Criterion C: Costs	Criterion D: Feasibility	Total score	Notes
5.4	Software to replace human operation													
5.5	Hardware to replace human operation													
5.6	Adapt human organization													
	…													
6.	**Software relaibility**													
6.1	Redevelop software		Yes	Yes	Yes				4	4	2	1	32	No consensus among experts, some score improvement percentage much lower.
6.2	Optimize without changing functional requirements		Yes	Yes	Yes				4	2	3	3	72	Testing of optimizations mainly determines the costs. It is mentioned that removing "dead code" is not complex.
6.3	Wider range of testing		Yes	Yes	Yes			referred to as "OTAP strategy"	4	1	3	2	24	
6.4	Use Field Data		Yes	Yes	Yes				4	1	5	4	80	
6.5	Improved hardware to run software		Yes	No			Not included in (old) model							
6.6	More preventive maintenance		Yes	No			Not included in (old) model							
6.7	Software reliability review		Yes	No			Small effect in model							
6.8	Redundant software		Yes	Yes	Yes			Separated software	4	4	2	2	64	Note: 2-out-of-3 systeem is substantially more reliable.
6.9	Reduce number of tasks Noded to		No				systeem 2005 bevatte							
6.10	Human actions replacing or redundant measure for software		Yes	Yes	Yes			Human recovery as is already described in HAD-database [7].	4	5	5	3	300	
6.11	Hardware replacing software		No				Ancient technique and thus not feasible anymore							
6.a	Analysis behaviour during (test)closures, together with simulators		Yes	Yes	Yes				4	2	4	3	96	Costs are based on yearly analysis
6.b	Human interface interaction control systems	No	Yes	Yes	Yes									
7a.	**Maintenance (strategy)**													
7a.1	More preventive maintenance	No												
7a.2	More predictive maintenance		Yes	No			model assumes a constant failure rate							
7a.3	More periodic maintenance	No												
7a.4	Maintenance at other decomposition level		Yes	No			Model does not include unavailability due to maintenance errors.							
7b.	**Maintenance (dormant failures)**													

#	Performance improvements	*Maximum effect > 5%*	*1. Technically feasible?*	*2. Lowers failure probability substantially?*	*3. Other functions still possible?*	*4. Other reasons why unpromising?*	*Considerations to rule out & other notes*	*Examples case*	*Criterion A: Maximum effect*	*Criterion B: Improvement percentage*	*Criterion C: Costs*	*Criterion D: Feasibility*	*Total score*	*Notes*
7b.1	Continue failure modelling		Yes	No			no additional options							
7b.2	Raise test frequency		Yes	Yes	Yes			Lower test intervals to 1 month	2	4	5	5	200	OS5 analyzed to determine score.
7b.3	Optimize test frequency		Yes	No			Test closure is already planned smartly.							
7b.4	Staggered testing		Yes	No			Not in model 2005							
7b.5	Test a wider range of operating conditions	No												
7b.6	Test at other decomposition level		Yes	Yes	Yes			Test where sector gates float and are moved a short distance within the dock (New Waterway does not need to be closed).	1	1	5	5	25	
7b.a	Make dormant failures noticable.		Yes	Yes	Yes				2	5	5	2	100	Difficulty is to find the right variable to predict failure. Costs are associated with this research process.
7c.	**Maintenance (unavailability due to repair)**													
7c.1	More spare parts		Yes	No			Repair times were already optimized							
7c.2	Spare parts closer to site		Yes	No			Repair times were already optimized							
7c.3	Repair equipment closer to / faster at site		Yes	No			Repair times were already optimized							
7c.4	Reduce repair/install time		Yes	No			Repair times were already optimized							
7c.5	Improve mobilization of staff		Yes	Yes	Yes			Repair crew at site	2	1	3	3	18	
7c.6	Improve maintainability		Yes	No			Repair times were already optimized							
7c.7	Backup in case of unavailability		Yes	No			Repair times were already optimized							
7c.8	Repair at other decomposition level		Yes	No			Repair times were already optimized							
8.	**Operation**													
8.1	Close barrier faster (lower mission time)		No				would cause issues (translation wave running upstream through the basin, structural requirements).							

#	Performance improvements	*Maximum effect > 5%*	*1. Technically feasible?*	*2. Lowers failure probability substantially?*	*3. Other functions still possible?*	*4. Other reasons why unpromising?*	*Considerations to rule out & other notes*	*Examples case*	*Criterion A: Maximum effect*	*Criterion B: Improvement percentage*	*Criterion C: Costs*	*Criterion D: Feasibility*	*Total score*	*Notes*
8.2	Close gate earlier		Yes	Yes	Yes		Only for example	Jack up ball joint earlier, all other options have too much effect on other functions.	2	4	5	5	200	
8.3	Operate in less failure-prone	No												
8.4	Adapt failure effect into fail-safe	No												
8.5	If unavailable/malfunctioning, close/open preventively		No				Many technical and economical issues							
	…													

[1] Holland barrier is a concept storm surge barrier: https://flowsplatform.nl/#/it-takes-two-to-tango-with-sea-level-rise-1682542508929________

F List of definitions

Term	Definition
Availability	This term has two definitions: 1) The fraction of time during which an object, object (sub)system or component can perform its intended function, and 2) the probability that an object performs its intended function at a given time under a given set of conditions. Mathematically these definitions are the same.
Barrier failure mode	A state and/or position of the storm surge barrier during a potential coastal flood event, which is undesired. For instance, failed closure, partially closed or structurally failed.
Barrier mode	A state and/or position of the storm surge barrier during a potential coastal flood event. Examples of these modes are: open, closed.
Closure decision level	A forecasted water level that is the main closure criterion.
Closure regime	The barrier modes during a storm surge event
Closure reliabity	The frequency that the barrier successfully closes in severe storm conditions. These storm conditions are that severe that otherwise interior flood defenses fail and result in coastal flooding.
Closure strategy	A plan with criteria when and how to close the barrier considering the uncertainties with respect to water level predictions and other storm characteristics.
Component	The lowest level of a hardware decomposition in an reliability and availability analysis.
Critical water level	The lowest water level near an interior flood defense which results in a breach and a consequent flood.
Decomposition resolution	The degree to which the object is subdivided into components. The more components, the higher the decomposition resolution.
End closure level	The water level when barrier closure is realized.
Exceedance frequency	The frequency at which a certain value, in this thesis always a water level maximum, is exceeded.
Failure	A loss of the element's functionality.

Failure category	There are five failure categories: 1) hardware failure (inherent failure of physical components), 2) external events, 3) common cause failure, 4) human error and 5) software error. Hardware failures are all hardware failures except for failures due to external events and common cause failure.
Failure criterion	A criterion which determines how much of the functionality can be lost before it is considered to be failed.
Failure event model	A model to determine the failure probability/frequency of a single failure event, for example, the probability of human error, or the frequency a storm surge barrier is hit by lightening.
Failure mechanism	The physical path to failure. For example: a barriers failure to close resulting in a coastal flood.
Failure mode	A way in which the element can fail to meet the design intent. For example: a failure to close
Failure scenario	A group of failure events resulting in failure of the analyzed object.
Failure to close	A failure to close after a closure decision is taken.
Frequency	The number of occurrences of a repeating event per unit of time. In this thesis, frequency is used to indicate how often extreme water levels and floods are expected per year on average.
Hardware decomposition	A hierarchical structure consisting of an object, object system, subsystem(s) and components which schematizes the object for a reliability and availability analysis.
Hydraulic loads	The exceedance frequency of extreme water level maxima behind the barrier near an interior flood defense.
Importance Analysis	Analysis of the importance of single events, relevant groups of events and variables in an reliability and availability analysis
Improvement dimensions	There are three improvement dimensions defined in this thesis: improvement type, failure category and hierarchical level.
Improvement types	There are four improvements types: improvement of the object properties, its maintenance, its operation and model improvement, that is, removing model conservatisms.

Inner basin	The water body behind/upstream of the barrier where water level maxima are affected by the barrier.
Interior flood defense	Flood protection surrounding the inner basin, consisting of dikes, flood walls and elevated land. Dikes are referred to as embankments in the UK and levees in the USA.
Logic model	Logic models relate how failure events logically result in an - mostly undesired - outcome. Examples of logic models are fault trees, event trees and reliability block diagrams.
Model parameter	A validated value in a model. In contrast to model variables changing this parameter results in loss of the model's validity. Therefore, a model parameter is considered to be part of the model structure.
Model structure	A parameterized mapping from inputs to outputs.
Model variable	An element of a model which numerical value can be chosen depending on the situation analyzed and the preferences of the analyst.
Object	In this thesis, the object of concern is always a storm surge barrier. The term is used to indicate that the developed methods could be tested at other objects such as locks, sluices, nuclear power plants and so forth.
Object system	The subelement of an object.
Performance improvement	An adjustment to the object properties, its maintenance, its operation or the way its performance is modelled that results in a higher performance.
Performance killer	A single event or group of events that greatly contribute to overall unreliability, unavailability, and/or probability of failure on demand fo the object, the influence of which could be lowered by a single performance improvement.
Principal performance improvement (PPI)	A performance improvement that can generally be applied to different types of objects.
Principal system failure mechanisms	The three main storm surge barrier flood protection system failure mechanisms which result in a coastal flood: 1) operational failure, 2) structural failure and 3) hydraulic overload. The hydraulic overload failure mechanism are all failure mechanisms where barrier operation and structure are successful. The most important sub-failure mechanism are: insufficient height, internal wind set-up and river discharge accumulating behind the barrier.

Probability	In this thesis, the bayesian interpretation of probability is applied, that is, a - subjective - degree of belief
Probability of failure on demand	The probability that an object fails to perform its intended function at a given time under a given set of conditions
Reliability	The probability that an object, object (sub)system or component will perform its intended function for a specified period of time under a given set of conditions.
Reliability and availability analysis (RA analysis)	RA analyses are applied to a variety of technological objects (nuclear plants, airplanes, space missions, chemical facilities) to analyze events with low probability and large consequences, where data to quantify risk are sparse (Bier and Cox Jr., 2007). In other industries, RA analyses are also referred to as probabilistic safety assessments, quantitative risk analyses or other combinations of these words. In the Netherlands, a probability of a failure to close is determined with a reliability and availability analysis.
Risk	A set of scenarios, each of which has a probability and an undesired consequence.
Start closure level	The water level near the barrier when the closure starts.
Storm surge barrier	A large hydraulic structure with movable gates, which temporarily closes during storm surges.
Storm surge barrier flood protection system	The storm surge barrier(s), inner basin and interior flood defenses.
Storm surge barrier performance	The difference between the hydraulic loads at the interior flood defense with and without the storm surge barrier.
Subsystem	The subelement of an object system. In the case there are more hierarchical levels than four, subsystems are numbered, i.e. subsystem level 1, subsystem level 2 and etc.
Unavailability type	Type of failure behaviour resulting in unavailability. In this thesis, four unavailability types are addressed: 1) dormant failure, 2) unavailability due to repair, 3) failure during mission and 4) failure on demand. Dormant failure refers to a failure which was undetected during normal conditions.
Water level maximum	The highest water level during an extreme storm surge event.

CURRICULUM VITAE

Curriculum Vitae

17/02/1985	Born in Groningen, the Netherlands

Education

2008 – 2009	MSc Civil engineering, specialization Hydraulic Structures, Delft University of Technology
2003 – 2007	BSc Civil engineering, Delft University of Technology
1997 – 2003	Coornhert Gymnasium Gouda

Employment

03/2021 – present	PhD researcher, Delft University of Technology
03/2021 – present	Senior advisor (1 day a week), Rijkswaterstaat, department storm surge barriers and guard locks
09/2009 – 03/2021	Hydraulic engineer, Royal Haskoning
01/2013 – 09/2016	Researcher Delft University of Technology (1 day a week)

LIST OF PUBLICATIONS

List of publications

Peer-reviewed journals

Mooyaart, L. F., Bakker, A. M.R., van den Bogaard, J.A., van den Boomen, M., Jonkman, S. N., 2025, A checklist to systematically improve safety-critical infrastructure: case study storm surge barrier in the Netherlands, Reliability Engineering and System Safety (submitted).

Bakker A.M.R., Rovers, D.L.T., **Mooyaart, L.F.**, 2025, Storm Surge Clusters, Multi-Peak Storms and Their Effect on the Performance of the Maeslant Storm Surge Barrier (The Netherlands),
Journal of Marine Science Engineering 2025, *13*(2), 298; https://doi.org/10.3390/jmse13020298

Mooyaart, L. F., Bakker, A. M. R., van den Bogaard, J. A., Jorissen, R. E., Rijcken, T., & Jonkman, S. N., 2025, Storm surge barrier performance: The effect of barrier failures on extreme water level frequencies. Journal of Flood Risk Management, 18(1), https://doi.org/10.1111/jfr3.13048

Mooyaart, L. F., Bakker, A. M. R., van den Bogaard, J. A., Rijcken, T., & Jonkman, S. N., 2023, Economic optimization of coastal flood defence systems including storm surge barrier closure reliability, Journal of Flood Risk Management 16(3). https://doi.org/10.1111/jfr3.12904

Mooyaart L.F., Jonkman S.N., 2017, Overview and design considerations of storm surge barriers, Journal of Waterway, Port, Coastal and Ocean Engineering, Issue 4, DOI: 10.1061/(ASCE)WW.1943-5460.0000383

Conference contributions

Mooyaart, L. F., Bakker, A. M.R., van den Bogaard, J.A., Jonkman, S. N., 2023, A Systematic Approach to Improve Reliability of Storm Surge Barrier Closures, ESREL 2023

Mooyaart, L. F., Bakker, A. M.R., van den Bogaard, J.A., Jonkman, S. N., 2023, A framework for storm surge barrier performance, ESREL2022

Mooyaart, L.F., Peters D.J., Kerpen N., Huis in 't Veld M., 2019, Design aspects of torqued concrete columns, Coastal structures '19

Mooyaart, L.F., Van Den Noortgaete T., oktober 2012, Tidal Power Plant in Antwerp, Proceedings Hydro 2012.

Mooyaart, L.F., Van Den Noortgaete T., van Berkel J., oktober 2011, Tidal Power Plant at Brouwersdam, Proceedings Hydro 2011.

↘

Storm surge barrier are large movable hydraulic structures that close during a storm surge to prevent coastal floods in bays and estuaries. These barriers are continuously maintained to rely on their operation when needed. Due to rising sea levels and coastal urbanization, coastal flood risk is increasing. Which barrier improvements are needed to cope with this risk increase, is unknown. This thesis presents a systematic method to find, select and evaluate barrier improvements focusing on lowering the probability of a failure to close a barrier. The method is applied to the Maeslant barrier to demonstrate its applicability.